ABSTRACT

Title of Dissertation: RELAY DEPLOYMENT AND SELECTION IN COOPERATIVE WIRELESS NETWORKS

Ahmed Salah Ibrahim, Doctor of Philosophy, 2009

Dissertation directed by: Professor K. J. Ray Liu
Department of Electrical and Computer Engineering

In cooperative communication protocols, multiple terminals can cooperate together forming a virtual antenna array to improve their performance. This thesis contributes to the advancement of cooperative communications by proposing new relay deployment and selection protocols across the network layers that can increase the bandwidth efficiency, reduce the end-to-end transmission power needed to achieve a desired network throughput, maximize the lifetime of a given network, rebuild a disconnected network, and mitigate the effect of channel estimation error and co-channel interference (CCI) problems.

Conventional cooperative schemes achieve full diversity order with low bandwidth efficiency. In this thesis we propose a relay selection cooperative protocol, which achieves higher bandwidth efficiency while guaranteeing full diversity order. We provide answers to two main questions, namely, "When to cooperate?" and

"Whom to cooperate with?". Moreover, we obtain optimal power allocation and present the tradeoff between the achievable bandwidth efficiency and the corresponding symbol error rate performance.

We illustrate that the cooperation gains can be leveraged to the network layer. In particular, we propose a cooperation-based routing algorithm, namely, the Minimum Power Cooperative Routing (MPCR) algorithm, which optimally selects relays while constructing the minimum-power route. Moreover, the MPCR can be implemented in a distributed manner. Using analytical and simulation results, we show that the MPCR algorithm achieves significant power savings compared to the current cooperation-based routing algorithms.

We also consider maximizing the network lifetime in sensor networks via deployment of relays. First, we propose a network maintenance algorithm that obtains the best locations for a given set of relays. Second we propose a routing algorithm, namely, Weighted Minimum Power Routing algorithm, that significantly increases the network lifetime due to the efficient utilization of the deployed relays. Finally, we propose an iterative network repair algorithm that finds the minimum number of relays along with their best locations, needed to reconnect a disconnected network.

We complete this thesis by investigating the impact of cooperative communications on mitigating the effect of channel estimation error and CCI. We show that cooperative transmission schemes are less susceptible to the effect of channel estimation error or CCI compared to the direct transmission. Finally we study the tradeoff between the timing synchronization error, emerging in the case of having simultaneous transmissions of the cooperating relays, and the channel estimation error, and show their net impact on the system performance.

RELAY DEPLOYMENT AND SELECTION IN COOPERATIVE WIRELESS NETWORKS

by

Ahmed Salah Ibrahim

Dissertation submitted to the Faculty of the Graduate School of the
University of Maryland, College Park in partial fulfillment
of the requirements for the degree of
Doctor of Philosophy
2009

Advisory Committee:

Professor K. J. Ray Liu, Chairman
Professor Thomas Charles Clancy
Professor Richard J. La
Professor Prakash Narayan
Professor Amr M. Baz

DEDICATION

To my family

ACKNOWLEDGEMENTS

I am very grateful to my advisor- Professor K. J. Ray Liu- for his continuous guidance and support in many aspects including, but not limited to, strengthening the scientific research capabilities, encouraging technical discussions with him at any time, supervising weekly group meetings that have significant impact on the presentation skills and self confidence, and creating opportunities for developing team-work skills. I am very honored for conducting my Ph.D. research work under the supervision of Professor Liu.

Many thanks to my colleagues in the Signals and Information Group at the University of Maryland for their fruitful discussions and social activities. I have learned so much from them and will always keep the good memories, which we have shared together. Special thanks to Dr. Ahmed Sadek, Professor Weifeng Su, Professor Karim Seddik, Professor Zhu Han, Amr El Sherif, and Mohammed Baidas.

My gratitude to Professor Prakash Narayan, Professor Richard La, Professor Charles Clancy, and Professor Amr Baz for agreeing to be in my dissertation committee, and for devoting the time to revising the thesis.

I am deeply indebted to my parents and my two sisters for all their prayers and encouragements in the past years. Finally, all praise is due to Allah for making me be able to achieve this important step.

TABLE OF CONTENTS

LIST OF TABLES

LIST OF FIGURES

Chapter 1

Introduction

Everyday, we witness new demands for services which require high data rates to be reliably provided through wireless networks, e.g., multimedia service through cellular networks. In wireless communication systems, transmitted signals experience multipath propagation. In particular, the received signal varies as a result of the destructive and constructive interference of the multipath signals. Destructive interference results in a fading phenomenon, which has a dramatic effect on the overall system performance compared to that caused by additive noise. Therefore, there is an urgent need for wireless communication protocols that can mitigate the fading effect and improve the system performance.

Various diversity techniques in time, frequency, and space domains have been proposed in the last decades to mitigate the fading phenomenon [1]. In principle diversity techniques provide a destination with multiple replicas of the transmitted signal, which experience independently faded channels. The probability of having all the channels in deep fade is much lower than that of any individual channel. Time diversity can be achieved by coding and interleaving across independently faded time slots. However in delay-sensitive applications with slow fading envi-

ronment, time diversity is not applicable due to the delay constraints. Frequency diversity can be achieved in frequency-selective wideband systems, for instance, by coding across independently faded sub-carriers in orthogonal frequency division multiplexing (OFDM) systems. However, frequency diversity degrades the bandwidth efficiency in coded OFDM systems and is not applicable in narrowband systems.

Spatial diversity using multiple antennas at the transmitter and/or the receiver is of special interest as it enhances the signal quality while not degrading the system performance in terms of delay and bandwidth efficiency. Various space-time codes have been proposed to provide spatial diversity such as space-time trellis codes and space-time block codes proposed in [2] and [3], respectively. Moreover, the multiple-input multiple-output (MIMO) channels add more degrees of freedom to the conventional single antenna channels, which result in higher channel capacity as was shown in [4] and [5]. However in wireless networks such as cellular networks, it may not be feasible to install multiple antennas at the mobile terminals due to cost and size limitations. This gave rise to a revolutionary concept, namely, cooperative diversity [6].

Cooperative diversity exploits the broadcast nature of the wireless medium. In cooperative communication protocols, a number of relay nodes are assigned to help a source in forwarding its information to its destination, hence forming a virtual antenna array. In the rest of this section, first we present a motivating example to illustrate the main idea of cooperative communications. Second we present related prior work, and finally we introduce the outline of this dissertation along with the main contributions.

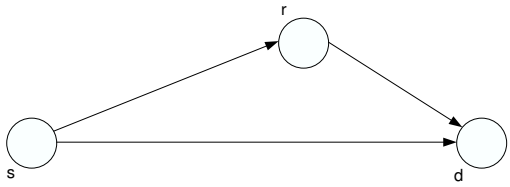

Figure 1.1: Single-relay cooperative communication system.

1.1 Motivating Example

We consider a cooperative communication system as shown in Figure 1.1. It consists of the source, s, the destination, d, and a relay, r. The relay receives and transmit information to enhance the the communication between the source and destination. Two cooperative protocols, namely, decode-and-forward and amplify-and-forward, are described as follows.

The decode-and-forward protocol is implements in two transmission phases and can be described as follows. In the first phase, the source broadcasts its information, which is received by both the relay and destination. The received signals at the destination and the relay can be written as

$$\begin{aligned} y_{s,d} &= \sqrt{P_1}\, h_{s,d}\, x + \eta_{s,d} \\ \text{and} \quad y_{s,r} &= \sqrt{P_1}\, h_{s,r}\, x + \eta_{s,r}\,, \end{aligned} \tag{1.1}$$

respectively, where P_1 is the source transmitted power, x is the transmitted information symbol with unit energy, and $\eta_{s,d}$ and $\eta_{s,r}$ are additive noise terms. Also, $h_{s,d}$ and $h_{s,r}$ are the source-destination and source-relay channel coefficients, respectively. If the relay decodes the received symbol correctly, then it forwards the decoded symbol to the destination in the second phase, otherwise it remains idle.

The received symbol at the destination from the relay is written as

$$y_{r,d}^{D} = \sqrt{\widetilde{P_2}}\, h_{r,d}\, x + \eta_{r,d}\,, \tag{1.2}$$

where the superscript D denotes decode-and-forward protocol, $\widetilde{P}_2 = P_2$ if the relay decodes the symbol correctly, otherwise $\widetilde{P}_2 = 0$, $\eta_{r,d}$ is an additive noise, and $h_{r,d}$ is the relay-destination channel coefficient.

Power is distributed between the source and the relay subject to the power constraint $P_1 + P_2 = P$. We assume that the relay can tell whether the information is decoded correctly or not [7]. Practically, this can be done at the relay by applying a simple signal-to-noise ratio (SNR) threshold on the received data. Although, it can lead to some error propagation, but for practical ranges of operating SNR, the event of error propagation can be assumed negligible. The destination applies maximal-ratio combining (MRC) [8] on the received signals from the source and the relay. The output of the MRC can be written as

$$y^{D} = \frac{\sqrt{P_1}\, h_{s,d}^{*}}{N_0}\, y_{s,d} + \frac{\sqrt{\widetilde{P_2}}\, h_{r,d}^{*}}{N_0}\, y_{r,d}^{D}\,. \tag{1.3}$$

The performance of the decode-and-forward protocol is discussed after introducing the amplify-and-forward protocol. The amplify-and-forward protocol is also implemented in two transmission phases and can be described as follows. Source broadcasts its information in the first phase as modeled in (1.1). In the second phase, the relay amplifies the received signal and transmits it to the destination with transmit power P_2 as

$$y_{r,d}^{A} = \sqrt{\frac{P_2}{P_1\,|h_{s,r}|^2 + N_0}}\, h_{r,d}\, y_{s,r} + \eta_{r,d}\,, \tag{1.4}$$

where the superscript A denotes amplify-and-forward protocol. The destination applies MRC on the received signals from the source and the relay and the output

of the MRC is

$$y^A = \frac{\sqrt{P_1}\, h^*_{s,d}}{N_0}\, y_{s,d} + \frac{\sqrt{\frac{P_1\, P_2}{P_1\, |h_{s,r}|^2 + N_0}}\, h^*_{s,r}\, h^*_{r,d}}{(\frac{P_2\, |h_{r,d}|^2}{P_1\, |h_{s,r}|^2 + N_0} + 1)\, N_0}\, y^A_{r,d}\,. \tag{1.5}$$

The channel coefficients $h_{s,d}$, $h_{s,r}$, and $h_{r,d}$ are modeled as zero-mean complex Gaussian random variables with variances $\delta^2_{s,d}$, $\delta^2_{s,r}$, and $\delta^2_{r,d}$, respectively. In addition, the noise terms $\eta_{s,d}$, $\eta_{s,r}$, and $\eta_{r,d}$ are modeled as zero-mean complex Gaussian random variables with variance N_0. In [7], symbol error rate (SER) expressions were derived for both techniques. At high SNR $\gamma = P/N_0$, it was shown that the SER, denoted by $\Pr(e)$, can be tightly upper bounded as

$$\Pr(e) \leq (CG\,\gamma)^{-2}\,, \tag{1.6}$$

where CG is referred to as the cooperation gain and it is equal to

$$CG = \begin{cases} \frac{b\delta_{s,d}\delta_{s,r}\delta_{r,d}}{\sqrt{(A^2/r^2)\delta^2_{r,d} + (B/r(1-r))\delta^2_{s,r}}} & \text{for decode-and-forward} \\ \frac{b\delta_{s,d}\delta_{s,r}\delta_{r,d}}{\sqrt{B((1/r^2)\delta^2_{r,d} + (1/r(1-r))\delta^2_{s,r})}} & \text{for amplify-and-forward} \end{cases}, \tag{1.7}$$

where $r = P_1/P$ is the power allocation ratio, $b = \sin^2(\pi/M)$, $A = \frac{1}{\pi}\int_0^{\frac{(M-1)\pi}{M}} \sin^2\theta\; d\theta = \frac{M-1}{2M} + \frac{\sin(\frac{2\pi}{M})}{4\pi}$, and $B = \frac{1}{\pi}\int_0^{\frac{(M-1)\pi}{M}} \sin^4\theta\; d\theta = \frac{3(M-1)}{8M} + \frac{\sin(\frac{2\pi}{M})}{4\pi} - \frac{\sin(\frac{4\pi}{M})}{32\pi}$ for M-PSK modulation type. The diversity order is defined as $d = -\lim_{\gamma\longrightarrow\infty} \log(\Pr(e))/\log(\gamma)$. Thus, from (1.6), it can be shown that both the amplify-and-forward and decode-and-forward protocols achieve full diversity order equal to two.

In Figure 1.2, we show simulation results of the amplify-and-forward and decode-and-forward for QPSK signals. We assume unity channel variances and equal power allocation between the source and the relay. It is shown that both cooperation schemes achieve full diversity, equal to two. The tight upper bound in (1.6) is also plotted for both cooperation schemes. We note that the decode-and-forward

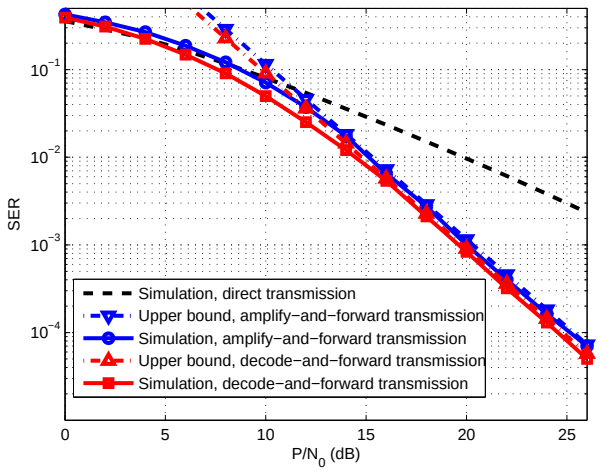

Figure 1.2: The SER of the amplify-and-forward and decode-and-forward cooperative techniques with equal power allocation and unity channel variances.

performs slightly better than the amplify-and-forward. The direct transmission performance, using a total transmission power P, is also plotted for comparison and it achieves diversity order equal to one.

In [7], a practical comparison between the amplify-and-forward and decode-and-forward was introduced. It was illustrated that for the case when the source-relay channel is statistically better than the source-destination and relay-destination channels, then decode-and-forward performs better than the amplify-and-forward but not at a remarkable degree. However, if the source-relay channel is bad then the amplify-and-forward and decode-and-forward perform similarly.

1.2 Related Prior Work

As shown in the previous example, cooperative diversity can mitigate fading effects via providing spatial diversity. Spatial diversity can be also utilized to reduce the transmission power required to achieve certain Quality of Service (QoS). There-

fore, cooperative communications can increase the battery life of the transmitting nodes. Alternatively, cooperative communications can extend the coverage area (e.g. in cellular networks) as was investigated in [9]. On the other hand, there are many challenges that need to be considered such as reducing the error probability at the helping terminals (relays), increasing the bandwidth efficiency of the conventional cooperative schemes, and the time synchronization among the simultaneous cooperating nodes. In the sequel, we present some of the prior work related to relay networks and cooperative communication protocols.

The classical relay channel model, which consists of three terminals: a source, a destination, and a relay, was first introduced in [10]. An upper bound on the channel capacity as well as an achievable lower bound for the additive white Gaussian noise (AWGN) relay channels were provided in [11]. Generally, the lower and upper bounds do not coincide except for special cases as in the degraded relay channels. In [12], different coding strategies haven been proposed, which achieve the ergodic capacity with phase fading if the phase information is known locally and if the relays are near the source.

User cooperation diversity was first introduced in [13] and [14]. A two-user code division multiple access (CDMA) cooperative system, where both users are active and use orthogonal codes, was implemented in this two-part series. It was illustrated that in a two-user system assuming the knowledge of channel phases at the transmitter sides, user cooperation can achieve high data rate for both users and that users are less sensitive to channel variations. In fast-fading scenario, it was shown that the achievability region of a two-user cooperative system includes the capacity region of the two-user multiple access system, i.e., when there is no cooperation among the users. Furthermore in slow-fading scenario, it was shown

that the outage probability of the cooperative system is less than that of the non-cooperative system.

Various techniques of cooperative communication have been described in [15] such as amplify-and-forward, decode-and-forward, selection relaying, and incremental relaying. As described in Section 1.1, in amplify-and-forward protocol each relay forwards the received information after amplifying it. In decode-and-forward cooperative protocol, each relay decodes the information received from the source, re-encodes it then forwards it to the destination. This is slightly different from the protocol defined in Section 1.1, in which the relay only forwards the received data if correctly decoded. In selection relaying protocol, the relay decides whether to cooperate with the source or not based on the channel conditions between the source and the relay. Finally in incremental relaying protocol, the relay cooperates only if the destination asked through feedback to receive another replica of the transmitted symbol. It was shown that the decode-and-forward and amplify-and-forward protocols achieve bandwidth efficiency equal to 1/2 symbols per channel use (SPCU), while the selection relaying and incremental relaying schemes achieve higher bandwidth efficiency.

The concept of multi-hop diversity, where each relay combines the signals received from all of the previous transmissions, was introduced in [16]. This kind of spatial diversity is specially applicable in multihop ad-hoc networks. Multi-node cooperative communications with decode-and-forward and amplify-and forward strategies, described in Section 1.1, have been analyzed in [17] and [18], respectively. In [17], a family of cooperative protocols in which each relay can combine an arbitrary subset from the previous transmissions was considered. SER performance analysis for the decode-and-forward multi-node schemes was provided. It

was shown that full diversity order is achieved if each relay combines the received signals from the previous relay and the source. Analysis for general multibranch multihop amplify-and-forward cooperative protocol was provided in [18]. It was shown that the multibranch scheme, in which there exists a number of parallel relay-based branches from the source to its destination, achieves full-diversity order.

Distributed space-time codes can achieve high bandwidth efficiency, while guaranteeing full diversity order. In [19], a distributed space-time coded (STC) cooperative scheme was proposed, in which the relays decode the received symbols from the source and utilize a distributed space-time code. In this scheme, each relay is assigned a column in a space-time matrix and it sends this column if it has decoded the source's message correctly. It was shown that decode-and-forward distributed space-time codes can achieve full diversity order in the number of cooperating relays and not just in the number of decoding ones. However, timing synchronization among the cooperating terminals problems are among the challenges to implement distributed space-time codes. In [20], distributed space time codes for decode-and-forward and amplify-and-forward cooperative protocols have been analyzed.

Coded cooperation, which combines error-control coding with cooperative communications, was introduced in [21]. The coded information is divided over two consecutive frames. The source broadcasts the first frame, which is received by the destination and the relay. The relay tries to decode this frame and sends the second frame if correctly decoded. Otherwise, the source sends the second frame. It was shown that full-diversity order and large coding gain are achieved via coded cooperation.

The optimal location for a single-relay communication system has been investigated for decode-and-forward and amplify-and-forward in [9] and [18], respectively. For incremental relaying decode-and-forward, it was shown in [9] that the optimal relay location is in the middle between the source and destination with no MRC at the destination. If MRC is utilized, then the optimal relay location is towards the source. In amplify-and-forward, it was shown that the relay is best to be deployed in the mid-way between the source and the destination [18].

Cooperative communications can also enhance the performance of MIMO systems. It was proven in [22] that relays can significantly increase the capacity of rank-deficient MIMO channels. Intuitively the cooperating relays create the rich scattering environment, needed for maximum throughput, by acting as scatters. In [23], the optimum design of the relay weighting matrix for the multiple-antenna amplify-and-forward relay was proposed. It was shown that the optimum relay matrix represents a matched filter along the singular vectors of the source-relay and relay-destination channel matrices.

1.3 Dissertation Organization and Contributions

In this thesis, we develop and analyze a cross-layer framework for utilizing the cooperative communication paradigm in wireless networks. The ultimate goal of our research is to develop new relay deployment and selection protocols across the network layers that can increase the bandwidth efficiency, reduce the required transmission power needed to achieve a desired network throughput, maximize the lifetime of a given network, maintain a given network to be connected as long as possible, rebuild a disconnected network, and mitigate the effect of channel estimation error and co-channel interference problem. In the following, we present

the main contributions of each chapter.

1.3.1 Cooperative Communications with Relay Selection (Chapter 2)

As explained in Section 1.1, the conventional cooperative scheme achieves full diversity order. However, it results in low bandwidth efficiency due to utilizing orthogonal channels for the transmission of the source and the relays. Increasing the bandwidth efficiency of the cooperative communications scheme is of great importance to satisfy the demand for high data rate. In Chapter 2, we propose a new cooperative communication protocol that achieves higher bandwidth efficiency while guaranteeing the same diversity order as that of the conventional cooperative scheme. The proposed scheme considers relay selection via the available partial channel state information (CSI) at the source and the relays. Hence, it is a form of cross-layer relay-selection scheme across the network and physical layers.

We consider the multi-node decode-and-forward cooperative scenarios, where arbitrary N relays are available. The source determines when it needs to cooperate with one relay only, and which relay to cooperate with in case of cooperation, i.e., "When to cooperate?" and "Whom to cooperate with?". An optimal relay is the one which has the maximum instantaneous scaled harmonic mean function of its source-relay and relay-destination channel gains. We derive an approximate expression of the bandwidth efficiency and obtain an upper bound on the symbol error rate (SER) performance. We show that full diversity is guaranteed and that a significant increase of the bandwidth efficiency is achieved. Finally, we obtain optimal power allocation and present the tradeoff between the achievable bandwidth efficiency and the corresponding symbol error rate performance [24–26].

1.3.2 Cooperative Routing (Chapter 3)

We focused in Chapter 2 on a special network setting, in which the source can reach the destination in a maximum of two hops. In Chapter 3 we consider a general network setting, in which the source can reach the destination in an arbitrary number of hops. We aim at finding the optimum route, which utilizes cooperative communications and optimally selects a set of the available relays. Such routing schemes are referred to as cooperative routing. Cooperative routing in wireless networks has gained much interest due to its ability to exploit the broadcast nature of the wireless medium in designing power-efficient routing algorithms. Most of the existing cooperation-based routing algorithms are implemented by finding a shortest-path route first and then improving the route using cooperative communication. As such, these routing algorithms do not fully exploit the merits of cooperative communications, since the optimal cooperative route might not be similar to the shortest-path one.

In Chapter 3, we consider the minimum-power routing problem in which we find the route that requires the minimum end-to-end transmission power. We propose a cooperation-based routing algorithm, namely, the Minimum Power Cooperative Routing (MPCR) algorithm, which makes full use of the cooperative communications while constructing the minimum-power route. The MPCR algorithm constructs the minimum-power route, which guarantees certain throughput, as a cascade of the minimum-power single-relay building blocks from the source to the destination. Thus, any distributed shortest path algorithm can be utilized to find the optimal cooperative route with polynomial complexity. Finally, we consider arbitrary networks as well as regular networks, namely, linear and grid regular networks and calculate the power saving due to utilizing cooperation [27, 28].

1.3.3 Connectivity-Aware Network maintenance (Chapter 4)

We proposed in Chapter 3 a cooperative routing scheme that reduces the end-to-end transmission power via considering some of the nodes in the network as relays. In Chapter 4, we focus on sensor networks and show that network lifetime can be extended by optimally deploying relays in the network.

In the last few years, sensor networks have gained much interest due to their potential for some civil and military applications as discussed in [29]. A Sensor network is composed of a large number of sensor nodes, which are deployed inside the phenomenon, and are generally limited in power, computational capabilities, and memory. In sensor networks, each sensor needs to be connected to the central processing unit in order to deliver its data. Furthermore, maximizing the network lifetime, i.e., keeping the network connected as long as possible, is one of the major issues in sensor networks.

In Chapter 4, we address the network maintenance problem, in which we aim to maximize the lifetime of a sensor network by adding a set of relays to it. The network lifetime is defined as the time until the network becomes disconnected. The Fiedler value, which is the algebraic connectivity of a graph, is used as an indicator of the network health. The network maintenance problem is formulated as a semi-definite programming (SDP) optimization problem that can be solved efficiently in polynomial time.

First, we propose a network maintenance algorithm that obtains the locations for a given set of relays. Second we propose a routing algorithm, namely, Weighted Minimum Power Routing (WMPR) algorithm, that significantly increases the network lifetime due to the efficient utilization of the deployed relays. Third, we

propose an adaptive network maintenance algorithm that relocates the deployed relays based on the network health indicator. Further, we study the effect of two different transmission scenarios, with and without interference, on the network maintenance algorithm. Finally, we consider the network repair problem, in which we find the minimum number of relays along with their locations to reconnect a disconnected network. We propose an iterative network repair algorithm that utilizes the network maintenance algorithm [30–32].

1.3.4 Mitigating Channel Estimation Error and Co-channel Interference Effects via Cooperative Communications (Chapter 5)

In the previous chapters, we investigated the impact of cooperative communications on increasing the bandwidth efficiency, reducing the end-to-end transmission power, and maximizing the lifetime of sensor networks. In these works, we have assumed perfect channel estimation error and no interference effect at the receivers. In Chapter 5, we consider a more practical communication system that suffers from channel estimation error and co-channel interference (CCI).

Channel estimation error and CCI problems are among the main causes of performance degradation in wireless networks. In Chapter 5, we investigate the impact of cooperative communications on mitigating the effect of channel estimation error and CCI. Two main performance criteria, namely, the traditional outage probability and the proposed signal-to-noise ratio (SNR) gap ratio, are utilized to characterize such impact. The SNR gap ratio measures the reduction in the SNR due to channel estimation error or CCI. Taking into consideration the channel estimation error, we show that the outage probability is reduced by utilizing

cooperative transmission protocols. We also show that cooperative transmission scenarios, in which each cooperating relay forwards its signal over an orthogonal channel, result in lower SNR gap ratio compared to that of the direct transmission. Thus, cooperative transmission schemes are less susceptible to the effect of channel estimation error compared to direct transmission. Moreover, increasing the number of cooperating relays reduces the effect of the channel estimation error more.

Timing synchronization error arises in distributed space-time cooperative schemes, in which the cooperating relays are simultaneously transmitting their signals over the same channel. Unlike the channel estimation error, the effect of the timing synchronization error gets worse as the the number of cooperating relays increases. In this work we also study the tradeoff between the timing synchronization error and the channel estimation error, and show their net impact on the system performance. Finally, we illustrate that the cooperative transmission schemes are also less susceptible to the effect of CCI [33, 34].

Chapter 2

Cooperative Communications with Relay-Selection: When to Cooperate and Whom to Cooperate with?

As discussed in Chapter 1, cooperative communications for wireless networks have gained much interest due to its ability to mitigate fading in wireless networks through achieving spatial diversity, while resolving the difficulties of installing multiple antennas on small communication terminals. The decode-and-forward and amplify-and-forward cooperative protocols, explained in Section 1.1, achieve bandwidth efficiency equal to 1/2 symbols per channel use (SPCU). For a system of arbitrary N relays, $N+1$ time slots are needed to send 1 symbol. Thus, the bandwidth efficiency is $1/(N+1)$ symbols per channel use (SPCU). Motivated by the great need to increase such bandwidth efficiency to satisfy the demand for high data rate, we aim in this chapter to increase the bandwidth efficiency while not

sacrificing the performance. This objective is achieved via relay selection.

There are various protocols proposed to choose the best relay among a collection of available relays in the literature. In [35], the authors proposed to choose the best relay depending on its geographic position, based on the geographic random forwarding (GeRaF) protocol proposed in [36] and [37]. In GeRaF, the source broadcasts its data to a collection of nodes and the node that is closest to the destination is chosen in a distributed manner to forward the source's data to the destination. In [38], the authors considered a best-select relay scheme in which only the relay, which has received the transmitted data from the source correctly and has the highest mean signal-to-noise ratio (SNR) to the destination node, is chosen to forward the source's data.

In this chapter, we propose a new cooperative communication protocol that achieves higher bandwidth efficiency while guaranteeing the same diversity order as that of the conventional cooperative schemes. The rational behind this protocol is that no need for the relay to forward the information if the direct link, between the source and the destination, is of high quality. The proposed scheme considers relay selection via the available partial channel state information (CSI) at the source and the relays. Partial CSI expresses the instantaneous channel gain without the phase component.

In the multi-node scenario, where arbitrary N relays are available, the source determines when it needs to cooperate with one relay only, and which relay to cooperate with, i.e., *"When to cooperate?"* and *"Whom to cooperate with?"*. We propose a relay's metric, which is motivated by the symbol error rate of the conventional cooperative scheme derived in [7]. The proposed relay's metric is a modified harmonic mean function of its source-relay and relay-destination channels gain.

The optimal relay, among a set of arbitrary N relays, is the one that has the maximum value of this metric. After identifying the optimal relay, the source decides whether to utilize this optimal relay or not based on the ratio between the source-destination channel gain and the optimal relay's metric. For the proposed scheme, we show that full diversity is guaranteed and that a significant increase of the bandwidth efficiency is achieved. We derive an approximate expression for the bandwidth efficiency and an upper bound on the symbol error rate performance for the symmetric scenario. Finally, we obtain optimal power allocation and present the tradeoff between the achievable bandwidth efficiency and the corresponding symbol error rate performance.

The rest of this chapter is organized as follows. In Section 2.1, we revisit the conventional decode-and-forward cooperative scenario, which leads to the motivation behind choosing an appropriate metric to indicate the relay's ability to help. Furthermore, we introduce the multi-node relay-selection decode-and-forward cooperative scenario. In Section 2.2, the performance analysis of the proposed scheme is presented with formulas for the approximate bandwidth efficiency and the SER upper bound. Section 2.3 presents a solution to the optimum power allocation problem. Moreover, bandwidth efficiency-SER tradeoff curves for different SNR are also shown in this section. Finally, we present some simulation results in Section 2.4, which verify the analytical results.

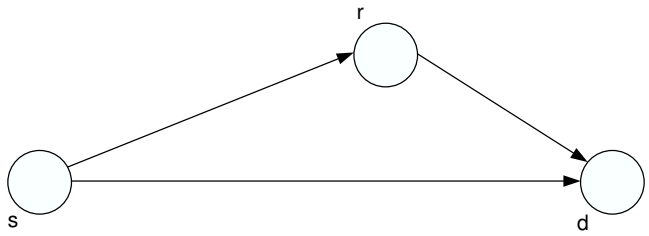

Figure 2.1: Single-relay cooperative communication system.

2.1 Motivation and Proposed Relay-Selection Protocol

In this section, we revisit the system model of the conventional single-relay decode-and-forward cooperative scenario, which was presented in Section 1.1, along with the SER results obtained in [7]. This helps in illustrating the motivation behind choosing a modified harmonic mean function of the source-relay and relay-destination channels gain as an appropriate metric to represent the relay's ability to help the source. Finally, we introduce the proposed multi-node relay-selection decode-and-forward cooperative scenario.

2.1.1 Conventional Single-Relay Decode-and-Forward Cooperative Scenario

The communication system of a conventional single-relay decode-and-forward cooperative scheme is shown in Figure 2.1. It consists of the source, s, the destination, d, and a relay, r. The transmission protocol requires two consecutive phases as follows. In the first phase, the source broadcasts its information to the relay and the destination. The received symbols at the destination and relay can be modeled

as $y_{s,d} = \sqrt{P_1}\ h_{s,d}\ x + \eta_{s,d}$ and $y_{s,r} = \sqrt{P_1}\ h_{s,r}\ x + \eta_{s,r}$, where P_1 is the source transmitted power, x is the transmitted information symbol, and $\eta_{s,d}$ and $\eta_{s,r}$ are additive noises. Also, $h_{s,d}$ and $h_{s,r}$ are the source-destination and source-relay channel gains, respectively.

The relay decides whether to forward the received information or not according to the quality of the received signal. If the relay decodes the received symbol correctly, then it forwards the decoded symbol to the destination in the second phase, otherwise it remains idle. The received symbol at the destination from the relay is written as $y_{r,d} = \sqrt{\widetilde{P_2}}\ h_{r,d}\ x + \eta_{r,d}$, where $\widetilde{P}_2 = P_2$ if the relay decodes the symbol correctly, otherwise $\widetilde{P}_2 = 0$, $\eta_{r,d}$ is an additive noise, and $h_{r,d}$ is the relay-destination channel coefficient. The destination applies maximal-ratio combining (MRC) [8] for the received signals from the source and the relay. The output of the MRC can be written as $y = \frac{\sqrt{P_1}\ h^*_{s,d}}{N_0}\ y_{s,d} + \frac{\sqrt{\widetilde{P_2}}\ h^*_{r,d}}{N_0}\ y_{r,d}$. The channel coefficients $h_{s,d}$, $h_{s,r}$, and $h_{r,d}$ are modeled as zero-mean complex Gaussian random variables with variances $\delta^2_{s,d}$, $\delta^2_{s,r}$, and $\delta^2_{r,d}$, respectively. The noise terms $\eta_{s,d}$, $\eta_{s,r}$, and $\eta_{r,d}$ are modeled as zero-mean complex Gaussian random variables with variance N_0.

It has been shown in [7] that the SER for M-PSK signalling can be upper bounded as

$$Pr(e) \leq \frac{N_0^2}{b^2}.\frac{A^2\ P_2\ \delta^2_{r,d} + B\ P_1\ \delta^2_{s,r}}{P_1^2\ P_2\ \delta^2_{s,d}\ \delta^2_{s,r}\ \delta^2_{r,d}}\ , \tag{2.1}$$

where $b = \sin^2(\pi/M)$,

$$\begin{aligned} A &= \frac{1}{\pi}\int_0^{\frac{(M-1)\pi}{M}} \sin^2\theta\ d\theta = \frac{M-1}{2M} + \frac{\sin(\frac{2\pi}{M})}{4\pi}\ , \\ \text{and}\ \ B &= \frac{1}{\pi}\int_0^{\frac{(M-1)\pi}{M}} \sin^4\theta\ d\theta = \frac{3(M-1)}{8M} + \frac{\sin(\frac{2\pi}{M})}{4\pi} - \frac{\sin(\frac{4\pi}{M})}{32\pi}\ . \end{aligned} \tag{2.2}$$

Moreover, it was shown in [7] that the SER upper bound in (2.1) is tight at high enough SNR.

2.1.2 Relay-Selection Criterion

In this subsection, we introduce a relay-selection criterion from the SER expression in (2.1). Let $\gamma \triangleq \frac{P}{N_0}$ denote the signal-to-noise ratio (SNR), where $P = P_1 + P_2$ is the total power. Hence, (2.1) can be written as

$$Pr(e) \leq (CG\ \gamma)^{-2}\ , \tag{2.3}$$

where CG denotes the cooperation gain and it is equal to

$$CG = \sqrt{b^2\ \delta_{s,d}^2 \left(\frac{\delta_{s,r}^2\ \delta_{r,d}^2}{q_1\ \delta_{r,d}^2 + q_2\ \delta_{s,r}^2} \right)}\ , \tag{2.4}$$

where

$$q_1 = \frac{A^2}{r^2}\ \ , \quad q_2 = \frac{B}{r\,(1-r)}\ , \tag{2.5}$$

and $r \triangleq \frac{P_1}{P}$ is referred to as *power ratio*. The diversity order is defined as $d = -\lim_{\gamma \longrightarrow \infty} \log(Pr(e))/\log(\gamma)$. So, in (2.3) the tight SER upper bound expression has diversity order equal to two. Hence, the actual SER of the system has diversity order two as well. Generally, diversity of order K means that there are K statistically independent paths from the source to the destination.

We note that maximizing the cooperation gain in (2.4) results in minimizing the SER in (2.3). By investigating the CG in (2.4), we can see that the term $m \triangleq \frac{\delta_{s,r}^2\ \delta_{r,d}^2}{q_1\ \delta_{r,d}^2 + q_2\ \delta_{s,r}^2}$ is the only term that depends on the relay channels (source-relay and relay-destination). Thus, if N relays are available and we need to choose one relay only, we will choose the relay with maximum m. By doing so, the multi-relay scheme becomes a single-relay scheme that uses the best relay during the whole transmission time, because the metric m depends on the average channel gains. Thus, the SER of this scheme is upper bounded as in (2.3). In other words, this scheme achieves diversity order 2 and not $N + 1$ as we aim to achieve.

The main reason for this system not achieving full diversity order is that one relay is chosen at the beginning of the transmission and it is used until the end of the transmission. If we can have the chance to choose the best relay at each time instant and utilize that relay only, then full diversity order can be achieved. Intuitively, this can be explained as follows. In order for the transmitted data to be lost, the direct path and the best-relay path have to be in deep fade. Consequently, all the other $N-1$ relay-dependent paths have to be in deep fade as the best-relay path is in deep fade. Thus a total of $N+1$ paths must be in deep fade to lose the transmitted signal. This corresponds to full diversity of order $N+1$ as explained above.

Since the average metric m cannot achieve the full diversity order, we propose to replace the source-relay and relay-destination channel gains by their corresponding instantaneous channel gains, i.e., $\delta_{s,r}^2$ and $\delta_{r,d}^2$ are replaced by $|h_{s,r}|^2$ and $|h_{r,d}|^2$, respectively. By doing so, we are combining what we have concluded from the single-relay SER (i.e., the relay average metric m) along with the instantaneous information that can achieve full diversity order if utilized properly. Thus, the instantaneous relay metric can be written as $m' = \frac{|h_{s,r}|^2 \, |h_{r,d}|^2}{q_1 \, |h_{r,d}|^2 + q_2 \, |h_{s,r}|^2}$. Finally, the metric m' is scaled to be in a standard harmonic mean function as $2\,q_1\,q_2\,m'$. Therefore, we propose the relay's metric β_m, which is given by

$$\beta_m = \mu_H(q_1 \, \beta_{r,d}, q_2 \, \beta_{s,r}) \triangleq \frac{2 \, q_1 \;\; q_2 \, \beta_{s,r} \, \beta_{r,d}}{q_1 \, \beta_{r,d} + q_2 \, \beta_{s,r}} \, , \tag{2.6}$$

where $\beta_{s,r} = |h_{s,r}|^2$, $\beta_{r,d} = |h_{r,d}|^2$, and $\mu_H(.,.)$ denotes the standard harmonic mean function. The relay's metric β_m (2.6) gives an instantaneous indication about the relay's ability to cooperate with the source.

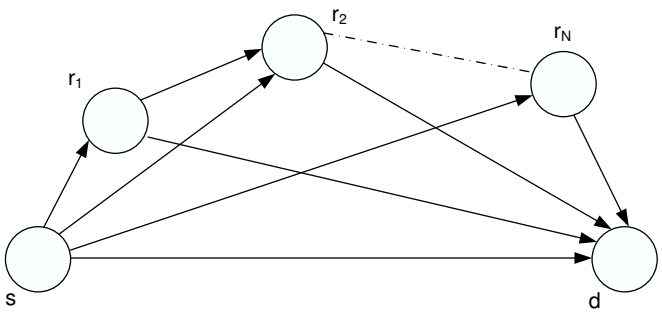

Figure 2.2: Multi-node cooperative communication system.

2.1.3 Proposed Relay-Selection Protocol

The communication system of a conventional multi-node decode-and-forward cooperative scheme is shown in Figure 2.2. The conventional multi-node decode-and-forward scheme is implemented in $N+1$ time slots (phases) as follows. In the first phase, the source broadcasts its data, which is received by the destination as well as the N relays. The first relay decodes what it has received from the source and checks if it has received the data correctly. If it has received the data correctly, it re-encodes the data to be broadcasted in the second phase. Otherwise, it remains idle. Generally in the i-th phase, the $(i-1)$-th relay combines the signals coming from all the previous relays and the source, re-transmits the data if it has decoded correctly, and remains idle otherwise. Based on that model, $N+1$ time slots are needed to send 1 symbol. Thus, the bandwidth efficiency is $1/(N+1)$ symbols per channel use (SPCU).

The basic idea of the proposed multi-node relay-selection cooperative scenario depends on selecting one relay among the N relays to cooperate with the source, if it needs cooperation. There are two main questions to be answered. The first question is how to determine the optimal relay to cooperate with, in case of coop-

eration. The answer comes from the motivation described earlier. The modified harmonic mean function of the source-relay and relay-destination channel gains is an appropriate measure on how much help a relay can offer. Thus, the optimal relay is the relay with the maximum modified harmonic mean function of its source-relay and relay-destination channel gains among all the N relays. With this optimal relay being decided, the system consists of the source, the destination, and the optimal relay, which is similar to the single-relay system shown in Figure 2.1. The second question is how the source determines whether to cooperate with this optimal relay or not, and its answer is explained in the sequel while explaining the transmission protocol.

Let the metric for each relay be defined as the modified harmonic mean function of its source-relay and relay-destination channel gains as

$$\beta_i = \mu_H(q_1\ \beta_{r_i,d}, q_2\ \beta_{s,r_i}) = \frac{2\ q_1\ \ q_2\ \beta_{r_i,d}\ \beta_{s,r_i}}{q_1\ \beta_{r_i,d} + q_2\ \beta_{s,r_i}}\ ,\ for\ i = 1, 2, \cdots, N\ . \tag{2.7}$$

Consequently the optimum relay will have a metric, which is equal to

$$\beta_{max} = \max\{\ \beta_1, \beta_2, \ldots, \beta_N\ \}\ . \tag{2.8}$$

The transmission protocol can be described as follows. In the first phase, the source computes the ratio $\beta_{s,d}/\beta_{max}$ and compares it to the cooperation threshold α. If $\frac{\beta_{s,d}}{\beta_{max}} \geq \alpha$, then the source decides to use direct transmission only. This mode is referred to as the *direct-transmission* mode. Let $\phi = \{\ \beta_{s,d} \geq \alpha\ \beta_{max}\ \}$ be the event of direct transmission. The received symbol at the destination can then be modeled as

$$y_{s,d}^{\phi} = \sqrt{P}\ h_{s,d}\ x + \eta_{s,d}, \tag{2.9}$$

where P is the total transmitted power, x is the transmitted symbol with unit average energy, $h_{s,d}$ is the source-destination channel coefficient, and $\eta_{s,d}$ is an

additive noise.

On the other hand, if $\frac{\beta_{s,d}}{\beta_{max}} < \alpha$, then the source employs the optimal relay r to transmit its information as in the conventional single-relay decode-and-forward cooperative protocol [7]. This mode is denoted by *relay-cooperation* mode and can be described as follows. In the first phase, the source broadcasts its symbol to both the optimal relay and the destination. The received symbols at the destination and the optimal relay can be modeled as

$$y_{s,d}^{\phi^c} = \sqrt{P_1}\, h_{s,d}\, x + \eta_{s,d}, \qquad y_{s,r}^{\phi^c} = \sqrt{P_1}\, h_{s,r}\, x + \eta_{s,r}, \tag{2.10}$$

respectively, where P_1 is the source transmitted power, $h_{s,r}$ is the source-relay channel coefficient, $\eta_{s,r}$ is an additive noise, and ϕ^c denotes the complement of the event ϕ. The optimal relay decodes the received symbol and re-transmits the decoded symbol if correctly decoded in the second phase, otherwise it remains idle. The received symbol at the destination is written as

$$y_{r,d}^{\phi^c} = \sqrt{\widetilde{P_2}}\, h_{r,d}\, x + \eta_{r,d}, \tag{2.11}$$

where $\widetilde{P}_2 = P_2$ if the relay decodes the symbol correctly, otherwise $\widetilde{P}_2 = 0$, $h_{r,d}$ is the relay-destination channel coefficient, and $\eta_{r,d}$ is an additive noise. Power is distributed between the source and the optimal relay subject to the power constraint $P_1 + P_2 = P$. We note that the optimal relay decides whether to forward the received information or not according to the quality of the received signal. For mathematical tractability, we assume that the relay can tell whether the information is decoded correctly or not [7, 17].

We assume that the channels are reciprocal as in the Time Division Duplex (TDD) mode, hence each relay knows its source-relay and relay-destination channel gains and calculates their harmonic mean function. Then, each relay sends this

metric to the source through a feedback channel. Furthermore, we assume that the source knows its source-destination channel gain. Thus, the source uses its source-destination channel gain and the maximum metric of the relays, to determine whether to cooperate with one relay only or not. Finally, the source sends a control signal to the destination and the relays to indicate its decision and the optimal relay it is going to cooperate with, in case of cooperation. This procedure is repeated every time the channel gains vary. We assume that the channel gains vary slowly so that the overhead resulting from sending the relays' metrics is negligible. We should note here that the source and the relays are not required to know the phase information of their channels. Hence, only partial CSI is needed for this proposed algorithm.

Flat quasi-static fading channels are considered, hence the channel coefficients are assumed to be constant during a complete frame, and can vary from a frame to another independently. Rayleigh fading channel model is considered for the channel between each two nodes. Let $h_{i,j}$ be a generic channel coefficient representing the channel between any two nodes. $h_{i,j}$ is modeled as zero-mean complex Gaussian random variables with variance $\delta_{i,j}^2$. Thus, the channel gain $|h_{i,j}|$ is modeled a Rayleigh random variable. Furthermore the channel gain squared $|h_{i,j}|^2$ is modeled as an exponential random variable with mean $\delta_{i,j}^2$, i.e., $p(|h_{i,j}|^2) = 1/\delta_{i,j}^2 \exp(-|h_{i,j}|^2/\delta_{i,j}^2)\, U(|h_{i,j}|^2)$ is the probability density function (PDF) of $|h_{i,j}|^2$ in which $U(.)$ is the unit step function. The noise terms, $\eta_{s,d}, \eta_{s,r}$, and $\eta_{r,d}$, are modeled as zero-mean, complex Gaussian random variables with equal variance N_0. In this section, we have presented the proposed relay's metric and the motivation behind choosing it. In addition, we have explained the proposed relay-selection protocol. In the next section, we provide the performance analysis of the proposed

scheme.

2.2 Performance Analysis

In this section, first we calculate the probability of the direct-transmission and relay-cooperation modes for the multi-node relay-selection decode-and-forward cooperative scenario. Then, they are used to obtain an approximate expression of the bandwidth efficiency and an upper bound on the SER performance.

2.2.1 Average Bandwidth Efficiency Analysis

We derive the average achievable bandwidth efficiency as follows. The cumulative distribution function (CDF) of β_i for $i = 1, 2, \cdots, N$, denoted by $P_{\beta_i}(.)$, can be written as given in [39] as

$$P_{\beta_i}(\beta_i) \;=\; 1 - \frac{\beta_i}{t_{1,i}}\ \exp(-\frac{t_{2,i}}{2}\ \beta_i)\ K_1(\frac{\beta_i}{t_{1,i}})\ , \tag{2.12}$$

where $t_{1,i} = \sqrt{q_1\ q_2\ \delta^2_{s,r_i}\ \delta^2_{r_i,d}}$, $t_{2,i} = \frac{1}{q_2\ \delta^2_{s,r_i}} + \frac{1}{q_1\ \delta^2_{r_i,d}}$, and $K_1(x)$ is first-order modified Bessel functions of the second kind, defined in [[40], (9.6.22)]. The CDF of β_{max} can be written as

$$P_{\beta_{max}}(\beta) = Pr(\ \beta_1 \leq \beta\ , \ldots, \beta_N \leq \beta\ ) = \prod_{i=1}^{N}\ P_{\beta_i}(\beta)\ , \tag{2.13}$$

and the PDF of β_{max} is written as

$$p_{\beta_{max}}(\beta) = \frac{\partial P_{\beta_{max}}(\beta)}{\partial \beta} \approx \sum_{j=1}^{N} p_{\beta_j}(\beta) \Big(\prod_{i=1, i\neq j}^{N} \Big(1 - \exp(-\frac{t_{2,i}}{2}\ \beta) \Big) \Big), \tag{2.14}$$

where $p_{\beta_j}(.)$ is the PDF of β_j. In (2.14), we approximated $K_1(.)$ as given in [[40], (9.6.9)] by

$$K_1(x) \approx \frac{1}{x}\ . \tag{2.15}$$

The expression in (2.14) is complex and will lead to more complex and intractable expressions. For mathematical simplicity, we consider the symmetric scenario where all the relays have the same source-relay and relay-destination channel variances, i.e., $\delta^2_{s,r_i} = \delta^2_{s,r}$ and $\delta^2_{r_i,d} = \delta^2_{r,d}$ for $i = 1, 2, \ldots, N$. Let $t_1 = \sqrt{q_1\ q_2\ \delta^2_{s,r}\ \delta^2_{r,d}}$ and $t_2 = \frac{1}{q_2\ \delta^2_{s,r}} + \frac{1}{q_1\ \delta^2_{r,d}}$. The CDF and PDF of β_{max} can be written as

$$\begin{aligned} P_{\beta_{max}}(\beta) &= \left(1 - \frac{\beta}{t_1}\ \exp(-\frac{t_2}{2}\ \beta)\ K_1(\frac{\beta}{t_1})\right)^N \\ \text{and}\ \ p_{\beta_{max}}(\beta) &= N\ \left(1 - \frac{\beta}{t_1}\ \exp(-\frac{t_2}{2}\ \beta)\ K_1(\frac{\beta}{t_1})\right)^{N-1}\ p_{\beta_m}(\beta)\ , \end{aligned} \quad (2.16)$$

respectively, where $p_{\beta_m}(.)$ is the PDF of β_m (2.6) and it is given by

$$p_{\beta_m}(\beta_m) = \frac{\beta_m}{2\ t_1^2}\ \exp(-\frac{t_2}{2}\ \beta_m)\ \left(t_1\ t_2\ K_1(\frac{\beta_m}{t_1}) + 2\ K_0(\frac{\beta_m}{t_1})\right)\ U(\beta_m) \quad (2.17)$$

The probability of the direct-transmission mode can be obtained as follows.

$$\begin{aligned} & Pr(\phi) = Pr(\beta_{s,d} \geq \alpha\ \beta_{max}) = \int_0^\infty P_{\beta_{max}}(\frac{\beta_{s,d}}{\alpha})\ p_{\beta_{s,d}}(\beta_{s,d})\ d\beta_{s,d} \\ = & \sum_{n=0}^{N} \binom{N}{n} (-1)^n \frac{1}{(\alpha t_1)^n \delta^2_{s,d}} \int_0^\infty \beta^n_{s,d}\ \exp\left(-(\frac{1}{\delta^2_{s,d}} + \frac{t_2\ n}{2\alpha})\ \beta_{s,d}\right) \left(K_1(\frac{\beta_{s,d}}{\alpha t_1})\right)^n d\beta_{s,d}. \\ \approx & \sum_{n=0}^{N} \binom{N}{n} (-1)^n \frac{2\alpha}{2\alpha + t_2\ \delta^2_{s,d}\ n}\ , \end{aligned} \quad (2.18)$$

where we approximated $K_1(.)$ as in (2.15) and $\beta_{s,d}$ is an exponential random variable with parameter $1/\delta^2_{s,d}$. The probability of the relay-cooperation mode is $Pr(\phi^c) = 1 - Pr(\phi)$. Since the bandwidth efficiency of the direct-transmission mode is 1 SPCU, and that of the relay-cooperation mode is 1/2 SPCU, thus the average bandwidth efficiency can be written as

$$R = Pr(\phi) + \frac{1}{2}\ Pr(\phi^c)\ . \quad (2.19)$$

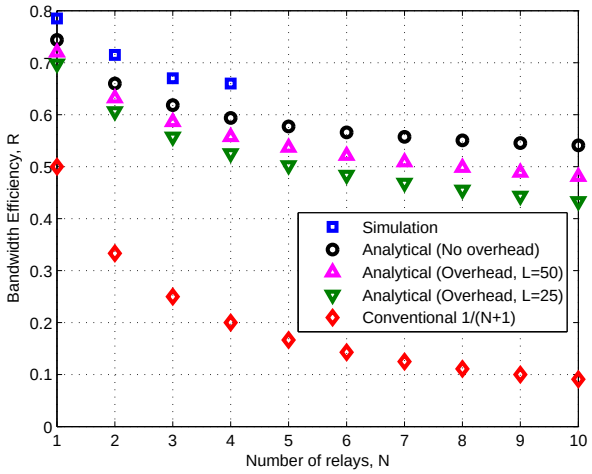

Figure 2.3: Bandwidth efficiency dependence on the number of relays with QPSK modulation and unity channel variances, $\alpha = 1$, and $r = 0.5$.

Thus, the bandwidth efficiency of the multi-node relay-selection decode-and-forward symmetric cooperative scenario, employing N relays, is approximated as

$$R \approx \frac{1}{2} \cdot \left(1 + \sum_{n=0}^{N} \binom{N}{n} (-1)^n \frac{2\alpha}{2\alpha + \left(\frac{1-r}{B\,\delta_{s,r}^2} + \frac{r}{A^2\,\delta_{r,d}^2} \right) r\,\delta_{s,d}^2\,n} \right) \quad SPCU\ . \quad (2.20)$$

Figure 2.3 depicts the bandwidth efficiency of the relay-selection assuming $\alpha = 1$ and $r = 0.5$ and the conventional cooperative schemes for different number of relays and unity channel variances. It is clear that the bandwidth efficiency decreases down to 0.5 as N increases, because the probability of the direct-transmission mode decreases down to 0 as N goes to ∞. Intuitively, increasing the number of relays increases the probability of having the optimal relay's metric higher than the source-destination channel gain. Furthermore, we plot the simulated bandwidth efficiency results for the proposed relay selection algorithm. Also, we plot the bandwidth efficiency of the conventional cooperative scheme, $R_{conv} = \frac{1}{N+1}$ SPCU, to show the significant increase in the bandwidth efficiency of the proposed relay-selection cooperative scenario over the conventional cooperative

scheme.

We address the system overhead issue as follows. Particularly, we compute the bandwidth efficiency of the proposed scheme taking into consideration the overhead. We assume slow fading channels, where the channels are constant during a transmission block (channel coherence time) and may vary from a block to another. For moderate to high data rate the block length L, measured in terms of the number of transmitted data symbols during the channel coherence time, can be relatively large. We assume that the feedback channel is an orthogonal channel. Each relay sends a quantized version of the harmonic mean function to the source. For simplicity, we assume that it uses the same modulation order (M-PSK) as that of the original data. For slowly varying channels, we expect that the change in each relay's metric will be relatively small across each two consecutive blocks. In this case, it is more reasonable to modulate the difference in the relays' metrics rather than the absolute values. This helps in having a small quantization error and the performance can be very close to the one without quantization. Thus, the overhead for each block is $N+1$ symbols, where N symbols are transmitted from the N relays and the last symbol is sent from the source to indicate whether to cooperate or not and which relay to cooperate with in case of cooperation.

Taking the overhead into consideration the bandwidth efficiency, given previously in (2.19), can be recalculated as

$$R_{overhead} = \frac{L}{L+(N+1)} Pr(\phi) + \frac{L}{2\,L+(N+1)} Pr(\phi^c) , \qquad (2.21)$$

where $Pr(\phi)$ is the direct transmission probability. Figure 2.3 depicts the effect of the overhead on the bandwidth efficiency for different block lengths. For moderate block length, $L = 25$, and $N = 3$ relays the bandwidth efficiency is 0.56, while it is 1/4 for the conventional scheme. Hence, an increase of 124% is achieved by our

proposed algorithm.

An alternative protocol to send the feedback information can be explained as follows. As we mentioned, we assume slow fading channel that can be statistically modeled. For instance, we assume that the channel follows Jakes Rayleigh fading model. The Jakes tap gain process is stationary and can be modeled as an auto-regressive (AR) model. Thus, each relay can send the AR coefficients representing its relay-destination channels to the source. The source utilizes these parameters to predict the relay-destination channel for each relay. Obviously, these AR coefficients are sent at the start of the transmission. This reduces the overhead significantly compared to the scheme explained above. In order to reduce the prediction error, each relay updates the source with its current instantaneous relay-destination channel with a period that lasts for a certain number of transmission blocks that depends on how slow the channel varies. Assuming a TDD system, the source can estimate its source-relay channel with each relay with no extra cost as follows. In the conventional scheme, it is assumed that each relay broadcasts a pilot signal so that the destination can estimate the relay-destination channel. The destination utilizes the estimated relay-destination channel in order to decode the signal received from each relay. So, the source can make use of these pilots too to estimate its source-relay channels. Then, the source computes all the relays metrics based on the estimated source-relay channels and the predicted relay-destination channels. It determines the optimal relay and decides whether to cooperate with it or not based on its source-destination channel gain.

2.2.2 SER Analysis and Upper Bound

In order to prove full diversity order for our proposed scheme, we make use of the following lemma.

Lemma 1 *For any x, y, and N*

$$\sum_{n=0}^{N} \binom{N}{n} \; (-1)^n \; \frac{1}{x + n\, y} = \frac{(N)!\; y^N}{\prod_{n=0}^{N}(x + n\, y)} \; . \tag{2.22}$$

Proof of Lemma 1 is given in the Appendix.

The probability of symbol error, or SER, is defined as

$$Pr(e) = Pr(e/\phi) \cdot Pr(\phi) + Pr(e/\phi^c) \cdot Pr(\phi^c) \; , \tag{2.23}$$

where $Pr(e/\phi) \cdot Pr(\phi)$ represents the SER of the direct-transmission mode and $Pr(e/\phi^c) \cdot Pr(\phi^c)$ represents the relay-cooperation mode SER. The SER of the direct-transmission mode can be calculated as follows. First, the instantaneous direct-transmission SNR is $\gamma^{\phi} = \frac{P\, \beta_{s,d}}{N_0}$. The conditional direct-transmission SER can be written, as given in [41], as

$$Pr(e/\phi, \beta_{s,d}) = \Psi(\gamma^{\phi}) = \frac{1}{\pi} \int_0^{\frac{(M-1)\pi}{M}} \exp(-\frac{b\, \gamma^{\phi}}{\sin^2 \theta}) \; d\theta \; , \tag{2.24}$$

where $b = \sin^2(\pi/M)$. Thus, the SER of the direct-transmission is calculated as

$$\begin{aligned} Pr(e/\phi)\; Pr(\phi) &= \int_0^{\infty} Pr(e/\phi, \beta_{s,d})\; Pr(\phi/\beta_{s,d}) \;\cdot p_{\beta_{s,d}}(\beta_{s,d})\; d\beta_{s,d} \\ &\approx \sum_{n=0}^{N} \binom{N}{n} (-1)^n F_1\big(1 + \frac{t_2\; \delta_{s,d}^2\; n}{2\alpha} + \frac{b\; P}{N_0\; \sin^2 \theta}\; \delta_{s,d}^2\big) \; , \end{aligned} \tag{2.25}$$

where we applied the approximation in (2.15) and $F_1\big(x(\theta)\big) = \frac{1}{\pi} \int_0^{\frac{(M-1)\pi}{M}} \frac{1}{x(\theta)} \; d\theta$.

For the relay-cooperation mode, maximal-ratio combining (MRC) [8] is applied at the destination. The output of the MRC [8] can be written as

$$y^{\phi^c} = \frac{\sqrt{P_1}\ h^*_{s,d}}{N_0}\ y^{\phi^c}_{s,d} + \frac{\sqrt{\widetilde{P_2}}\ h^*_{r,d}}{N_0}\ y^{\phi^c}_{r,d}\ , \tag{2.26}$$

and the instantaneous SNR of the MRC output is given by $\gamma^{\phi^c} = \frac{P_1\beta_{s,d}+\widetilde{P_2}\beta_{r,d}}{N_0}$. Taking into account the two scenarios of $\widetilde{P_2} = 0$ and $\widetilde{P_2} = P_2$, the conditional SER of the relay-cooperation mode is given, as in [7], as

$$\begin{aligned} Pr(e/\phi^c, \beta_{s,d}, \beta_{s,r}, \beta_{r,d}) = \Psi(\gamma^{\phi^c})|_{\widetilde{P_2}=0}\ \Psi(\frac{P_1\beta_{s,r}}{N_0}) \\ + \Psi(\gamma^{\phi^c})|_{\widetilde{P_2}=P_2}\ \left(1 - \Psi(\frac{P_1\beta_{s,r}}{N_0})\right)\ . \end{aligned} \tag{2.27}$$

Let $Pr(A/\phi^c, \beta_{s,d}, \beta_{s,r}, \beta_{r,d}) = \Psi(\gamma^{\phi^c})\Psi(\frac{P_1\beta_{s,r}}{N_0})$ and $Pr(B/\phi^c, \underline{\beta}) = \Psi(\gamma^{\phi^c})$. Since,

$$\begin{aligned} Pr(A/\phi^c, \beta_{s,d}, \beta_{s,r}, \beta_{r,d}) &= \frac{1}{\pi}\int_{\theta_1=0}^{\frac{(M-1)\pi}{M}} \exp\big(-\frac{b\ P_1}{N_0\ \sin^2\theta_1}\ \beta_{s,d}\big) \\ &\times \exp\big(-\frac{b\ \widetilde{P_2}}{N_0\ \sin^2\theta_1}\ \beta_{r,d}\big)\ d\theta_1 \\ &\times \frac{1}{\pi}\int_{\theta_2=0}^{\frac{(M-1)\pi}{M}} \exp\big(-\frac{b\ P_1}{N_0 \sin^2\theta_2}\ \beta_{s,r}\big)\ d\theta_2\ , \end{aligned} \tag{2.28}$$

thus,

$$Pr(A/\phi^c)\ Pr(\phi^c) = \int_{\underline{\beta}} Pr(A/\phi^c, \underline{\beta})\ Pr(\phi^c/\underline{\beta})\ p_{\underline{\beta}}(\underline{\beta})\ d\underline{\beta}\ , \tag{2.29}$$

where $\underline{\beta} \triangleq [\beta_{s,d},\ \beta_{s,r},\ \beta_{r,d}]$. Furthermore,

$$Pr(\phi^c/\underline{\beta}) = Pr(\beta_{s,d} < \alpha\beta_{max}/\beta_{s,d}, \beta_{s,r}, \beta_{r,d}) = U(\alpha\beta_{max} - \beta_{s,d})\ , \tag{2.30}$$

where $U(.)$ is the unit step function. Substituting (2.28) and (2.30) into (2.29), we get

$$\begin{aligned} Pr(A/\phi^c)\ Pr(\phi^c) &= \int_{\underline{\beta}} \frac{1}{\pi^2} \int_{\theta_1=0}^{\frac{(M-1)\pi}{M}} \int_{\theta_2=0}^{\frac{(M-1)\pi}{M}} \exp\big(-P_1\ C(\theta_1)\ \beta_{s,d}\big) \\ &\times \exp\big(-\widetilde{P}_2\ C(\theta_1)\ \beta_{r,d}\big) \exp\big(-P_1\ C(\theta_2)\ \beta_{s,r}\big) \\ &\times U(\alpha\beta_{max} - \beta_{s,d})\ p_{\underline{\beta}}(\underline{\beta})\ d\theta_2\ d\theta_1\ d\underline{\beta}\ , \end{aligned} \tag{2.31}$$

where $C(\theta) = \frac{b}{N_0 \sin^2\theta}$. Since $\beta_{s,d}$, $\beta_{s,r}$, and $\beta_{r,d}$ are statistically independent, thus

$$p_{\underline{\beta}}(\underline{\beta}) = p_{\beta_{s,d}}(\beta_{s,d})\ p_{\beta_{s,r}}(\beta_{s,r})\ p_{\beta_{r,d}}(\beta_{r,d}) = p_{\beta_{s,d}}(\beta_{s,d})\ p_{\underline{\widetilde{\beta}}}(\underline{\widetilde{\beta}})\ \ , \tag{2.32}$$

where $\underline{\widetilde{\beta}} \triangleq [\beta_{s,r},\ \beta_{r,d}]$. Integrating (2.31) with respect to $\beta_{s,d}$, we get

$$\begin{aligned} Pr(A/\phi^c)Pr(\phi^c) = \int_{\underline{\widetilde{\beta}}} \frac{1}{\pi^2} \int_{\theta_1=0}^{\frac{(M-1)\pi}{M}} \int_{\theta_2=0}^{\frac{(M-1)\pi}{M}} & \frac{p_{\underline{\widetilde{\beta}}}(\underline{\widetilde{\beta}})}{1 + P_1\ C(\theta_1)\delta_{s,d}^2} \\ \times \bigg(1 - \exp\Big(-\big(P_1 C(\theta_1) + \frac{1}{\delta_{s,d}^2}\big)\alpha\beta_{max}\Big)\bigg) & \\ \times \exp\Big(-\big(\widetilde{P}_2 C(\theta_1)\beta_{r,d} + P_1 C(\theta_2)\beta_{s,r}\big)\Big) & d\theta_2\, d\theta_1\, d\underline{\widetilde{\beta}}, \end{aligned} \tag{2.33}$$

It is difficult to get an exact expression of (2.33) for β_{max} defined in (2.8). Thus, we obtain an upper bound via a worst-case scenario. We replace $\beta_{s,r}$ and $\beta_{r,d}$ in (2.33) by their worst-cast values in terms of β_{max}. Then, we average (2.33) over β_{max} only. Since $\beta_{max} = \mu_H(q_1\ \beta_{r,d}, q_2\ \beta_{s,r})$, we can write $\frac{1}{\beta_{max}} = \frac{1}{2\ q_2\ \beta_{s,r}} + \frac{1}{2\ q_1\ \beta_{r,d}}$. Then, we replace $\beta_{s,r}$ and $\beta_{r,d}$ by their worst values in terms of β_{max} as $\beta_{s,r} \longrightarrow \frac{\beta_{max}}{2\ q_2}$ and $\beta_{r,d} \longrightarrow \frac{\beta_{max}}{2\ q_1}$. Thus, (2.33) can be upper bounded as

$$\begin{aligned} Pr(A/\phi^c)Pr(\phi^c) \leq \frac{1}{\pi^2} \int_{\theta_1=0}^{\frac{(M-1)\pi}{M}} & \frac{d\theta_1}{1 + P_1\ C(\theta_1)\delta_{s,d}^2} \\ \int_{\theta_2=0}^{\frac{(M-1)\pi}{M}} & \bigg(M_{\beta_{max}}\Big(\frac{\widetilde{P_2}\ C(\theta_1)}{2\ q_1} + \frac{P_1\ C(\theta_2)}{2\ q_2}\Big) - \\ & M_{\beta_{max}}\Big(\big(P_1 C(\theta_1) + \frac{1}{\delta_{s,d}^2}\big)\alpha + \frac{\widetilde{P_2} C(\theta_1)}{2\ q_1} + \frac{P_1 C(\theta_2)}{2\ q_2}\Big)\bigg) d\theta_2, \end{aligned} \tag{2.34}$$

where $M_{\beta_{max}}(.)$ is the moment generation function (MGF) of β_{max} and it can be approximated as

$$M_{\beta_{max}}(\gamma) \approx N \sum_{n=0}^{N-1} \binom{N-1}{n} \ (-1)^n \ M_{\beta_m}(\gamma + \frac{n \ t_2}{2}) \ , \tag{2.35}$$

where we have applied (2.15) and $M_{\beta_m}(.)$ is the MGF of β_m. It was shown in [39] that for two independent exponential random variables with parameters λ_1 and λ_2, the MGF of their harmonic mean function is written as

$$\begin{aligned} M_{\beta_m}(\gamma) = E_{\beta_m}\big(\exp(-\gamma \ \beta_m)\big) = \frac{16 \ \lambda_1 \ \lambda_2}{3 \ (\lambda_1 + \lambda_2 + 2 \ \sqrt{\lambda_1 \ \lambda_2} + \gamma)^2} \\ \times \Big(\frac{4(\lambda_1 + \lambda_2)_2 F_1\big(3, \frac{3}{2}; \frac{5}{2}; \frac{\lambda_1+\lambda_2-2 \ \sqrt{\lambda_1 \ \lambda_2}+\gamma}{\lambda_1+\lambda_2+2\sqrt{\lambda_1 \ \lambda_2}+\gamma}\big)}{(\lambda_1 + \lambda_2 + 2\sqrt{\lambda_1 \lambda_2} + \gamma)} \\ +_2 F_1\big(2, \frac{1}{2}; \frac{5}{2}; \frac{\lambda_1 + \lambda_2 - 2 \ \sqrt{\lambda_1 \ \lambda_2} + \gamma}{\lambda_1 + \lambda_2 + 2 \ \sqrt{\lambda_1 \ \lambda_2} + \gamma}\big)\Big), \end{aligned} \tag{2.36}$$

where $E_{\beta_m}(.)$ represents the statistical average with respect to β_m and ${}_2F_1(.,.;.;.)$ is the Gauss' hypergeometric function defined in [[40], (15.1.1)]. Following similar steps as done in (2.28)-(2.34), we get

$$\begin{aligned} &Pr(B/\phi^c) \ Pr(\phi^c) \leq \\ &\frac{1}{\pi} \int_{\theta=0}^{\frac{(M-1)\pi}{M}} \left(\frac{M_{\beta_{max}}\Big(\frac{\widetilde{P_2} \ C(\theta)}{2 \ q_1}\Big)}{1 + P_1 \ C(\theta)\delta_{s,d}^2} - \frac{M_{\beta_{max}}\Big(\big(P_1 \ C(\theta) + \frac{1}{\delta_{s,d}^2}\big)\alpha + \frac{\widetilde{P_2} \ C(\theta)}{2 \ q_1}\Big)}{1 + P_1 \ C(\theta)\delta_{s,d}^2} \right) d\theta. \end{aligned} \tag{2.37}$$

The unconditional SER of the relay-cooperation mode can be written from (2.27) as

$$\begin{aligned} Pr(e/\phi^c) \ Pr(\phi^c) = Pr(A/\phi^c) \ Pr(\phi^c)|_{\widetilde{P_2}=0} - Pr(A/\phi^c) \ Pr(\phi^c)|_{\widetilde{P_2}=P_2} \\ + Pr(B/\phi^c) \ Pr(\phi^c)|_{\widetilde{P_2}=P_2} \ . \end{aligned} \tag{2.38}$$

Since $Pr(A/\phi^c) \ Pr(\phi^c)|_{\widetilde{P_2}=P_2}$ in (2.33) is a positive value, therefore an upper bound on the SER of the relay-cooperation mode can be obtained by removing this term

from (2.38). Moreover, we can remove the subtracted terms in (2.34) and (2.37). Therefore, an upper bound on the total SER can be obtained by adding (2.25), (2.34), and (2.37), after removing the subtracted terms, as

$$\begin{aligned} Pr(e) \leq N! \Big(\frac{t_2 \delta_{s,d}^2}{2\alpha}\Big)^N F_1 \left(\prod_{n=0}^{N} \big(1 + \frac{t_2\ \delta_{s,d}^2\ n}{2\alpha} + \frac{b\ P\ \delta_{s,d}^2}{N_0\ sin^2\theta}\big) \right) \\ + \sum_{n=0}^{N-1} \binom{N-1}{n} \frac{(-1)^n}{\pi} \int_{\theta_1=0}^{\frac{(M-1)\pi}{M}} \left(\frac{M_{\beta_m}\left(\frac{b\ P_2}{2\ q_1\ N_0\ \sin^2\theta_1} + \frac{n\ t_2}{2}\right)}{1 + \frac{b\ P_1\ \delta_{s,d}^2}{N_0\ \sin^2\theta_1}} + \right. \\ \left. \frac{\frac{1}{\pi}\int_{\theta_2=0}^{\frac{(M-1)\pi}{M}} M_{\beta_m}\left(\frac{b\ P_1}{2\ q_2\ N_0\ \sin^2\theta_2} + \frac{n\ t_2}{2}\right) d\theta_2}{1 + \frac{b\ P_1\ \delta_{s,d}^2}{N_0\ \sin^2\theta_1}} \right) d\theta_1 \ , \end{aligned} \tag{2.39}$$

where we applied Lemma 1 for the direct-transmission SER in (2.25).

In order to show that full diversity order is achieved, we derive an upper bound on the SER performance at high SNR. At high SNR, we neglect the terms 1 and $(1 + \frac{t_2\ \delta_{s,d}^2\ n}{2\alpha})$ in (2.39). Thus, the SER upper bound is written as

$$\begin{aligned} Pr(e) \leq N!\ \left(\frac{t_2\ \delta_{s,d}^2}{2\alpha}\right)^N\ F_1\left(\big(\frac{b\ P}{N_0\ sin^2\theta}\ \delta_{s,d}^2\big)^{N+1} \right) \\ + \sum_{n=0}^{N-1} \binom{N-1}{n}\ (-1)^n\ \frac{1}{\pi} \int_{\theta_1=0}^{\frac{(M-1)\pi}{M}} \frac{N_0\ \sin^2\theta_1}{b\ P_1\ \delta_{s,d}^2} \Big(M_{\beta_m}\big(\frac{b\ P_2}{2\ q_1\ N_0\ \sin^2\theta_1} + \frac{n\ t_2}{2}\big) \\ + \frac{1}{\pi} \int_{\theta_2=0}^{\frac{(M-1)\pi}{M}} M_{\beta_m}\big(\frac{b\ P_1}{2\ q_2\ N_0\ \sin^2\theta_2} + \frac{n\ t_2}{2}\big) d\theta_2 \Big) d\theta_1 \end{aligned} \tag{2.40}$$

The SER upper bound expression in (2.40) is in terms of the MGF $M_{\beta_m}(.)$, which is mathematically intractable. In [7], the authors have presented an approximation to the MGF of two independent exponential random variables at high enough SNR as

$$M_{\beta_m}(\gamma) \approx \frac{q_1\ \delta_{r,d}^2 + q_2\ \delta_{s,r}^2}{2\ \gamma}\ . \tag{2.41}$$

Using the MGF approximation given in (2.41) and Lemma 1, we obtain

$$
\begin{aligned}
Pr(e) \leq\ & N!\,(\frac{N_0}{b\,P})^{N+1}(\frac{t_2}{2\alpha})^{N}\ \frac{I(2N+2)}{\delta_{s,d}^2} \\
& + N!\ t_2^{N-1}\ (q_1\ \delta_{r,d}^2 + q_2\ \delta_{s,r}^2)\frac{1}{\pi}\int_{\theta_1=0}^{\frac{(M-1)\pi}{M}}\ \frac{N_0\ \sin^2\theta_1}{b\ P_1\ \delta_{s,d}^2}\Big(\ \frac{1}{\prod_{n=0}^{N-1}(\frac{b\ P_2}{q_1\ N_0\ \sin^2\theta_1}+n\ t_2)} \\
& + \frac{1}{\pi}\int_{\theta_2=0}^{\frac{(M-1)\pi}{M}}\ \frac{1}{\prod_{n=0}^{N-1}(\frac{b\ P_1}{q_2\ N_0\ \sin^2\theta_2}+n\ t_2)}\ d\theta_2\Big)d\theta_1\ ,
\end{aligned}
\tag{2.42}
$$

where

$$
I(p) = \frac{1}{\pi}\int_{\theta=0}^{\frac{(M-1)\pi}{M}}\ \sin^p\theta\ d\theta\ . \tag{2.43}
$$

Neglecting the term $(n\ t_2)$ at high SNR, we get

$$
\begin{aligned}
Pr(e)\ \ &\leq\ \ N!\,(\frac{N_0}{b\,P})^{N+1}(\frac{t_2}{2\alpha})^{N}\ \frac{I(2N+2)}{\delta_{s,d}^2} + N!(\frac{N_0}{b})^{N+1}\ t_2^{N-1}\ \frac{(q_1\ \delta_{r,d}^2 + q_2\ \delta_{s,r}^2)}{P_1\ \delta_{s,d}^2} \\
&\times\ \ \left(\ \left(\frac{q_1}{P_2}\right)^N\ I(2\ N+2) + \left(\frac{q_2}{P_1}\right)^N\ A\ I(2\ N)\right)\ .
\end{aligned}
\tag{2.44}
$$

Replacing $q_1 = \frac{A^2}{r^2}$, $q_2 = \frac{B}{r\,(1-r)}$, and $t_2 = \frac{1}{q_2\ \delta_{s,r}^2} + \frac{1}{q_1\ \delta_{r,d}^2}$, and using $P_1 = r\ P$ and $P_2 = (1-r)\ P$, we get the following result. At high SNR $\gamma = \frac{P}{N_0}$, the SER of the multi-node relay-selection decode-and-forward symmetric cooperative scenario, utilizing N relays, is upper bounded by

$$
Pr(e)\ \ \leq\ \ (CG\cdot\gamma)^{-(N+1)}\ , \tag{2.45}
$$

where

$$
\begin{aligned}
CG = & \left(\frac{N!\ (\frac{r(1-r)}{B\ \delta_{s,r}^2}+\frac{r^2}{A^2\ \delta_{r,d}^2})^{N-1}}{b^{N+1}\ \delta_{s,d}^2}\ \right)^{-\frac{1}{(N+1)}}\ \left(\frac{(\frac{r(1-r)}{B\ \delta_{s,r}^2}+\frac{r^2}{A^2\ \delta_{r,d}^2})\ I(2\ N+2)}{(2\ \alpha)^N}\right. \\
& \left. + \frac{\left(\frac{A^2\delta_{r,d}^2}{r^2}+\frac{B\delta_{s,r}^2}{r(1-r)}\right)\left(A^{2N}\ I(2\ N+2) + B^N\ A\ I(2\ N)\right)}{r^{N+1}\ (1-r)^N}\right)^{-\frac{1}{(N+1)}}\ .
\end{aligned}
\tag{2.46}
$$

As defined earlier, the diversity order is $d = -\lim_{\gamma\longrightarrow\infty}\log(Pr(e))/\log(\gamma)$. By substituting (2.44), the diversity order of the proposed algorithm is $N+1$.

2.2.3 Single-relay Scenario: When to Cooperate?

In the conventional single-relay decode-and-forward cooperative scheme, one symbol is sent each two time slots. Hence, the bandwidth efficiency is 0.5 SPCU. In the single-relay scenario, it is meaningful to consider only the question: *"When to cooperate?"*, as only one relay is available. Based on the general multi-node scheme described in Section 2.1.3, the proposed single-relay scheme is described as follows.

First, the relay calculates the scaled harmonic mean function of its source-relay and relay-destination instantaneous channel gains (2.7), then sends it to the source. The source decides when to cooperate by taking the ratio between the source-destination channel gain and the relay's metric and comparing it to the cooperation threshold. If this ratio is greater than or equal to the cooperation threshold, then the source sends its information to the destination directly without the need for the relay. Otherwise, the source employs the relay in forwarding its information to the destination as in the conventional cooperative scheme. The source broadcasts its decision before the start of the data transmission.

We calculate the bandwidth efficiency and the SER of the proposed single-relay scheme as follows. By substituting $N = 1$ in (2.20), the bandwidth efficiency of the relay-selection decode-and-forward cooperative scenario, utilizing single relay, can be approximated as

$$R \approx \frac{\alpha + (\frac{1-r}{B\,\delta^2_{s,r}} + \frac{r}{A^2\,\delta^2_{r,d}})\; r\,\delta^2_{s,d}}{2\alpha + (\frac{1-r}{B\,\delta^2_{s,r}} + \frac{r}{A^2\,\delta^2_{r,d}})\; r\,\delta^2_{s,d}} \quad SPCU. \tag{2.47}$$

It is clear that the bandwidth efficiency is $R \geq 0.5$. By substituting $N = 1$ in (2.44), the SER of the single-relay relay-selection decode-and-forward cooperative scheme is upper bounded as $Pr(e) \leq (CG{\cdot}\gamma)^{-2}$, where CG denotes the cooperation

gain and is equal to

$$CG = \sqrt{\frac{b^2\ \delta_{s,d}^2}{B\left(\frac{\frac{r(1-r)}{B\ \delta_{s,r}^2}+\frac{r^2}{A^2\ \delta_{r,d}^2}}{2\ \alpha}+\frac{2\ A^2\ \left(\frac{A^2\ \delta_{r,d}^2}{r^2}+\frac{B\ \delta_{s,r}^2}{r(1-r)}\right)}{r^2\ (1-r)}\right)}}\ . \tag{2.48}$$

Note that $I(2) = \frac{1}{\pi}\int_0^{\frac{(M-1)\pi}{M}} \sin^2\theta\ d\theta = A$ and $\frac{1}{\pi}\int_0^{\frac{(M-1)\pi}{M}} \sin^4\theta\ d\theta = B$ as defined in (2.2).

In this section, we have obtained the approximate bandwidth efficiency expression and the SER upper bound. We showed a significant increase in the bandwidth efficiency over the conventional cooperative scheme. Furthermore, we proved that full diversity order is guaranteed if $\alpha > 0$. In the next section, we show how to choose optimum values for the cooperation threshold and the power ratio to maximize the system performance.

2.3 Power Allocation and Cooperation Threshold

In this section, an analytical expression of the optimum power allocation is derived, and bandwidth efficiency-SER tradeoff curves are shown to obtain the cooperation threshold. We clarify that as the cooperation threshold α increases, the probability of choosing the relay-cooperation mode increases. Therefore, the bandwidth efficiency and the SER, given by (2.20) and (2.44), respectively, decrease monotonically with α. In addition, the bandwidth efficiency is a monotonically increasing or decreasing function of the power ratio $r = P_1/P$, depending on the channel variances. On the contrary, there exists an optimum power ratio r^*, which minimizes the SER. We determine the optimum power allocation as follows.

In the direct-transmission mode, all the power is transmitted through the source-destination channel. In the relay-cooperation mode, we determine the optimum powers P_1 and P_2 which minimize the SER upper bound expression in (2.44) subject to constraint $P_1 + P_2 = P$. Substituting (2.5) into (2.44), we can approximate[2] the optimization problem as

$$\begin{aligned} \min_{P_1} \; & \left(\frac{A^2\ \delta_{r,d}^2}{r^2\ P_1} + \frac{B\ \delta_{s,r}^2}{r\ (1-r)\ P_1}\right)\left(\left(\frac{A^2}{r^2\ P_2}\right)^N\ I(2\ N+2)\right. \\ & \left. + \left(\frac{B}{r\ (1-r)\ P_1}\right)^N\ A\ I(2\ N)\right) \\ & s.t.\ \ P_1 + P_2 = P\ . \end{aligned} \tag{2.49}$$

By substituting $r = P_1/P$ into (2.49), we get

$$\begin{aligned} \min_{P_1} \; & \frac{\left(A^{2N+2}\ I(2\ N+2) + A^3\ B^N\ I(2\ N)\right)\delta_{r,d}^2}{P_1^{2\,N+3}\ P_2^N} \\ & + \frac{\left(A^{2N}\ B\ I(2\ N+2) + A\ B^{N+1}\ I(2\ N)\right)\delta_{s,r}^2}{P_1^{2\,N+2}\ P_2^{N+1}} \\ & s.t.\ \ P_1 + P_2 = P\ . \end{aligned} \tag{2.50}$$

Solving (2.50) using the standard lagrangian method results in the following result. The optimum power allocation of the multi-node relay-selection decode-and-forward symmetric cooperative scenario, employing N relays, is obtained as

$$\begin{aligned} P_1 &= \frac{1 - \frac{N\ X_1}{2\,(N+1)\ X_2} + \sqrt{1 + \frac{(N+3)\ X_1}{(N+1)\ X_2} + (\frac{N\ X_1}{2\,(N+1)\ X_2})^2}}{2 - \frac{N\ X_1}{2\,(N+1)\ X_2} + \sqrt{1 + \frac{(N+3)\ X_1}{(N+1)\ X_2} + (\frac{N\ X_1}{2\,(N+1)\ X_2})^2}}\ P\ , \\ P_2 &= \frac{1}{2 - \frac{N\ X_1}{2\,(N+1)\ X_2} + \sqrt{1 + \frac{(N+3)\ X_1}{(N+1)\ X_2} + (\frac{N\ X_1}{2\,(N+1)\ X_2})^2}}\ P\ , \end{aligned} \tag{2.51}$$

[2]It can be shown that this approximation has a very minor effect on the value of the optimum power ratio.

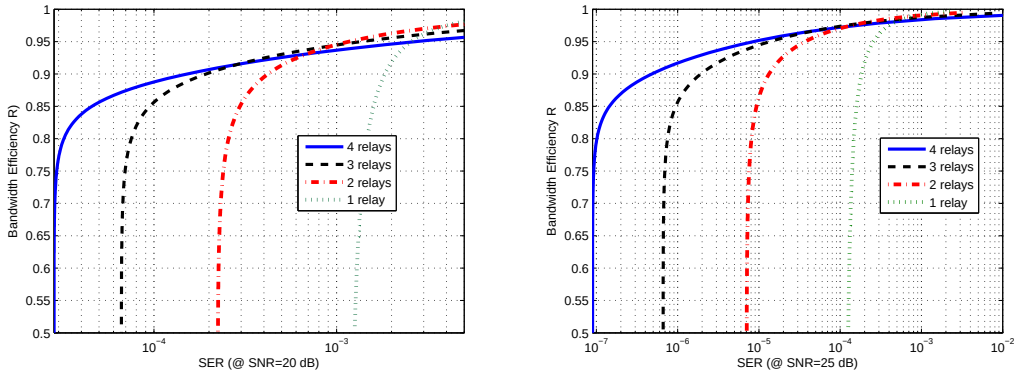

(a) (b)

Figure 2.4: Bandwidth efficiency versus SER at (a) SNR=20 dB, (b) SNR=25 dB.

where

$$\begin{aligned} X_1 &= \left(A^{2N+2}\, I(2\,N+2) + A^3\, B^N\, I(2\,N)\right) \delta_{r,d}^2\,, \\ X_2 &= \left(A^{2N}\, B\, I(2\,N+2) + A\, B^{N+1}\, I(2\,N)\right) \delta_{s,r}^2\,. \end{aligned} \tag{2.52}$$

It is shown in (2.51) that the optimum power allocation does not depend on the source-destination channel variance. It depends basically on the modulation order M and the source-relay and relay-destination channel variances. If $\delta_{r,d}^2 \gg \delta_{s,r}^2$ then P_1 goes to P and P_2 goes to zero. Intuitively, this is because the source-relay link is of bad quality. Thus, it is reasonable to send the total power through the source-destination channel. In addition, if $\delta_{s,r}^2 \gg \delta_{r,d}^2$ then P_1 goes to $P/2$ and P_2 goes to $P/2$ as well, which is expected because if the source-relay channel is so good, then the symbols will be received correctly by the relay with high probability. Thus, the relay will be almost the same as the source, thus both source and relay share the power equally.

The obtained optimum power ratio will be used to get the cooperation threshold as follows. Figure 2.4 depicts the bandwidth efficiency-SER tradeoff curves for

$\delta^2_{s,d}$	$\delta^2_{s,r}$	$\delta^2_{r,d}$	$r = P_1/P$	α	Bandwidth Efficiency (R)	Coop. Gain (CG)
1	1	1	0.6902	0.55	0.8624	0.247
1	1	10	0.7487	0.09	0.9075	0.1613
1	10	1	0.6697	0.14	0.9443	0.0939

Table 2.1: Single-relay optimum values using the $(CG \cdot R)$ optimization criterion.

different number of relays at SNR equal to 20 dB and 25 dB. This tradeoff is the achievable bandwidth efficiency and SER for different values of cooperation threshold. At a certain SER value, the maximum achievable bandwidth efficiency while guaranteeing full diversity order, can be obtained through Figure 2.4. In Figure 2.4, it is shown that the tradeoff achieved using four relays is the best among the plotted curves at low SER region. Moreover, it is clear in Figure 2.4 (a) that the SER is almost constant at $2\text{x}10^{-5}$ while the bandwidth efficiency increases from 0.5 to 0.8 SPCU for four relays. Thus, about 60% increase in the bandwidth efficiency can be achieved with the same SER performance.

We consider three different channel-variances cases for the single-relay case as follows. Case 1 which corresponds to the unity channel variances, where $\delta^2_{s,d} = \delta^2_{s,r} = \delta^2_{r,d} = 1$ and it is represented at the first row of Table 2.1. Case 2 expresses a stronger relay-destination channel $\delta^2_{r,d} = 10$, while case 3 expresses a stronger source-relay channel $\delta^2_{s,r} = 10$. Cases 2 and 3 are represented at the second and third rows of Table 2.1, respectively. Table 2.1 shows the optimum values of the power allocation ratio (2.51) for the three cases. Since we aim at maximizing both the cooperation gain and the bandwidth efficiency, we choose- as an *example*- an optimization metric, which is the product of the cooperation gain and bandwidth efficiency, to find the cooperation threshold. This optimization metric can

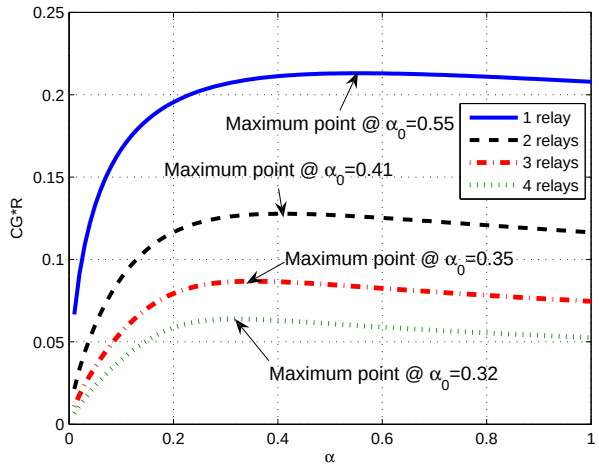

Figure 2.5: Cooperation thresholds for different number of relays with unity channel variances.

be written as

$$\max_{\alpha} \;\; CG(\alpha) \cdot R(\alpha) \;, \tag{2.53}$$

where R and CG are obtained from (2.20) and (2.46), respectively.

The cooperation threshold for the three different cases defined above are $\alpha_o = 0.55$, $\alpha_o = 0.09$, and $\alpha_o = 0.14$, respectively. These values of cooperation thresholds result in bandwidth efficiencies equal to $R_o = 0.8624$, $R_o = 0.9075$, and $R_o = 0.9443$ SPCU, respectively. Notably for $\delta^2_{r,d} = 10$, the optimum power ratio is $r_o = 0.7487$, which is greater than $r_o = 0.6902$ for $\delta^2_{r,d} = 1$; $\delta^2_{s,r} = 1$ in both cases. This is in agreement with the conclusion that more power should be put for P_1 if $\delta^2_{r,d} \gg \delta^2_{s,r}$.

As shown in Figure 2.5, increasing the number of relays affects the cooperation threshold values according to the $CG \cdot R$ optimization criterion. Table 2.2 describes the effect of changing the number of relays on the power ratio, cooperation threshold, bandwidth efficiency, and the cooperation gain using the unity channel-

N	$r = P_1/P$	α	Bandwidth Eff. (R)	Coop. Gain (CG)
1	0.6902	0.55	0.8624	0.247
2	0.6826	0.41	0.8397	0.1512
3	0.6787	0.35	0.8297	0.1046
4	0.6764	0.32	0.82	0.0776

Table 2.2: $CG \cdot R$ multi-node optimum values for unity channel variances.

variances case. A few comments on Table 2.2 are as follows. 1) The optimum power ratio is slightly decreasing with the number of relays. Because, increasing the number of relays will increase the probability of finding a better relay, which can receive the symbols from the source more correctly. Thus, it can send with almost equal power with the source. 2) The bandwidth efficiency is slightly decreasing with increasing the number of relays, because the probability that the source-destination channel is better than all the relays' metrics goes to 0 as N goes to ∞.

In this section, we have derived analytical expression of the optimum power allocation of the multi-node relay-selection decode-and-forward cooperative scenarios. Furthermore, we have shown the bandwidth efficiency-SER tradeoff curves, which are used to obtain the optimum cooperation threshold.

2.4 Simulation Results

In this section, some computer simulations for the relay-selection decode-and-forward cooperative system are presented to illustrate the previous theoretical analysis. It is assumed that the noise variance is set to 1, $N_0 = 1$. For fair comparison, the SER curves are plotted as a function of P/N_0. Finally, QPSK signalling

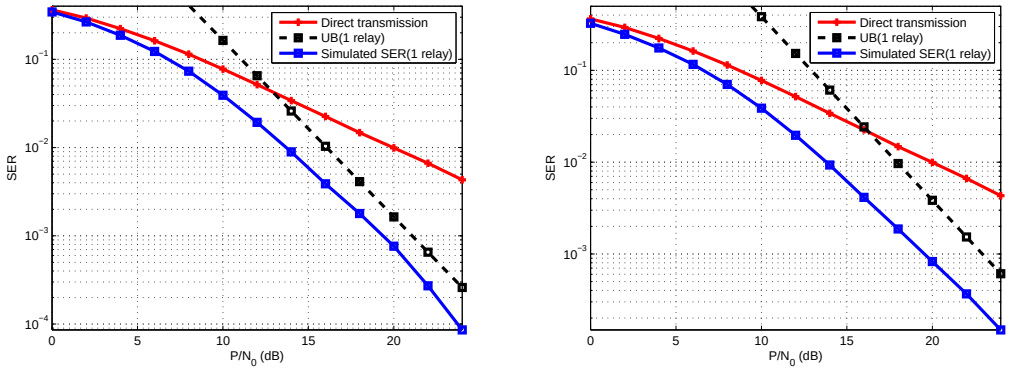

(a) (b)

Figure 2.6: SER simulated with optimum and equal power ratio, SER upper bound, and direct transmission curves for single-relay relay-selection decode-and-forward cooperative scheme with QPSK modulation, (a) $\alpha = 0.55$, and unity channel variances, (b) $\alpha = 0.09$, $\delta^2_{s,d}$=1, $\delta^2_{s,r}$=1, and $\delta^2_{r,d}$=10.

is used in all the simulations.

Figure 2.6 (a) depicts the simulated SER curves for the single-relay relay-selection decode-and-forward cooperative scheme with unity channel variances. According to Table 2.1, the optimum cooperation threshold and the optimum power ratio are $\alpha_o = 0.55$ and $r_o = 0.6902$, respectively. We plot the SER curve using the previous optimum values. Moreover, we plot the SER upper bound (2.44), which achieves full diversity order as was previously proven. Also, we plot the direct transmission curve which achieves diversity order 1, to show the advantage of using the cooperative scenario. Figure 2.6 (b) shows the simulated SER curve for single-relay relay-selection decode-and-forward cooperative scheme when the relay-destination channel is stronger, $\delta^2_{r,d} = 10$. As shown in the second row of Table (2.1), the resultant power ratio, cooperation threshold, bandwidth efficiency, and cooperation gain are 0.7487, 0.09, 0.9075, and 0.1613, respectively. We plot

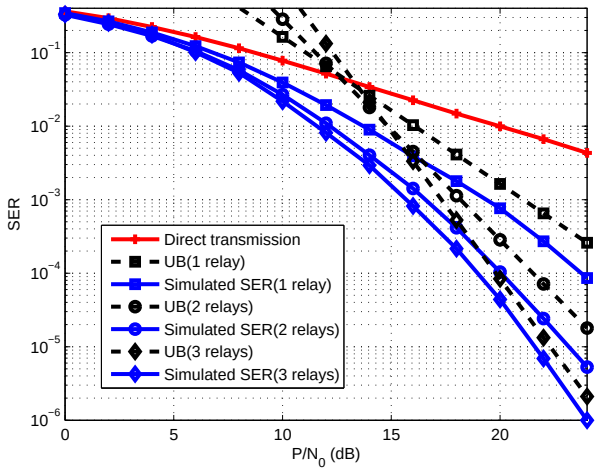

Figure 2.7: SER simulated with optimum power ratio and SER upper bound curves for multi-node relay-selection decode-and-forward cooperative scheme with QPSK modulation and unity channel variances.

the SER upper bound using the optimum power ratio. We have shown that the SER upper bound achieves full diversity order, which guarantees that the actual SER performance has full diversity order as well.

Figure 2.7 depicts the SER performance employing one, two, and three relays for unity channel variances. We plot the simulated SER curves using the optimum power ratios and the cooperation thresholds obtained in Table 2.2. Moreover, we plot the SER upper bounds obtained in (2.44). It was shown in (2.44) that these upper bounds achieve full diversity order. It is obvious that the simulated SER curves are bounded by these upper bounds, hence they achieve full diversity order as well. The direct-transmission SER curve is plotted as well to show the effect of employing the relays in a cooperative way. Moreover, the simulated bandwidth efficiencies are 0.8973, 0.8805, and 0.8738 employing one, two, and three relays, respectively. These results are slightly higher than the analytical results shown in

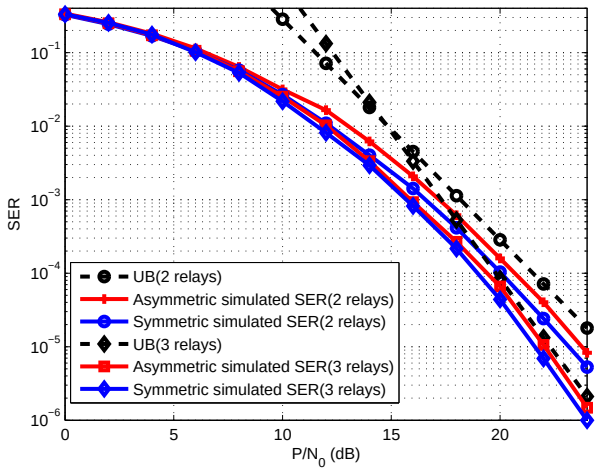

Figure 2.8: SER simulated for symmetric (unity channel variance) and asymmetric cases for multi-node relay-selection decode-and-forward cooperative scheme with QPSK modulation.

Table 2.2.

We also show some simulation results for the asymmetric case. In Figure 2.8, we show the SER of the asymmetric case along with the symmetric results for two and three relays. For $N = 2$ relays, the average channel gains are $\delta^2_{s,r_1} = \delta^2_{r_2,d} = 1.5$ and $\delta^2_{s,r_2} = \delta^2_{r_1,d} = 0.5$. For $N = 3$, two of the three relays have the same average channel gains as in $N = 2$. The third relay has $\delta^2_{s,r_3} = \delta^2_{r_3,d} = 1$. We also compare the results with the symmetric case with unity channel variances. Hence, both the symmetric and asymmetric cases have the same average source-relay and relay-destination channel gains. The power ratio and cooperation threshold are obtained from Table 2.2. As shown, the symmetric and asymmetric SER performance curves are very close to each other for both the two and three relays. More importantly, the asymmetric simulation results are upper bounded by the upper bound derived in (2.44) for the symmetric case.

Appendix

Proof of Lemma 1 is as follows. First, we prove that

$$\sum_{n=0}^{N} \frac{\binom{N}{n}\,(-1)^n}{1+n\,z} = \frac{N!\,z^N}{\prod_{n=0}^{N}(1+n\,z)}\,. \tag{2.54}$$

Let $A(z) = \sum_{n=0}^{N} \frac{\binom{N}{n}\,(-1)^N}{1+n\,z}$, $B(z) = \prod_{n=0}^{N}(1+n\ z)$, and $G(z) = A(z)\cdot B(z)$. The order of $G(z)$ is N, thus it can be written as $G(z) = \sum_{i=0}^{N} g_i\ z^i$, where $g_i = \frac{1}{i!}\frac{\partial^i G(z)}{\partial z^i}|_{z=0}$. It can be easily shown that

$$\frac{\partial^i A(z)}{\partial z^i} = (-1)^i\ i! \sum_{n=0}^{N} \frac{\binom{N}{n}\,(-1)^n\,n^i}{(1+n\,z)^{i+1}}\,. \tag{2.55}$$

Using the identity obtained in [[42], (0.154, 3-4)] as

$$\sum_{n=0}^{N}\binom{N}{n}\,(-1)^n\,n^i = \begin{cases} 0\,, & 0\le i<N \\ (-1)^N N!\,, & i=N \end{cases}, \tag{2.56}$$

we get

$$\frac{\partial^i A(z)}{\partial z^i}|_{z=0} = (-1)^i\ i!\left(\sum_{n=0}^{N}\binom{N}{n}\,(-1)^n\,n^i\right) = \begin{cases} 0\,, & 0\le i<N \\ (N!)^2\,, & i=N \end{cases}. \tag{2.57}$$

Since, $A(z)|_{z=0} = 0$ and $B(z)|_{z=0} = 1$, thus

$$g_i = \frac{1}{i!}\frac{\partial^i\,(\ A(z)\cdot B(z)\ )}{\partial z^i}|_{z=0} = \frac{1}{i!}\frac{\partial^i A(z)}{\partial z^i}|_{z=0}\cdot B(z)|_{z=0} = \begin{cases} 0\,, & 0\le i<N \\ N!\,, & i=N \end{cases}. \tag{2.58}$$

Thus,

$$A(z) = \frac{G(z)}{B(z)} = \frac{N!\,z^N}{\prod_{n=0}^{N}(1+n\,z)}\,, \tag{2.59}$$

which proves (2.54). Replacing $z = \frac{y}{x}$ in (2.54), we obtain Lemma 1 and the proof is complete.

Chapter 3

Distributed Energy-Efficient Cooperative Routing in Wireless Networks

In Chapter 2, we have proposed a cross-layer design for relay-selection cooperative communication scheme to achieve high bandwidth efficiency while guaranteeing full diversity order. It was assumed that the source can reach the destination in a maximum of two hops. In this chapter we consider the general case of larger networks, in which we aim to propose a cross-layer design of cooperation-based routing algorithms that minimize the end-to-end transmission power while guaranteeing a desired throughput.

Energy saving is one of the main objectives of routing algorithms for different wireless networks such as mobile ad hoc networks [43] and sensor networks [44]. In [45], it was shown that in some wireless networks such as ad hoc networks, nodes spend most of their power in communication, either sending their own data or relaying other nodes' data. In addition to saving more energy, selected routes

may guarantee certain Quality of Service (QoS). *QoS routing* is of great importance to some wireless applications (e.g. multimedia applications) [46].

As discussed in Chapter 1, cooperative communication for wireless networks has gained much interest due to its ability to mitigate fading through achieving spatial diversity, while offering flexibility in addition to traditional Multiple-Input Multiple-Output (MIMO) communication. Routing algorithms, which are based on the cooperative communications, are known in the literature as *cooperative routing* algorithms [47]. Designing cooperative routing algorithms is an interesting research area and can lead to significant power savings. The cooperative routing makes use of two facts: the Wireless Broadcast Advantage (WBA) in the broadcast mode and the Wireless Cooperative Advantage (WCA) in the cooperative mode. In the broadcast mode each node sends its data to more than one node, while in the cooperative mode many nodes send the same data to the same destination.

The cooperative routing problem has been recently considered in the literature [38, 47–51]. In [47], the optimum route is found through a dynamic programming algorithm which is a complexity that increases exponentially with the number of the nodes in the network. Two heuristic algorithms (Cooperation Along the Minimum Energy Non-Cooperative Path (CAN-L) and Progressive Cooperation (PC-L)) are proposed in a centralized manner. In [48], two heuristic routing algorithms, namely, Cooperative routing along Truncated Non-Cooperative Route (CTNCR) and Source Node Expansion Routing (SNER) are proposed. These algorithms choose the minimum-power route while guaranteeing fixed transmission rate. In CTNCR, the shortest path is constructed first, then some of the nodes are truncated according to a specific power allocation. In SNER, the network is divided into two disjoint subsets: one that has the source initially and the other has the

rest of the nodes. In each iteration one node that requires the least transmission power is added to the first set until the destination is reached. It is assumed that both the transmitter and receiver have perfect channel state information about the channel in a centralized manner.

In [49], Li *et al.* proposed the Cooperative Shortest Path (CSP) algorithm, which chooses the next node in the route that minimizes the power transmitted by the last L nodes added to the route. Sikora *et al.* presented in [50] an information-theoretic viewpoint of the cooperative routing in linear wireless network for both the power-limited and bandwidth-limited regimes. In addition, the authors in [50] analyzed the transmission power, required to achieve a desired end-to-end rate. In [51], Pandana *et al.* studied the impact of cooperative communication on maximizing the lifetime of wireless sensor networks. Finally, the authors in [38] proposed three cooperative routing algorithms, namely, relay-by-flooding, relay-assisted routing, and relay-enhanced routing. In the relay-by-flooding, the message is propagated by flooding and multiple hops. The relay-assisted routing uses cooperative nodes of an existing route and the relay-enhanced routing adds cooperative nodes to an existing route. Both of these routing schemes start with a route determined without cooperation.

Most of the existing cooperation-based routing algorithms are implemented by finding a shortest-path route first and then building the cooperative route based on the shortest-path one. Indeed, these routing algorithms do not fully exploit the merits of cooperative communications at the physical layer, since the optimal cooperative route might be completely different from the shortest-path route. In addition, most of these cooperation-based routing algorithms require a central node, which has global information about all the nodes in the network, in order

to calculate the best route given a certain source-destination pair. Having such a central node may not be possible in some wireless networks. Particularly, in infrastructureless networks (e.g. ad hoc networks), routes should be constructed in a *distributed* manner, i.e., each node is responsible for choosing the next node towards the destination. These are our main motivations to propose a distributed cooperation-based routing algorithm that takes into consideration cooperative communications while constructing the minimum-power route.

In this chapter, we consider the minimum-power routing problem with cooperation in wireless networks. We consider a set of users, who are trying to communicate with each other and propose a cooperation-based routing algorithm, which requires less transmission power compared to the conventional routing schemes. In other words we try to find, in a polynomial complexity, the route that requires the minimum transmitted power while guaranteeing certain Quality of Service (QoS). The QoS is characterized by the end-to-end throughput. The main contribution of this chapter is the proposed cooperation-based routing algorithm, namely the Minimum Power Cooperative Routing (MPCR) algorithm, which can choose the minimum-power route while guaranteeing the desired QoS. For arbitrary network of 100 nodes, it will be shown that the MPCR algorithm can achieve power saving of 57.36% compared to the conventional shortest-path routing algorithms. Furthermore, it can achieve power saving of 37.64% with respect to the Cooperation Along the Shortest Non-Cooperative Path (CASNCP) algorithm, which finds the shortest-path route first then applies the cooperative communication upon the shortest-path route to reduce the transmission power. For regular linear network consisting of 100 nodes, we show in analysis that the power savings of the MPCR algorithm with respect to conventional shortest-path and CASNCP routing algo-

rithms are 73.91% and 65.61%, respectively. For regular grid networks consisting of 100 nodes, we show that the power savings of the MPCR algorithm with respect to the shortest-path and CASNCP routing algorithms are 65.63% and 29.8%, respectively.

The rest of the chapter is organized as follows. In the next section, we formulate the minimum-power routing problem and describe the network model. In Section 3.2, we derive closed-form expressions for the minimum transmission power per hop. We propose two cooperation-based routing algorithms in Section 3.3, which are the MPCR and CASNCP routing algorithms. Then, we consider the regular linear and grid wireless networks and derive the analytical results for the power savings due to cooperation in these two networks. In Section 3.4, we show the numerical results for the power savings of the proposed algorithm.

3.1 Network Model and Transmission Modes

In this section, we describe the network model and formulate the minimum-power routing problem. Then, we present the direct transmission and cooperative transmission modes.

3.1.1 Network Model

We consider a graph $G(V, E)$ where V is the vertex set and E is the edge set. The number of nodes is $|V| = N$ nodes and the number of edges is $|E| = M$ edges. Given any source-destination pair (S, D), the goal is to find the $S - D$ route that minimizes the total transmission power, while satisfying a specific throughput. For a given source-destination pair, denote Ω as the set of all possible routes, where

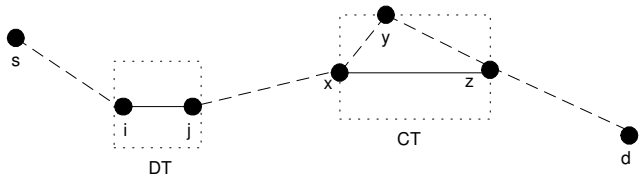

Figure 3.1: Cooperative Transmission (CT) and Direct Transmission (DT) modes as building blocks for any route.

each route is defined as a set consisting of its hops. For a route $\omega \in \Omega$, denote ω_i as the i-th hop of this route. Thus, the problem can be formulated as

$$\min_{\omega \in \Omega} \sum_{\omega_i \in \omega} P_{\omega_i} \quad \text{s.t.} \quad \eta_\omega \geq \eta_o \ , \tag{3.1}$$

where P_{ω_i} denotes the transmission power over the i-th hop, η_ω is the end-to-end throughput, and η_o represents the desired value of the end-to-end throughput. Let η_{ω_i} denote the throughput of the i-th hop, which is defined as the number of successfully transmitted bits per second per hertz (b/s/Hz) of a given hop. Furthermore, the end-to-end throughput of a certain route ω is defined as the minimum of the throughput values of the hops constituting this route, i.e.,

$$\eta_\omega = \min_{\omega_i \in \omega} \eta_{\omega_i} \ . \tag{3.2}$$

It has been proven in [49] that the Minimum Energy Cooperative Path (MECP) routing problem, i.e., to find the minimum-energy route using cooperative radio transmission, is *NP-complete*. This is due to the fact that the optimal path could be a combination of cooperative transmissions and point-to-point transmissions. Therefore, we consider two types of building blocks: direct transmission (DT) and cooperative transmission (CT) building blocks. In Figure 3.1 the DT block is represented by the link (i, j), where node i is the sender and node j is the receiver. In addition, the CT block is represented by the links $(x, y), (x, z)$, and (y, z), where

node x is the sender, node y is a relay, and node z is the receiver. The route can be considered as a cascade of any number of these two building blocks, and the total power of the route is the summation of the transmission powers along the route. Thus, the minimization problem in (3.1) can be solved by applying any distributed shortest-path routing algorithm such as the distributed Bellman-Ford algorithm [52].

3.1.2 Direct and Cooperative Transmission Modes

Let $h_{u,v}, d_{u,v}$, and $n_{u,v}$ represent the channel coefficient, length, and additive noise of the link (u, v), respectively. For the direct transmission between node i and node j, the received symbol can be modeled as

$$r_{i,j}^{D} = \sqrt{P^{D}\ d_{i,j}^{-\alpha}}\ h_{i,j}\ s + n_{i,j}\ , \tag{3.3}$$

where P^D is the transmission power in the direct transmission mode, α is the path loss exponent, and s is the transmitted symbol with unit power.

For the cooperative transmission, we consider a modified version of the decode-and-forward incremental relaying cooperative scheme, proposed in [15]. The transmission scheme for a sender x, a relay y, and a receiver z, can be described as follows. The sender sends its symbol in the current time slot. Due to the broadcast nature of the wireless medium, both the receiver and the relay receive noisy versions of the transmitted symbol. The received symbols at the receiver and the relay can be modeled as

$$r_{x,z}^{C} = \sqrt{P^{C}\ d_{x,z}^{-\alpha}}\ h_{x,z}\ s + n_{x,z} \tag{3.4}$$

and

$$r_{x,y}^{C} = \sqrt{P^{C}\ d_{x,y}^{-\alpha}}\ h_{x,y}\ s + n_{x,y}\ , \tag{3.5}$$

respectively, where P^C is the source transmission power in the cooperative transmission mode. Once the symbol is received, the receiver and the relay decode it. We assume that the relay and the receiver decide that the received symbol is correctly received if the received signal-to-noise ratio (SNR) is greater than a certain threshold, which depends on the transmitter and the receiver structures.

If the receiver decodes the symbol correctly, then it sends an acknowledgment (ACK) to the sender and the relay to confirm a correct reception. Otherwise, it sends a negative acknowledgment (NACK) that allows the relay, if it received the symbol correctly, to transmit this symbol to the receiver in the next time slot. This model represents a modified form of the Automatic Repeat Request (ARQ), where the relay retransmits the data instead of the sender, if necessary. The received symbol at the receiver can be written as

$$r_{y,z}^{C} = \sqrt{P^C \; d_{y,z}^{-\alpha}} \; h_{y,z} \; s + n_{y,z} \; . \tag{3.6}$$

In general, the relay can transmit with a power that is different from the sender power P^C. However, this complicates the problem of finding the minimum-power formula, as will be derived later. For simplicity, we consider that both the sender and the relay send their data employing the same power P^C.

In this chapter, flat quasi-static fading channels are considered, hence, the channel coefficients are assumed to be constant during a complete frame, and may vary from a frame to another. We assume that all the channel terms are independent complex Gaussian random variables with zero mean and unit variance. Finally, the noise terms are modeled as zero-mean, complex Gaussian random variables with equal variance N_0. In this section, we have formulated the minimum-power routing problem and we have defined the two main transmission modes. In the next section, we derive the closed-from expressions for the transmission power

in both direct and cooperative transmission modes required to achieve the desired throughput.

3.2 Link Analysis

In this section, we derive the required power for the direct and cooperative transmission modes in order to achieve certain throughput. Since the throughput is a continuous monotonously-increasing function of the transmission power, the optimization problem in (3.1) has the minimum when $\eta_\omega = \eta_o, \forall \omega \in \Omega$. Since the end-to-end throughput $\eta_\omega = \min_{\omega_i \in \omega} \eta_{\omega_i}$, then the optimum power allocation, which achieves a desired throughput η_o along the route ω, forces the throughput at all the hops η_{ω_i} to be equal to the desired one, i.e.,

$$\eta_{\omega_i} = \eta_o \ , \quad \forall \ \omega_i \in \omega \ . \tag{3.7}$$

This result can be explained as follows. Let $P^*_{\omega_1}, P^*_{\omega_2}, \cdots, P^*_{\omega_n}$ represent the required powers on a route consisting of n hops, where P^*_i results in $\eta_{\omega_i} = \eta_o$ for $i = 1, \cdots, n$. If we increase the power of the i-th block to $P_{\omega_i} > P^*_{\omega_i}$ then the resulting throughput of the i-th block increases, i.e. $\eta_{\omega_i} > \eta_o$, while the end-to-end throughput does not change as $\min_{\omega_i \in \omega} \eta_{\omega_i} = \eta_o$. Therefore, no need to increase the throughput of any hop over η_o, which is indicated in (3.7).

Since the throughput of a given link ω_i is defined as the number of successfully transmitted bits per second per hertz, thus it can be calculated as

$$\eta_{\omega_i} = p^S_{\omega_i} \times R_{\omega_i} \ , \tag{3.8}$$

where $p^S_{\omega_i}$ and R_{ω_i} denote the per-link probability of success and transmission rate, respectively. We assume that the desired throughput can be factorized as

$$\eta_o = p^S_o \times R_o \ , \tag{3.9}$$

where p_o^S and R_o denote the desired per-link probability of success and transmission rate, respectively. In the sequel, we calculate the required transmission power in order to achieve the desired per-link probability of success and transmission rate for both the direct and cooperative transmission modes.

For the direct transmission mode in (3.3), the mutual information between sender i and receiver j can be given by

$$I_{i,j} = \log\left(1 + \frac{P^D\ d_{i,j}^{-\alpha}\ |h_{i,j}|^2}{N_0}\right), \tag{3.10}$$

where $\frac{P^D\ d_{i,j}^{-\alpha}\ |h_{i,j}|^2}{N_0}$ is the signal-to-noise ratio (SNR). Without loss of generality, we have assumed unit bandwidth in (3.10). The outage probability is defined as the probability that the mutual information is less than the required transmission rate R_o. Thus, the outage probability of the link (i, j) is calculated as

$$p_{i,j}^O = \Pr(I_{i,j} \leq\ R_o)\ . \tag{3.11}$$

By substituting (3.10) into (3.11), we get

$$p_{i,j}^O = \Pr(|h_{i,j}|^2 \leq\ \frac{(2^{R_o} - 1)\ N_0\ d_{i,j}^{\alpha}}{P^D})\ . \tag{3.12}$$

The channel coefficients between each two nodes $h_{i,j}$ are modeled as independent circular symmetric complex Gaussian random variables with zero-mean and unit variance. In other words, the fading model of any of the channels is Rayleigh fading model [53]. Hence, the channel gain $|h_{i,j}|^2$ is modeled as exponential random variable, i.e., $p(|h_{i,j}|^2) = \exp(-|h_{i,j}|^2)$ for $|h_{i,j}|^2 \geqslant 0$ is the probability density function (PDF) of $|h_{i,j}|^2$. Thus, the outage probability in (3.12) is equal to

$$p_{i,j}^O = 1 - \exp\Big(-\frac{(2^{R_o} - 1)\ N_0\ d_{i,j}^{\alpha}}{P^D}\Big)\ . \tag{3.13}$$

If an outage occurs, the data is considered lost. The probability of success is calculated as $p_{i,j}^S = 1 - p_{i,j}^O$. Thus using (3.13), to achieve the desired p_o^S and R_o

for direct transmission mode, the required transmission power is

$$P^D(d_{i,j}) = \frac{(2^{R_o} - 1)\ N_0\ d_{i,j}^{\alpha}}{-\log(p_o^S)}\ . \tag{3.14}$$

For the cooperative transmission mode, the total outage probability is given by

$$\begin{aligned} p_{x,y,z}^O &= \Pr(I_{x,z} \le R^C) \cdot \Pr(I_{x,y} \le R^C) \\ &\quad + \Pr(I_{x,z} \le R^C) \cdot \big(1 - \Pr(I_{x,y} \le R^C)\big) \cdot \Pr(I_{y,z} \le R^C)\ , \end{aligned} \tag{3.15}$$

where R^C denotes the transmission rate for each time slot. In (3.15), the first term corresponds to the event when both the sender-receiver and the sender-relay channels are in outage, and the second term corresponds to the event when both the sender-receiver and relay-receiver channels are in outage but the sender-relay is not. Consequently, the probability of success of the cooperative transmission mode can be calculated as

$$\begin{aligned} p^S &= \exp\big(-g\, d_{x,z}^{\alpha}\big) + \exp\big(-g\,(d_{x,y}^{\alpha} + d_{y,z}^{\alpha})\big) \\ &\quad - \exp\big(-g\,(d_{x,y}^{\alpha} + d_{y,z}^{\alpha} + d_{x,z}^{\alpha})\big)\ , \end{aligned} \tag{3.16}$$

where

$$g = \frac{(2^{R^C} - 1)\ N_0}{P^C}\ . \tag{3.17}$$

In (3.15) and (3.16), we assume that the receiver decodes the signals received from the relay either at the first time slot or at the second time slot, instead of combining the received signals together. In general, Maximum Ratio Combining (MRC) [8] at the receiver gives the optimum result. However, it requires the receiver to store an analog version of the received data from the sender, which requires huge storage capacity. The probability that the source transmits only, denoted by $\Pr(\phi)$, is calculated as

$$\begin{aligned} \Pr(\phi) &= 1 - \Pr(I_{x,z} \le R^C) + \Pr(I_{x,z} \le R^C)\Pr(I_{x,y} \le R^C) \\ &= 1 - \exp\big(-g\ d_{x,y}^{\alpha}\big) + \exp\big(-g\ (d_{x,y}^{\alpha} + d_{x,z}^{\alpha})\big)\ , \end{aligned} \tag{3.18}$$

where the term $\big(1 - \Pr(I_{x,z} \leq \ R^C)\big)$ corresponds to the event when the sender-receiver channel is not in outage, while the other term corresponds to the event when both the sender-receiver and the sender-relay channels are in outage. The probability that the relay cooperates with the source is calculated as

$$\overline{\Pr(\phi)} = 1 - \Pr(\phi) \ . \tag{3.19}$$

Thus, the average transmission rate of the cooperative transmission mode can be calculated as

$$R = R^C \cdot \Pr(\phi) + \frac{R^C}{2} \cdot \overline{\Pr(\phi)} \ = \frac{R^C}{2} \ \big(1 + \Pr(\phi)\big) \ , \tag{3.20}$$

where R^C corresponds to the transmission rate if the sender is sending alone in one time slot and $R^C/2$ corresponds to the transmission rate if the relay cooperates with the sender in the consecutive time slot.

We set the probability of success in (3.16) as $p^S = p_o^S$ and the average transmission rate in (3.20) as $R = R_o$. By approximating the exponential functions in (3.16) as $\exp(-x) \approx 1 - x + x^2/2$, we obtain

$$g \approx \sqrt{\frac{1 - p_o^S}{d_{eq}}} \ , \tag{3.21}$$

where $d_{eq} \triangleq d_{x,z}^{\alpha}(d_{x,y}^{\alpha} + d_{y,z}^{\alpha})$. Thus, R^C can be obtained using (3.20) as

$$\begin{aligned} R^C &= \frac{2 \ R_o}{1 + \Pr(\phi)} \\ &\approx \frac{2 \ R_o}{2 - \exp\big(-\sqrt{\frac{1-p_o^S}{d_{eq}}} \ d_{x,y}^{\alpha}\big) + \exp\big(-\sqrt{\frac{1-p_o^S}{d_{eq}}} \ (d_{x,y}^{\alpha} + d_{x,z}^{\alpha})\big)} \ , \end{aligned} \tag{3.22}$$

where we substituted (3.21) in (3.18). In addition, the required power per link can be calculated using (3.17) and (3.21) as

$$P^C \approx (2^{R^C} - 1) \ N_0 \ \sqrt{\frac{d_{eq}}{1 - p_o^S}} \ . \tag{3.23}$$

Finally, the total transmission power of the cooperative transmission mode can be calculated as

$$\begin{aligned} P_{tot}^{C}(d_{x,z}, d_{x,y}, d_{y,z}) &= P^{C} \cdot \Pr(\phi) + 2\, P^{C} \cdot \overline{\Pr(\phi)} \\ &= P^{C}\big(2 - \Pr(\phi)\big)\ , \end{aligned} \tag{3.24}$$

where $\Pr(\phi)$ and P^{C} are given in (3.18) and (3.23), respectively. In this section, we have derived closed-from expressions for the transmission power in both the direct and the cooperative transmission modes required to achieve the desired throughput. In the next section, we describe our proposed cooperation-based routing algorithms.

3.3 Cooperation-Based Routing Algorithms

In this section, we propose two cooperation-based routing algorithms, which require polynomial complexity to find the minimum-power route. Then, we discuss the impact of cooperative cooperation on the routing in specific regular wireless networks, which are the regular linear and grid networks. We assume that each node broadcasts periodically HELLO packet to its neighbors to update the topology information. In addition, we consider a simple Medium Access Control (MAC) protocol, which is the conventional Time Division Multiple Access (TDMA) scheme with equal time slots.

3.3.1 Proposed Routing Algorithms

First, we propose a cooperation-based routing algorithm, namely, the Minimum-Power Cooperative Routing (MPCR) algorithm. The MPCR algorithm takes into consideration the cooperative communications while constructing the minimum-

Table 3.1: MPCR Algorithm.

Step 1: Each node $x \in \{1, \ldots, N\}$ behaving as a sender calculates the cost of the its outgoing link (x, z), where $z \in N(x)$ is the receiver, as follows. For each other node $y \in N(x), y \neq z$, node x calculates the cost of the cooperative transmission in (3.24) employing node y as a relay.
Step 2: The cost of the (x, z)-th link is the minimum cost among all the costs obtained in *Step 1*.
Step 3: If the minimum cost corresponds to a certain relay $y*$, node x employs this relay to help the transmission over that hop. Otherwise, it uses the direct transmission over this hop.
Step 4: Distributed Bellman-Ford shortest-path algorithm is applied using the calculated cooperation-based link costs. Each node $i \in \{1, \ldots, N\}$ executes the iteration $P_i = \min_{j \in N(i)} (P_{i,j} + P_j)$, where $N(i)$ denotes the set of neighboring nodes of node i, P_j represents the latest estimate of the shortest path from node j to the destination, and $P_{i,j}$ is the minimum possible transmission power from node i to node j.

power route. The derived power formulas for direct transmission and cooperative transmission are utilized to construct the minimum-power route. It can be distributively implemented by the Bellman-Ford shortest path algorithm [52]. In the conventional Bellman-Ford shortest path algorithm, each node $i \in \{1, \ldots, N\}$ executes the iteration $D_i = \min_{j \in N(i)} (d_{i,j}^{\alpha} + D_j)$, where $N(i)$ denotes the set of neighboring nodes of node i, $d_{i,j}^{\alpha}$ denotes the effective distance between node i and j, and D_j represents the latest estimate of the shortest path from node j to the destination [52] that is included in the HELLO packet.

The MPCR algorithm is implemented as follows. First, each node calculates the costs (required powers) of its outgoing links, and then applies the shortest-path

Bellman-Ford algorithm using these newly calculated costs. The required transmission power between two nodes is the minimum power obtained by searching over all the possible nodes in the neighborhood to act as a relay. If there is no available relay in the neighborhood, a direct transmission mode is considered. Second, the distributed Bellman-Ford shortest-path routing algorithm is implemented at each node. Each node updates its cost toward the destination as

$$P_i = \min_{j \in N(i)} \left(P_{i,j} + P_j \right) , \tag{3.25}$$

where P_i denotes the required transmission power from node i to the destination and $P_{i,j}$ denotes the minimum transmission power between node i and node j. $P_{i,j}$ is equal to either P^D in (3.14) if direct transmission is considered or P^C_{tot} in (3.24) if cooperative transmission is considered employing one of the nodes in the neighborhood as a relay. Table 3.1 describes the MPCR algorithm in details. The worst-case computational complexity of calculating the costs at each node is $O(N^2)$ since it requires two nested loops, and each has a maximum length of $N-1$ to calculate all the possible cooperative transmission blocks.

Second, we propose a cooperation-based routing algorithm, namely, Cooperation Along the Shortest Non-Cooperative Path (CASNCP) algorithm. The CASNCP algorithm is similar to the heuristic algorithms proposed by Khandani *et al.* in [47] and Yang *et al.* in [48] as it applies cooperative communications upon the shortest-path route. However, it is implemented in a different way using the proposed cooperation-based link cost formula. First, it chooses the shortest-path route. Second, for each three consecutive nodes in the route, it applies either the cooperative transmission mode; first node as the sender, second node as the relay, and third node as the receiver, or the direct transmission mode from the first to the third node. Table 3.2 describes the CASNCP algorithm.

Table 3.2: CASNCP Algorithm.

Step 1: Implement the Shortest Non-Cooperative Path (SNCP) algorithm using the distributed Bellman-Ford algorithm to choose the conventional shortest-path route ω_S as follows. Each node $i \in \{1, \ldots, N\}$ executes the iteration $D_i = \min_{j \in N(i)} (d_{i,j}^{\alpha} + D_j)$, where $N(i)$ denotes the set of neighboring nodes of node i and D_j represents the latest estimate of the shortest path from node j to the destination.
Step 2: For each three consecutive nodes on ω_S, either the cooperative transmission mode or the direct transmission mode is implemented. In the cooperative transmission mode, the first, second, and third nodes behave as the sender, relay, and receiver, respectively, i.e., the first node sends its data to the third node with the help of the second node as discussed in the cooperative transmission mode. In the direct transmission mode, the first node is the sender and the third node is the destination. The transmission mode that requires less power is chosen.

We point out that in this chapter, we restrict the cooperation scheme between any two nodes to the single-relay case. First, the required power between each two nodes is calculated taken into consideration the possibility of having any other node as a relay in a single-relay cooperative communication model. Second, the optimum shortest-path algorithm is calculated based on these cooperation-based link costs. Based on that, the proposed MPCR algorithm calculates the optimum-route subject to the single-relay cooperation model. In other words, if we allow cooperation to happen using more than one relay, then the optimum path in this case can possibly require transmission power that is less than that required by the MPCR algorithm. However, this can cause significant increase in communication and computation burdens, and the performance increase might be sufficiently

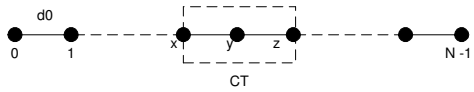

Figure 3.2: Linear wireless network, d_0 denote the distance between each two adjacent nodes.

small. In other words, adding more relays might not be cost effective, and the proposed scheme is optimal in the sense of up to one relay case.

3.3.2 Performance Analysis: Regular Linear Networks

The regular linear network, shown in Figure 3.2, is a one-dimensional chain of nodes placed at equal intervals d_0. Without taking into consideration the interference effect, nodes are placed at equal intervals to achieve the best performance in terms of the throughput and the energy consumption [50]. In order to illustrate the behavior of each routing algorithm, we consider the three consecutive nodes x, y, and z in Figure 3.2, where node x needs to transmit its data to node z. The SNCP routing algorithm transmits the data directly from node x to node y then from node y to node z. Thus, the required power for the SNCP routing algorithm is

$$P_{SNCP}(x,z) = 2\ P^D(d_0)\ , \tag{3.26}$$

where $P^D(d_0)$ is the required transmission power over one hop and it is given by (3.14) with $d_{i,j} = d_0$. The CASNCP routing algorithm applies cooperative communication transmission on the shortest-path route as follows. Node x transmits the data directly to node z. If node z does not decode the data correctly, then node y retransmits the data if it has correctly decoded it during the first transmission. The transmission power for the CASNCP routing algorithm is given by

$$P_{CASNCP}(x,z) = P^C_{tot}(2\,d_0, d_0, d_0)\ , \tag{3.27}$$

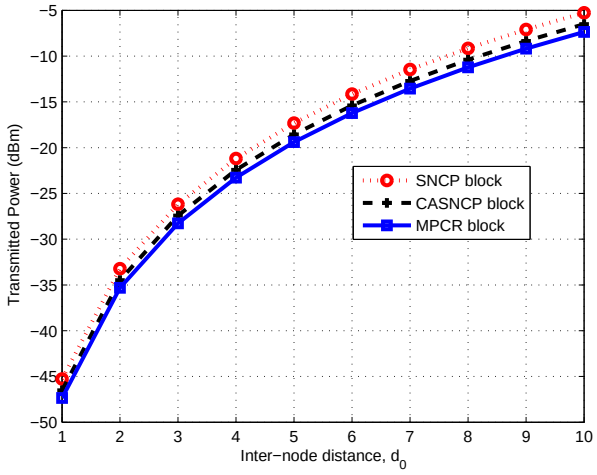

Figure 3.3: Required transmission power per one block of three nodes versus the inter-node distance d_0 for $N_0 = -70$ dBm, $\alpha = 4$, $\eta_0 = 1.96$ b/s/Hz, and $R_0 = 2$ b/s/Hz in regular linear networks.

where $P_{tot}^{C}(2\,d_0, d_0, d_0)$ represents the cooperative transmission power given in (3.24) with $d_{x,z} = 2\,d_0$, $d_{x,y} = d_0$, and $d_{y,z} = d_0$.

By applying the MPCR algorithm described above on this example, we find that the route is chosen on two consecutive phases as follows. First, node x transmits its data directly to node y utilizing direct transmission mode. Second, node y transmits its data to node z in a cooperative transmission mode utilizing node x as a relay. In other words, if node z does not receive the data correctly from node y, then node x will retransmit the data to node z. Thus, the total transmission power to transmit the data from node x to node z is

$$P_{MPCR}(x, z) = P^{D}(d_0) + P_{tot}^{C}(d_0, d_0, 2\,d_0)\ , \tag{3.28}$$

where $P_{tot}^{C}(d_0, d_0, 2\,d_0)$ is the required cooperative transmission power given in (3.24) with $d_{x,z} = d_0$, $d_{x,y} = d_0$, and $d_{y,z} = 2\,d_0$. Figure 3.3 depicts the required transmission power per block (x, y, z) as a function of the distance d_0 at

throughput $\eta_0 = 1.96$ b/s/Hz ,transmission rate $R_0 = 2$ b/s/Hz, noise variance $N_0 = -70$ dBm, and path loss exponent $\alpha = 4$. As shown, the MPCR algorithm requires the least transmission power compared to both the SNCP and CASNCP routing algorithm.

Based on this example, we explain the route chosen by each algorithm when the source is node 0 and the destination is node $N-1$. The SNCP routing algorithm constructs the shortest route as a sequence of all the nodes between the source and destination, i.e., $w_{SNCP} = \{(0,1),(1,2),\cdots,(N-2,N-1)\}$, where (i,j) denotes the direct transmission building block between sender i and receiver j. The CASNCP routing algorithm applies cooperative transmission mode on each three consecutive nodes in the SNCP route, i.e., $w_{CASNCP} = \{(0,1,2),(2,3,4),\cdots,(N-3,N-2,N-1)\}$, where (x,y,z) denotes a cooperative transmission building block with x, y, and z denoting the sender, relay, and receiver, respectively. Finally, the MPCR routing algorithm, applied on this linear network, chooses a different route, which is $w_{MPCR} = \{(0,1),(1,0,2),(2,1,3),\cdots,(N-2,N-3,N-1)\}$. In other words, each node sends its data to the adjacent node towards the destination utilizing its other adjacent node towards the source as a relay. In the following, we calculate the average required transmission power by each algorithm in a linear network.

For any routing scheme, the average end-to-end transmission power can be calculated as

$$P(\text{route}) = \sum_{l=1}^{N-1} P(\text{route}|l) \times \Pr(l) \ , \tag{3.29}$$

where $P(\text{route}|l)$ is the end-to-end transmission power when the destination is l hops away from the source and $\Pr(l)$ denotes the probability mass function (PMF) of having l hops between any source-destination pair. The PMF $\Pr(l)$ can be

calculated as

$$\Pr(l) = \begin{cases} \frac{1}{N}, & \text{l=0} \\ \frac{2\,(N-l)}{N^2}, & \text{l=1,2,}\cdots\text{,N-1} \end{cases} . \tag{3.30}$$

We illustrate how (3.30) is derived as follows. The probability of choosing a certain node is $\frac{1}{N}$. Thus, the probability of having the source and destination at certain locations is given by $\frac{1}{N} \times \frac{1}{N} = \frac{1}{N^2}$. At $l = 0$ hops there is N possible combinations of this event, where the source and destination are the same. Therefore, $\Pr(0) = \frac{N}{N^2} = \frac{1}{N}$. Considering one direction only (e.g., from left to right in Figure 3.2), at $l = 1$ there is $N-1$ distinct source-destination pairs: the first is the 0-to-1 pair and the last is the $(N-1)$-to-N pair. By considering the other direction, the number of different source-destination pairs is $2 \times (N-1)$. Therefore, the probability of having a source-destination pair with $l = 1$ hop in between is $\Pr(1) = \frac{2(N-1)}{N^2}$. In general, there is $2(N-l)$ different source-destination pairs with l hops in between, hence, the PMF of having source-destination pairs with l hops in between is given by (3.30).

For a route of l hops, the MPCR end-to-end transmission power can be calculated as

$$P_{MPCR}(\text{route}|l) = P^D(d_0) + P^C_{tot}(d_0, d_0, 2\,d_0) \times (l-1)\ , \tag{3.31}$$

where the term $P^D(d_0)$ accounts for the first transmission from the source to its adjacent node towards the destination and $P^C_{tot}(d_0, d_0, 2\,d_0)$ is the required cooperative transmission power over one hop, which is given in (3.24) with $d_{x,z} = d_0$, $d_{x,y} = d_0$, and $d_{y,z} = 2\ d_0$. The CASNCP end-to-end transmission power can be given as

$$P_{CASNCP}(\text{route}|l) = \begin{cases} P^C_{tot}(2\,d_0, d_0, d_0) \times \frac{l}{2} & \text{l is even} \\ P^C_{tot}(2\,d_0, d_0, d_0) \times \frac{l-1}{2} + P^D(d_0) & \text{l is odd} \end{cases} . \tag{3.32}$$

If l is even, there exist $\frac{l}{2}$ cooperative transmission blocks and each block requires a total power of $P^C_{tot}(2\,d_0, d_0, d_0)$. If l is odd, then a direct transmission mode is done over the last hop. Finally, the SNCP end-to-end transmission power is calculated as

$$P_{SNCP}(\text{route}|l) = P^D(d_0) \times l\ . \tag{3.33}$$

The average end-to-end transmission power for any routing scheme can be calculated by substituting the corresponding power formulas, which are (3.31), (3.32), and (3.33) for the MPCR, CASNCP, and SNCP, respectively in (3.29).

3.3.3 Performance Analysis: Regular Grid Networks

Figure 3.4 shows a regular 4 x 4 grid topology and d_0 denotes the distance between each two nodes in the vertical or horizontal directions. To illustrate the routes selected by different routing schemes, we assume that the source is node 0 and the destination is node 7. The SNCP routing algorithm chooses one of the possible shortest routes. For instance, the chosen shortest-route is $w_{SNCP} = \{(0,1),(1,5),(5,6),(6,7)\}$, where (i,j) denotes the direct transmission mode from node i to node j. Figure 3.4 (a) shows the route chosen by the SNCP routing algorithm, where the solid line between each two nodes indicates the direct transmission mode.

The CASNCP routing algorithm applies cooperation among each three consecutive nodes on the shortest-route, and the resulting route is $w_{CASNCP} = \{(0,1,5),(5,6,7)\}$, where (x,y,z) denotes the cooperative transmission mode between sender x, relay y, and destination z. Figure 3.4 (b) shows the route chosen by the CASNCP algorithm. The solid lines indicate the sender-receiver transmissions and the dashed lines indicate the sender-relay and relay-receiver transmissions. By applying the

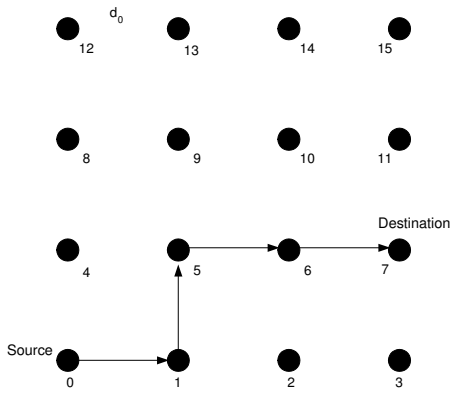

(a)

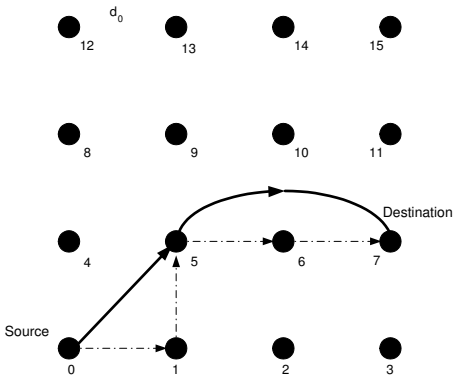

(b)

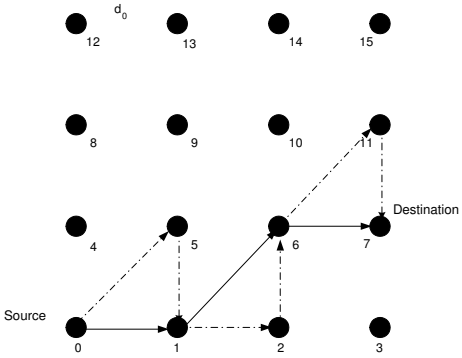

(c)

Figure 3.4: Route chosen by the three routing algorithms in grid wireless network. (a) SNCP constructed route, (b) CASNCP constructed route, and (c) MPCR constructed route.

MPCR algorithm described in Section 3.3.1 on this example, we find that MPCR chooses the route given by $w_{MPCR} = \{(0, 5, 1), (1, 2, 6), (6, 11, 7)\}$ as shown in Figure 3.4 (c). If the MPCR is routing the data in the horizontal (vertical) direction only, MPCR considers the receiver to be the sender's nearest node towards the destination and the relay to be the node nearest to the receiver along the vertical (horizontal) direction. In this example, we can visually notice the difference between the routes chosen by the MPCR and CASNCP routing algorithms.

We define the power saving of scheme 2 with respect to scheme 1 as

$$\text{Power Saving} = \frac{P_{Scheme1} - P_{Scheme2}}{P_{Scheme1}} \ \% \ . \tag{3.34}$$

At throughput $\eta_o = 1.96$ b/s/Hz and path loss exponent $\alpha = 4$, the power saving ratios of the MPCR with respect to the SNCP and CASNCP in this example are 64.14% and 30.47%, respectively. Also, the power saving of the CASNCP with respect to the SNCP is 48.42%.

The average required transmission power by each algorithm can be calculated as

$$P(\text{route}) = \sum_{i=1}^{N-1} \sum_{j=0}^{i} P(route|\sqrt{i^2 + j^2}) \times \Pr(\sqrt{i^2 + j^2}) \ , \tag{3.35}$$

where i and j denote the number of hops between the source and destination in the horizontal and vertical directions, respectively. In addition, $\sqrt{i^2 + j^2}$ denotes the distance between the source and the destination. The PMF $\Pr(\sqrt{i^2 + j^2})$, which depends on the number of hops between the source and destination as well as their

relative locations, is given by

$$\Pr(\sqrt{i^2+j^2}) = \begin{cases} \frac{1}{N^2}, & \text{i=j=0;} \\ \frac{4\,(N-i)\,(N-j)}{N^4}, & \text{i=j or j=0;} \\ \frac{8\,(N-i)\,(N-j)}{N^4}, & \text{otherwise} \end{cases} \quad \text{for } j \leq i \text{ and } 0 \leq i \leq (N-1). \tag{3.36}$$

We explain (3.36) similar to (3.30) as follows. The probability of choosing a certain node to be the source or the destination is $\frac{1}{N^2}$. Thus, the probability of choosing any source-destination pair is given by $\frac{1}{N^2} \times \frac{1}{N^2} = \frac{1}{N^4}$. There are N^2 possible combinations, in which the source and the destination are the same. Hence at $i = j = 0$, $\Pr(0) = \frac{N^2}{N^4} = \frac{1}{N^2}$. In the following, we consider only the lower triangular part, i.e., $j \leq i$. At $j = 0$, the grid network reduces to the linear case with $N - i$ possible source-destination pairs. For source-destination pair separated by $i = j$ hops in the horizontal and vertical directions, the number of possible source-destination pairs in one direction (e.g. left to right) is $(N - i) \times (N - j)$. This result is very similar to the one in (3.30) with considering the nodes on two dimensions instead of one dimension only in the linear case. At $i = j$ or $j = 0$, and considering the upper triangular part ($\times 2$) and reversing the source-destination pairs ($\times 2$), then the probability of having such source-destination pairs is $4\frac{(N-i)\,(N-j)}{N^4}$. For the third component in (3.36) i.e., at $j < i$, we additionally multiply this number by 2 to compensate the other combinations when i and j can be interchanged while giving the same distance of $\sqrt{i^2+j^2}$, which results in a total of 8.

The MPCR end-to-end transmission power can be calculated as

$$\begin{aligned} P_{MPCR}(\text{route}|\sqrt{i^2+j^2}) &= P^C_{tot}(\sqrt{2}\,d_0, d_0, d_0) \times j \\ &+ P^C_{tot}(d_0, \sqrt{2}\,d_0, d_0) \times |i-j|\,, \end{aligned} \tag{3.37}$$

where the first term represents the diagonal walk for j steps and the second term represents the horizontal $|i-j|$ steps. The CASNCP end-to-end transmission power is calculated by

$$P_{CASNCP}(\text{route}|\sqrt{i^2+j^2}) =$$
$$\begin{cases} P^C_{tot}(\sqrt{2}\,d_0, d_0, d_0) \times j + P^C_{tot}(2\,d_0, d_0, d_0) \times \frac{|i-j|}{2} & (|i-j|) \text{ is even;} \\ P^C_{tot}(\sqrt{2}\,d_0, d_0, d_0) \times j + P^C_{tot}(2\,d_0, d_0, d_0) \times \frac{|i-j-1|}{2} + P^D(d_0) & (|i-j|) \text{ is odd.} \end{cases} \tag{3.38}$$

Finally, the SNCP end-to-end transmission power is given by

$$P_{SNCP}(\text{route}|\sqrt{i^2+j^2}) = P^D(d_0) \times (i+j)\ , \tag{3.39}$$

which represents a direct transmission over $i+j$ hops, each of length d_0. The average end-to-end transmission power for any routing scheme can be calculated by substituting the power formulas for the MPCR, CASNCP, and SNCP (given by (3.37), (3.38), and (3.39), respectively) in (3.35).

3.3.4 Comparisons

We assume the required throughput is $\eta_0 = 1.96$ b/s/Hz, the transmission rate is $R_0 = 2$ b/s/Hz, the noise variance is $N_0 = -70$ dBm, and the path loss exponent is $\alpha = 4$. In Figure 3.5, we show the total required transmission power for the three routing algorithms as a function of the number of hops between the source and destination in regular networks. First, we consider a linear network of $N = 20$ nodes and the inter-node distance is $d_0 = 2$. Figure 3.5 (a) depicts the average transmission power, required by the three routing algorithms, as a function of the number of hops between the source and the destination. As shown, the MPCR algorithm requires the least transmission power for any particular number of hops.

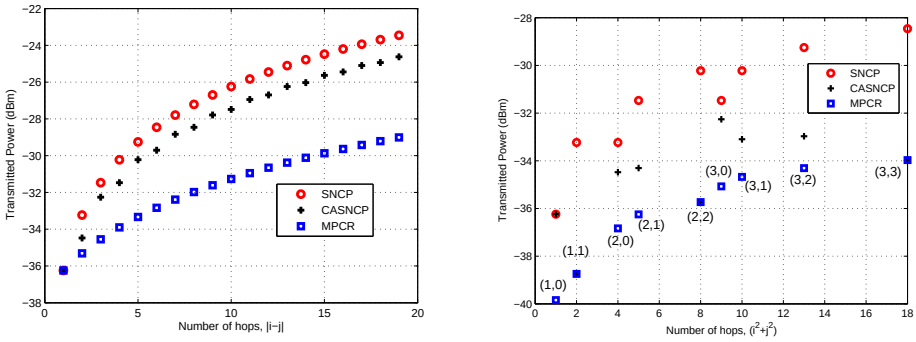

(a) (b)

Figure 3.5: Required transmission power per route versus the number of hops in regular (a) 20-node linear network, (b) 16-node grid network.

Second, we consider a 4×4 grid network, $N = 4$, and the inter-node distance is $d_0 = 2$. As described before, let i and j denote the number of hops between the source and the destination in the horizontal and vertical directions, respectively. In Figure 3.5 (b), we show the required transmission power by the various routing algorithms as a function of the squared distance $(i^2 + j^2)$ between the source and the destination. Each point is identified using the notation (i, j), where $j \leq i, 0 \leq i \leq 3$. This determines the relative positions of the source and destination. As shown, the MPCR algorithm requires the least transmission power for any source-destination pair. We note that in the diagonal case $i = j$, the MPCR and CASNCP algorithms require the same transmission power, as they both construct the same routes. In addition, the SNCP algorithm requires the same transmission power for different source-destination pairs, which have the same total number of hops $i + j$.

Figure 3.6 depicts the end-to-end transmission power in linear and grid networks of the three different routing algorithms for throughput $\eta_0 = 1.96$ b/s/Hz ,transmission rate $R_0 = 2$ b/s/Hz, noise variance $N_0 = -70$ dBm, and path loss

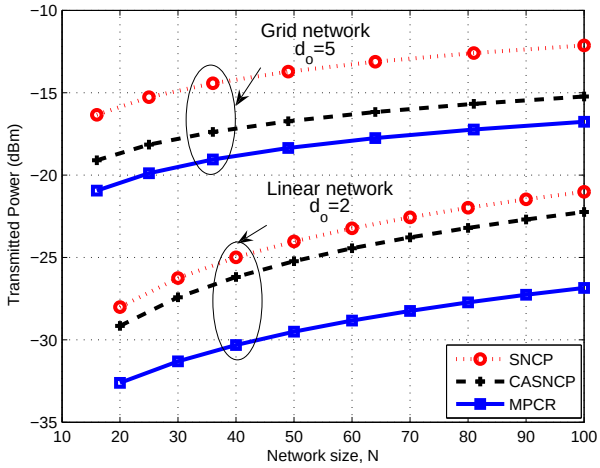

Figure 3.6: Required transmission power per route versus the network size for $N_0 = -70$ dBm, $\alpha = 4$, $\eta_0 = 1.96$ b/s/Hz, and $R_0 = 2$ b/s/Hz in regular linear and grid networks.

$\alpha = 4$. In both networks, the MPCR algorithm requires the minimum end-to-end transmission power compared to both CASNCP and SNCP routing algorithms.

For the linear network, Figure 3.7 (a) depicts the power saving (3.34) versus the network size for the network setup defined above. It is shown that at $N = 100$ nodes, the power savings of the MPCR with respect to SNCP and CASNCP algorithms are 73.91% and 65.61%, respectively. On the other hand, applying cooperation over the shortest-path route results in power saving of 24.57% only, as illustrated in the the CASNCP with respect to the SNCP curve. Similarly, Figure 3.7 (b) depicts the power savings for the grid network. At $N = 100$ nodes, the power savings of the MPCR with respect to SNCP and CASNCP algorithms are 65.63% and 29.8%, respectively. Applying cooperation over the shortest-path route results in power saving of 51.04%.

In this section, we have proposed two cooperation-based routing algorithms

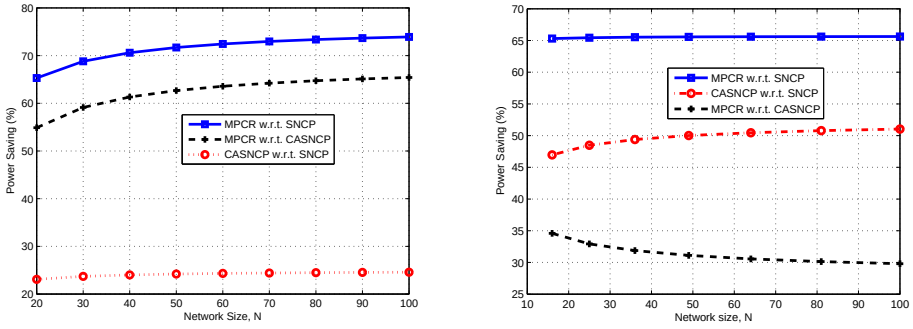

(a) (b)

Figure 3.7: Power saving due to cooperation versus the network size for $N_0 = -70$ dBm, $\alpha = 4$, $\eta_0 = 1.96$ b/s/Hz, and $R_0 = 2$ in regular (a) linear network, (b) grid network.

and applied them on regular networks. In the next section, we show the reduction in the end-to-end transmission power due to cooperation in random networks.

3.4 Numerical Results

In this section, we consider the random network case, in which nodes are deployed randomly in the network area. More precisely, we present computer simulations to illustrate the power savings of our proposed cooperation-based routing algorithms in random networks. We consider a 200m x 200m square, where N nodes are uniformly distributed. The additive white Gaussian noise has variance $N_0 = -70$ dBm and the path loss exponent is $\alpha = 4$. Given a certain network topology, we randomly choose a source-destination pair and apply the various routing algorithms, discussed in Section 3.3, to choose the corresponding route. For each algorithm, we calculate the total transmission power per route. Finally, these quantities are averaged over 1000 different network topologies.

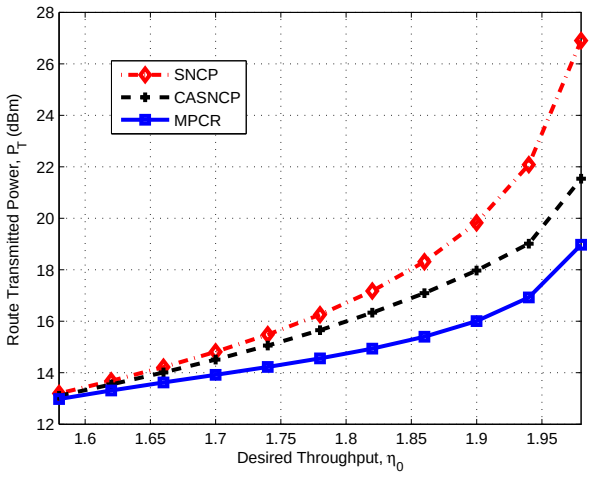

Figure 3.8: Required transmission power per route versus the desired throughput for $N = 20$ nodes, $\alpha = 4$, $N_0 = -70$ dBm, and $R_0 = 2$ b/s/Hz in a 200m x 200m random network.

First, we illustrate the effect of varying the desired throughput on the required transmission power per route. Figure 3.8 depicts the transmission power per route, required by the different routing algorithms. It is shown that the SNCP algorithm, which applies the Bellman-Ford shortest-path algorithm requires the most transmission power per route. Applying the cooperative communication mode on each three consecutive nodes in the SNCP route results in reduction in the required transmission power as shown in the CASNCP routing algorithm's curve. Moreover, the MPCR algorithm requires the least transmission power among the other routing algorithms.

One of the major results of this chapter is that the MPCR algorithm requires less transmission power than the CASNCP algorithm. Intuitively, this result is because the MPCR applies the cooperation-based link cost formula to construct the minimum-power route. On the contrary, the CASNCP algorithm first constructs

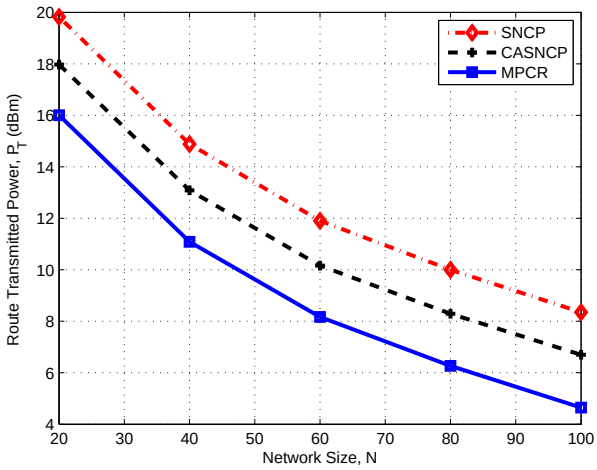

Figure 3.9: Required transmission power per route versus the number of nodes for $\eta_o = 1.9$ b/s/Hz and α=4 in a 200m x 200m random network.

shortest-path route then it applies the cooperative communication protocol on the established route. Therefore, the CASNCP algorithm is limited to applying the cooperative-communication protocol on a certain number of nodes, while the MPCR algorithm can consider any node in the network to be in the CT blocks, which constitute the route. Thus, the MPCR algorithm reduces the required transmission power more than the CASNCP algorithm.

Figure 3.9 depicts the required transmission power per route by the different routing algorithms for different number of nodes at $p_o^S = 0.95$ and $\eta_o = 1.9$ b/s/Hz. As shown, the required transmission power by any routing algorithm decreases with the number of nodes. Intuitively, the higher the number of nodes in a fixed area, the closer the nodes to each other, the lower the required transmission power between these nodes, which results in lower required end-to-end transmission power. We also calculate the power saving ratio as a measure of the improvement of the MPCR algorithm. At $N = 100$ nodes, $p_o^S = 0.95$, and $\eta_o = 1.9$ b/s/Hz, the power savings

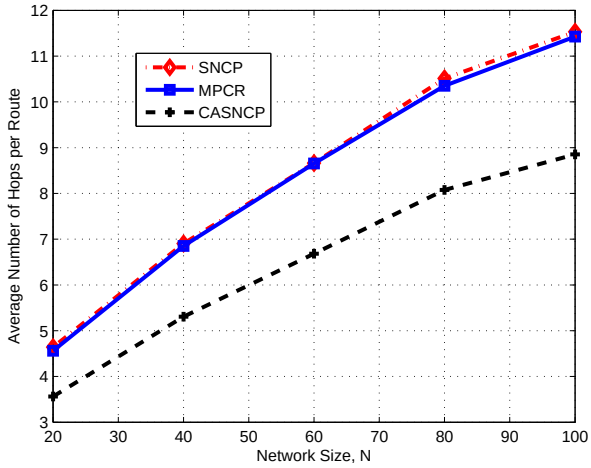

Figure 3.10: Average number of hops per route versus the number of nodes for $\eta_o = 1.9$ b/s/Hz and α=4 in a 200m x 200m random network.

of MPCR algorithm with respect to the SNCP and CASNCP algorithms are 57.36% and 37.64%, respectively. In addition, the power saving of the CASNCP algorithm with respect to the SNCP algorithm is 31.62%.

In Figure 3.10 the average number of hops in each route, constructed by the different routing algorithms, is shown versus the number of nodes in the network. For the cooperative transmission mode, the average number of hops is defined as

$$h^C = 1 \cdot \Pr(\phi) + 2 \cdot \overline{\Pr(\phi)} = 2 - \Pr(\phi) \ , \tag{3.40}$$

and the average number of hops for the direct transmission mode is one. As shown, the routes constructed by either the CASNCP or the MPCR algorithms consist of number of hops that is less than the routes constructed by the SNCP algorithm. Moreover, the average number of hops increases with N as there are more available nodes in the network, which can be employed to reduce the transmission power. Although the MPCR scheme requires less power than the CASNCP routing algorithm, but it requires longer delay. Intuitively, this is because the minimum-power

routes may involve more nodes. This shows the tradeoff between the required power and the delay in the routes chosen by the MPCR and CASNCP routing schemes.

Chapter 4

Connectivity-Aware Network Maintenance and Repair via Relays Deployment

In Chapter 3, we have proposed cooperative network algorithm that reduces the end-to-end transmission power given a certain throughput, by utilizing some of the nodes in the network as relays. Relays can be also utilized to increase the network lifetime in some networks such as wireless sensor networks. In this chapter, we focus on wireless sensor networks and investigate the possibility of maximizing the network lifetime by deploying a set of relays. Furthermore, we study the impact of deploying relays on reconnecting disconnected networks.

Recently, there have been much interest in wireless sensor networks due to its various application areas such as battlefield surveillance systems, target tracking, and industry monitoring systems [54]. A sensor network consists of a large number of sensor nodes, which are deployed in a particular area to measure certain phenomenon such as temperature and pressure. These sensors send their measured

data to a central processing unit (information sink), which collects the data and develops a decision accordingly. Often sensors have limited energy supply. Hence efficient utilization of the sensors' limited energy, and consequently extending the network lifetime, is one of the design challenges in wireless sensor networks.

The network lifetime is defined in this chapter as the time until the network becomes disconnected. The network is considered connected if there is a path, possibly a multi-hop one, from each sensor to the central processing unit. In various applications, sensors are deployed randomly in the field and there is no much control over the specific location of each sensor. In the scenario where relays are available, it could be possible to deploy relays in some particular locations to enhance the network performance and extend its lifetime. An example is that low-altitude unmanned air vehicle (UAV) can perform as a relay that can be deployed in particular locations. Throughout this work, we assume that the deployed relays have the same capability as that of the sensors. Particularly, the relays forward the received data without any processing operations.

Deploying a set of relays in a wireless sensor network is one of the main approaches to extend the network lifetime. More precisely, relays can forward the sensors' data and hence they contribute to reducing the transmission power required by many sensors per transmission, which can extend the lifetime of these sensors. However, the problem of finding the locations of these relays is shown to be NP-hard [55]. Therefore, there is a need to find a heuristic algorithm that can find near-optimum locations for the available set of relays in polynomial time. This problem is referred to in the literature as *network maintenance* problem.

In wireless sensor networks and after deploying the sensors for a while, some sensors may lose their available energy, which affects each sensor's ability to send

its own data as well as forward the other sensors' data. This affects the network connectivity and may result in the network being disconnected. In this case, there is a need to determine the minimum number of relays along with their locations that are needed to reconnect this network. Similar to the network maintenance problem, this problem is NP-complete [56] and there is a need for a heuristic algorithm to solve this problem in polynomial time. This problem is referred to as *network repair* problem.

In this chapter, we address the network maintenance and network repair problems in wireless sensor networks. We propose various cross-layer algorithms for relay deployment and data routing, which are jointly designed across the physical and network layers. First, we propose an efficient network maintenance algorithm that finds the locations for an available set of relays to extend the network lifetime. The network connectivity and consequently the network lifetime are quantified via the Fiedler value, which is the algebraic connectivity of the network graph. The Fiedler value is equal to the second smallest eigenvalue of the Laplacian matrix representing the network graph. The proposed network maintenance algorithm aims at formulating the network lifetime problem as a semi-definite programming (SDP) optimization problem that can be solved in polynomial time.

Building upon the proposed network maintenance algorithm, we propose a routing algorithm, namely, Weighted Minimum Power Routing (WMPR) algorithm, that can extend the network lifetime whenever the deployed relays have higher initial energy than that of the existing sensors. The WMPR assigns weights to the sensors that are different from that of the relays. It tends to use the relays more often and hence balance the network load among the existing sensors and relays, which results in longer network lifetime. Furthermore, we propose an adaptive

network maintenance algorithm that increases the network lifetime by relocating the relays depending on the network status. We consider the Fiedler value of the remaining network as a good *network health indicator*. Finally, we propose an iterative network repair algorithm which finds a solution for the minimum number of relays along with their locations needed to reconnect a disconnected network.

The proposed network maintenance algorithms are applied in two different transmission scenarios depending on the employed medium access control protocol. First, we consider a zero-interference scenario where each node is assigned an orthogonal channel and hence there is no interference among the nodes. Second, we consider an interference-based scenario where a set of nodes is allowed to send simultaneously and hence causing interference to each other. We show that the transmission power required by each sensor per transmitted packet is higher in the interference-based scenario compared to that in the zero-interference scenario. Therefore in a limited-energy network setup, where network lifetime is of big concern, a zero-interference transmission scenario should be favorably considered to extend the network lifetime.

The remainder of this chapter is organized as follows. In the next section, we summarize some related work. In Section 4.2, we describe the system model and present a brief revision on the algebraic connectivity of a graph. We formulate the network maintenance problem and describe the proposed algorithm in Section 4.3. We build upon that algorithm and propose different strategies to increase the network lifetime in Section 4.4. In Section 4.5, we address the network repair problem and describe the proposed algorithm. In Section 4.6, we present some simulation results that show the significance of our proposed algorithms.

4.1 Related Work

In this section, we briefly review some of the existing network maintenance and network repair strategies in wireless sensor networks. Most of the previous works consider the time until the first sensor dies, i.e., runs out of energy, as the network lifetime. In sensor networks, sensors are usually deployed with large numbers and each area is often covered by more than one sensor. Therefore, there is a strong correlation in the sensors' information and that the death of one sensor may not affect the performance of the others sending their measurements to the central unit. Thus, we consider the time until the network becomes disconnected as the network lifetime [57, 58].

Recently, there have been numerous network maintenance algorithms [55, 59, 60]. In [55], the problem of provisioning additional energy on the existing sensors along with deploying additional relays in two-tier wireless sensor networks was considered. It was shown that the problem of joint design of energy provisioning and relay node placement can be formulated as a mixed-integer nonlinear programming problem, which is NP-hard in general. A relay deployment algorithm that maximizes the minimum sensor lifetime by exploiting the cooperative diversity was proposed in [59]. In [60], a joint design of relay deployment and transmission power control was considered to maximize the network lifetime. In that work, there is no solution to deploy the relays in particular locations, instead the probability distribution of the relays' location is quantified. More precisely, the relay density is higher near the central unit.

There have been recent works that considered the connectivity in wireless sensor networks [61–63]. In [61], the problem of adding relays to improve the connectivity of multi-hop wireless networks was addressed. A set of designated points are given

and the available relays must be deployed in a smaller set of these designated points. The set of relay locations, are determined based on testing all the designated points and choosing the combination, which results in higher connectivity measure. Obviously, this scheme is very complex as the network size increases. In [62], three random deployment strategies, namely, connectivity-oriented, lifetime-oriented, and hybrid-oriented, were proposed. However, there is no explicit optimization problem for maximizing the network lifetime in that work. A mathematical approach to positioning and flying an unmanned air vehicle (UAV) over a wireless ad hoc network in order to optimize the network's connectivity for better Quality of Service (QoS) and coverage was proposed in [63].

Several works have considered the network repair problem, in which the objective is to find the minimum number of relays needed to have a connected graph. This is the same problem as the Steiner minimum tree with minimum number of Steiner points and bounded edge length problem defined in [64], which is NP-hard. Several approximate algorithms have been proposed to solve it in [56, 65–67]. For instance, in [67] the proposed algorithm first computes the minimum spanning tree (MST) of the given graph, then it adds relays on the MST edges, which are not existing in the original graph. The connectivity improvement using Delaunay Triangulation [56] constructs a Delaunay Triangulation in the disconnected network and deploy nodes in certain triangles according to several criteria. The network repair problem has been generalized to k-connectivity, both in the sense of edge and vertex connectivity, in [68].

Finally, we point out some of the unique aspects of our work compared to the existing works summarized above. First, the topology model is based on some of the physical layer parameters. More precisely, the graph edges are constructed

based on the desired bit error rate, maximum transmission power of the sensors, noise variance, and Rayleigh fading channel model parameters. This helps in proposing cross-layer design of relay deployment and data routing schemes. Second the Fiedler value, which is a good measure of the connectivity, is considered as the network health indicator. Third, the main relay deployment algorithm is less complex than the previously proposed algorithms, because it is based on a SDP formulation, which can be solved in polynomial time.

4.2 System Model

In this section, first we describe the wireless sensor network model. Second, we derive the required transmission power to achieve a particular Quality of Service (QoS), which is the bit error rate in this work. Finally, we briefly review some concepts related to the spectral graph theory.

A wireless sensor network can be modeled as an undirected weighted simple finite graph $G(V, E)$, where $V = \{v_1, v_2, \cdots, v_n\}$ is the set of all nodes (sensors) and E is the set of all edges (links). An undirected graph implies that all the links in the network are bidirectional, hence, if node v_i can reach node v_j then the opposite is also true. A simple graph means that there is no self loop in each node and there are no multiple edges connecting two nodes. Finally, a finite graph implies that the cardinality of the sets V and E is finite. Let n and m denote the number of nodes and edges in the graph, respectively, i.e., $|V| = n$ and $|E| = m$, where $|\,.\,|$ denotes the cardinality of the given set.

We assume that binary phase shift keying (BPSK) modulation scheme is employed for the transmission between any two nodes. BPSK is primarily chosen since the data rate in most of the sensor network applications is relatively low, and

the BPSK modulation is an intuitive choice for such applications. We point out that the proposed algorithms can be easily applied with other modulation types as well. Let $d_{i,j}$ denote the distance between two nodes $\{v_i, v_j\} \in V$ and let α denote the path loss exponent. The channel between each two nodes $\{v_i, v_j\} \in V$, denoted by $h_{i,j}$, is modeled as a complex Gaussian random variable with zero-mean and variance equal to $d_{i,j}^{-\alpha}$, i.e., $h_{i,j} \sim CN(0, d_{i,j}^{-\alpha})$. Thus, the channel gain $|h_{i,j}|$ follows a Rayleigh fading model [[53], Ch.14]. Furthermore, the channel gain squared $|h_{i,j}|^2$ is an exponential random variable with mean $d_{i,j}^{-\alpha}$, i.e., $p(|h_{i,j}|^2) = d_{i,j}^{\alpha} \exp(-|h_{i,j}|^2 d_{i,j}^{\alpha})$ is the probability density function (pdf) of $|h_{i,j}|^2$. The noise in each transmission is modeled as a Gaussian random variable with zero-mean and variance N_0.

Without loss of generality, we assume the zero-interference transmission scenario[1], in which sensors transmit their data over orthogonal channels whether in time or frequency domain. For instance, we consider the Time Division Multiple Access (TDMA) scenario. The transmission from node v_i to v_j can be modeled as

$$y_j = \sqrt{P_i}\, h_{i,j}\, x_i + n_j \;, \tag{4.1}$$

where x_i is the transmitted symbol with unit energy, i.e., $|x_i|^2 = 1$. In (4.1), P_i is the transmitted power, y_j is the received symbol, and n_j is the added noise term.

The probability of bit error, or bit error rate (BER), can be calculated as [[53], Ch.14]

$$\varepsilon = \frac{1}{2}\Big(1 - \sqrt{\frac{\gamma_{i,j}}{1+\gamma_{i,j}}}\Big) \;, \tag{4.2}$$

where $\gamma_{i,j} = \frac{P_i\, d_{i,j}^{-\alpha}}{N_0}$ denotes the average signal-to-noise ratio (SNR). The transmission power of node v_i, required to achieve a desired average BER of ε^o over link

[1]The transmission scenario that takes into consideration the interference effect is a simple extension of the zero-interference scenario, and it will be addressed in Section 4.6.1

(v_i, v_j), can be calculated from (4.2) as

$$P_i^o = d_{i,j}^{\alpha} \, N_0 \, \frac{(1 - 2\,\varepsilon^o)^2}{1 - (1 - 2\,\varepsilon^o)^2} \; , \tag{4.3}$$

which is the required transmission power for the zero-interference transmission scenario.

We assume that each node $v_i \in V$ can transmit with power $0 \leq P_i \leq P_{max}$, where P_{max} denotes the maximum transmission power of each node. Also, we assume that the noise variance and the desired BER are constant for all the transmissions in the network. Therefore, an undirected weighted edge (v_i, v_j) exists if $P_i^o \leq P_{max}$, where P_i^o is calculated as in (4.3). Furthermore, the weight of an edge l connecting v_i and v_j, denoted by $w_{i,j}$ or w_l, is a function of the transmitted power P_i^o that depends on the considered routing scheme, as will be discussed in Section 4.4.1.

For an edge l, $1 \leq l \leq m$, connecting nodes $\{v_i, v_j\} \in V$, define the edge vector $\mathbf{a_l} \in \mathbf{R^n}$, where the i-th and j-th elements are given by $a_{l,i} = 1$ and $a_{l,j} = -1$, respectively, and the rest is zero. The *incidence* matrix $\mathbf{A} \in \mathbf{R^{n \times m}}$ of the graph G is the matrix with l-th column given by $\mathbf{a_l}$. The weight vector $\mathbf{w} \in \mathbf{R^m}$ is defined as $\mathbf{w} = [w_1, w_2, ..., w_m]^T$, where T denotes transpose.

The *Laplacian* matrix $\mathbf{L} \in \mathbf{R}^{n \times n}$ is defined as

$$\mathbf{L} = \mathbf{A} \, \mathrm{diag}(\mathbf{w}) \, \mathbf{A}^T = \sum_{l=1}^{m} w_l \, \mathbf{a_l} \, \mathbf{a_l}^T \; , \tag{4.4}$$

where $\mathrm{diag}(\mathbf{w}) \in \mathbf{R}^{m \times m}$ is the diagonal matrix formed from $\mathbf{w}$. The diagonal entry $L_{i,i} = \sum_{j \in N(i)} w_{i,j}$, where $N(i)$ is the set of neighboring nodes of node v_i that have a direct edge with node v_i. $L_{i,j} = -w_{i,j}$ if $(v_i, v_j) \in E$, otherwise $L_{i,j} = 0$. Since all the weights are nonnegative, the Laplacian matrix is positive semi-definite, which is expressed as $\mathbf{L} \succeq 0$. In addition, the smallest eigenvalue is zero, i.e., $\lambda_1(\mathbf{L}) = 0$.

The second smallest eigenvalue of $\mathbf{L}$, $\lambda_2(\mathbf{L})$, is the algebraic connectivity of the graph G [69–72]. It is called *Fiedler value* and it measures how connected the graph is because of following main reasons. First, $\lambda_2(\mathbf{L}) > 0$ if and only if G is connected and the multiplicity of the zero-eigenvalue is equal to the number of the connected sub-graphs. Second, $\lambda_2(\mathbf{L})$ is monotone increasing in the edge set, i.e.,

$$\begin{aligned} &\text{if} \quad G_1 = (V, E_1)\ , G_2 = (V, E_2)\ , E_1 \subseteq E_2 \\ &\text{then} \quad \lambda_2(\mathbf{L_1}) \leq \lambda_2(\mathbf{L_2})\ , \end{aligned} \tag{4.5}$$

where $\mathbf{L_q}$ denotes the Laplacian matrix of the graph G_q for $q = 1, 2$.

As we mentioned previously, the smallest eigenvalue of the Laplacian matrix is $\lambda_1(\mathbf{L}) = 0$. In addition, its corresponding eigenvector is the all-ones vector $\mathbf{1} \in \mathbf{R}^n$, as the sum of the elements in each row (column) is zero. Let $\mathbf{y} \in \mathbf{R}^n$ be the eigenvector corresponding to $\lambda_2(\mathbf{L})$, which has unity norm $||\mathbf{y}|| = 1$ and is orthogonal to the all-ones vector, i.e., $\mathbf{1}^T\mathbf{y} = 0$. Since, $\mathbf{L}\,\mathbf{y} = \lambda_2\,\mathbf{y}$, hence $\mathbf{y}^T\,\mathbf{L}\,\mathbf{y} = \lambda_2\ \mathbf{y}^T\,\mathbf{y} = \lambda_2$. Therefore, the Fiedler value can be expressed as the smallest eigenvalue that satisfy these conditions, i.e.,

$$\lambda_2(\mathbf{L}) = \inf_{\mathbf{y}} \{\mathbf{y}^T\,\mathbf{L}\,\mathbf{y}\ ,\ ||\mathbf{y}||_2 = 1,\ \mathbf{1}^T\,\mathbf{y} = 0\}\ . \tag{4.6}$$

In this work, the network lifetime is defined as the time until the network becomes disconnected, which happens when there is no communication path from any existing sensor to the central unit [57, 58]. Consequently, the network dies (becomes disconnected) if there is no communication path between any two living nodes including the central unit. Therefore, there is a direct relation between keeping the network connected as long as possible and maximizing the network lifetime, as was shown in [57, 58]. As discussed before, the Fiedler value defines the algebraic connectivity of the graph and it is a good measure of how connected

the graph is. Intuitively the higher the Fiedler value is, the more edges that exist between the nodes, the longer the network can live without being disconnected, and thus the higher the network lifetime is. Based on that, we consider the Fiedler value as a quantitative measure of the network lifetime. In Section 4.6, we will validate this direct relation between the Fiedler value and the network lifetime.

4.3 Network Maintenance

The network maintenance problem can be stated as follows. Given a wireless network deployed in a $g \times g$ square area and represented by the graph $G_b = (V_b, E_b)$, as well as a set of K relays, what are the locations for placing relays in order to maximize the Fiedler value of the resulting network? Intuitively, adding a relay to the network may result in connecting two sensors or more, which were not connected together. Because this relay can be within the transmission range of these sensors, hence it can forward data from one sensor to the other. Therefore, adding a relay may result in adding an edge or more to the original graph.

Let $E_c(K)$ denote the set of edges resulting from adding a candidate set of K relays. Thus, the network maintenance problem can be formulated as

$$\max_{E_c(K)} \quad \lambda_2\Big(\mathbf{L}\big(E_b \cup E_c(K)\big)\Big) \ . \tag{4.7}$$

Since each relay can be deployed anywhere in the network, the location of each relay is considered as a continuous variable, which belongs to the interval $([0, g], [0, g])$. It has been shown that this problem is NP-hard in [55]. In the following subsection, we explain our proposed heuristic algorithm to solve this problem.

4.3.1 SDP-based Network Maintenance Algorithm

Our proposed algorithm to solve the network maintenance problem in (4.7) can be described as follows. First, we divide the $g \times g$ network area into n_c equal square regions, each with width h. Thus, $n_c = (\frac{g}{h})^2$. We represent each region by a relay deployed in its center. Thus, the problem can be viewed as having a set of n_c candidate relays, hence the subscript c, and we want to choose the optimum K relays among these n_c relays. This optimization problem can be formulated as

$$\begin{aligned} &\max \ \ \lambda_2\big(\mathbf{L}(\mathbf{x})\big) \\ &\text{s.t.} \ \ \mathbf{1}^T\mathbf{x} = K, \ \mathbf{x} \in \{0,1\}^{n_c} \ , \end{aligned} \tag{4.8}$$

where

$$\mathbf{L}(\mathbf{x}) = \mathbf{L}_b + \sum_{l=1}^{n_c} x_l \, \mathbf{A}_l \, \mathrm{diag}(\mathbf{w}_l) \, \mathbf{A}_l^T \ , \tag{4.9}$$

and $\mathbf{1} \in \mathbf{R}^{n_c}$ is the all-ones vector.

We note that the optimization vector in (4.8) is the vector $\mathbf{x} \in \mathbf{R}^{n_c}$. The i-th element of $\mathbf{x}$, denoted by x_i, is either 1 or 0, which corresponds to whether this relay should be chosen or not, respectively. In (4.9), $\mathbf{L}_b$ is the Laplacian matrix of the base graph. In addition, $\mathbf{A}_l$ and $\mathbf{w}_l$ are the incidence matrix and weight vector resulting from adding relay l to the original graph. Assuming that adding relay l results in I_l edges between the original n nodes in the base network, then the matrix $\mathbf{A}_l$ can be formed as $\mathbf{A}_l = [\mathbf{a}_l^1, \mathbf{a}_l^2, \cdots, \mathbf{a}_l^{I_l}]$, where $\mathbf{a}_l^z \in \mathbf{R}^n$, $z = 1, 2. \cdots, I_l$, represents an edge between two original nodes. Similarly, $\mathbf{W}_l = [\mathbf{w}_l^1, \mathbf{w}_l^2, \cdots, \mathbf{w}_l^{I_l}]$. We point out that the effect of adding relays appears only in the edge set E, and not in the node set V. The weight of a constructed edge equals the summation of the weights of the edges connecting the relay with the two sensors. Finally, the constraint $\mathbf{1}^T\mathbf{x} = K$ in (4.8) indicates that the number of chosen relays is K.

The exhaustive search scheme to solve (4.8) is done by computing $\lambda_2(\mathbf{L})$ for different $\binom{n_c}{K}$ Laplacian matrices, which requires huge amount of computation for large n_c. Therefore, we need an efficient and quick way to solve (4.8). The optimization problem (4.8) can be thought of as a general version of the one considered in [70]. By relaxing the Boolean constraint $\mathbf{x} \in \{0,1\}^{n_c}$ to be a linear constraint $\mathbf{x} \in [0,1]^{n_c}$, we can represent the optimization problem in (4.8) as

$$\begin{aligned} &\max \ \lambda_2\big(\mathbf{L}(\mathbf{x})\big) \\ &\text{s.t. } \mathbf{1}^T\mathbf{x} = K, 0 \leq \mathbf{x} \leq 1 \ . \end{aligned} \tag{4.10}$$

We note that the optimal value of the relaxed problem in (4.10) is an upper bound for the optimal value of the original problem (4.8), as it has a larger feasible set.

Similar to (4.6), the Fiedler value of $\mathbf{L}(\mathbf{x})$ can be expressed as

$$\lambda_2\big(\mathbf{L}(\mathbf{x})\big) = \inf_{\mathbf{y}} \{\mathbf{y}^T\mathbf{L}(\mathbf{x})\,\mathbf{y} \ , \ ||\mathbf{y}||_2 = 1, \ \mathbf{1}^T\mathbf{y} = 0\} \ . \tag{4.11}$$

It can be shown that $\lambda_2\big(\mathbf{L}(\mathbf{x})\big)$ in (4.11) is the point-wise infimum of a family of linear functions of $\mathbf{x}$. Hence, it is a concave function in $\mathbf{x}$. In addition, the relaxed constraints are linear in $\mathbf{x}$. Therefore, the optimization problem in (4.10) is a *convex optimization* problem [73]. Furthermore, the convex optimization problem in (4.10) is equivalent to the following semi-definite programming (SDP) optimization problem [70, 72]

$$\begin{aligned} &\max \ s \\ &\text{s.t. } s(\mathbf{I} - \frac{1}{n}\mathbf{1}\,\mathbf{1}^T) \preceq \mathbf{L}(\mathbf{x}), \ \mathbf{1}^T\mathbf{x} = K, \ 0 \leq \mathbf{x} \leq 1 \ , \end{aligned} \tag{4.12}$$

where $\mathbf{I} \in \mathbf{R}^{n\times n}$ is the identity matrix and $\mathbf{B} \preceq \mathbf{A}$ denotes that $\mathbf{A} - \mathbf{B}$ is a positive semi-definite matrix.

By solving the SDP optimization problem in (4.12) efficiently using any SDP standard solver such as the SDPA-M software package [74], the optimization variable $\mathbf{x}$ is obtained. Then, we use a heuristic algorithm to obtain a near-optimal

Boolean solution from the SDP solution. In this chapter, we consider a simple heuristic, which is to set the largest K elements in the vector $\mathbf{x}$ to 1 and the rest to 0. The obtained Boolean vector is the near-optimum solution of the original problem in (4.8). This described procedure will be repeated a few times, and each repetition is referred to as a level. As indicated earlier, each location x_k, $k = 1, 2, \cdots, K$, represents a square region of width h. Choosing $x_k = 1$ implies that the k-th region is more significant, in terms of the connectivity of the whole network, than other ones that have not been chosen.

In order to improve the current solution, we repeat the same procedure by dividing each k-th region into n_c smaller areas and representing each area by a relay at its center. Then, we find the near-optimum location in these n_c regions to have the relay deployed there. This problem is the same as the one in (4.12) by setting $K = 1$ relay. The same procedure is repeated for each region k, $1 \leq k \leq K$, obtained in the first level. The proposed network-maintenance algorithm applies a finite number of levels until there is no more improvement in the resulting Fiedler value. Table 4.1 summarizes the implementation of our proposed network-maintenance algorithm.

We also discuss the complexity issue of the proposed network maintenance algorithm. The interior point algorithms for solving SDP optimization problems are shown to be polynomial in time [74]. Thus, the network maintenance algorithm which applies a small number of iterations, each requires solving SDP optimization problem, has a polynomial complexity in time. Finally, we point out that our network maintenance algorithm is also suitable for the kind of applications, where there is a possible locations for the relays to be deployed [61]. In this section, we have proposed a SDP-based network maintenance algorithm that deploys a finite

number of relays to maximize the Fiedler value of the resulting graph and consequently the network lifetime. In the next section, we consider various strategies to increase the efficiency of the deployed relays.

4.4 Lifetime-Maximization Strategies

In this section, we build upon the network maintenance algorithm described in Table 4.1 and propose two strategies that can extend the network lifetime. First, we propose the WMPR algorithm, which efficiently utilizes the deployed relays in a wireless network. Second, we propose an adaptive network maintenance algorithm that relocates the relays based on the network status.

4.4.1 Weighted Minimum Power Routing (WMPR) Algorithm

In this subsection, first we explain the conventional Minimum Power Routing (MPR) algorithm then we present the proposed WMPR algorithm. The MPR algorithm constructs the minimum-power route from each sensor to the central unit, by utilizing the conventional Dijkstra's shortest-path algorithm [52]. The cost (weight) of a link (v_i, v_j) is given by

$$w_{i,j}|_{MPR} = P_i^o + P_r \ , \tag{4.13}$$

where P_i^o is the transmission power given in (4.3) and P_r denotes the receiver processing power, which is assumed to be fixed for all the nodes.

In (4.13), it is obvious that the MPR algorithm does not differentiate between the original sensors and the deployed relays while constructing the minimum-power route. In most of the applications, it is very possible that the few deployed relays

have higher initial energy than that of the many existing sensors. Intuitively to make the network live longer, the relays should be utilized more often than the sensors. Consequently, the loads of the sensors and relays will be proportional to their energies, which results in more balanced network. The WMPR algorithm achieves this balance by assigning weights to the sensors and the relays, and the cost of each link depends on these weights. Therefore, we propose to have the weight of the link (v_i, v_j) given by

$$w_{i,j}|_{WMPR} = e_i \, P_i^o + e_j \, P_r \ , \tag{4.14}$$

where e_i denotes the weight of node v_i. By assigning the relays smaller weight than that of the sensors, the network becomes more balanced and the network lifetime is increased. In summary, the WMPR utilizes the Dijkstra's shortest-path algorithm to compute the route from each sensor to the central unit using (4.14) as the link cost. More importantly, weights of the relays should be smaller than that of the sensors.

Figure 4.1 depicts a sensor network of $n = 20$ nodes deployed randomly in $6m \times 6m$ area. The central unit is located in the center of the network and we assume that $K = 1$ relay is available. The location of the relay is determined via the network maintenance algorithm, proposed in Table 4.1. Each routing algorithm, either the MPR or the WMPR, constructs a tree connecting all the nodes together that has the minimum weight between each two nodes. In Figure 4.1 (a), the relay is treated in a similar fashion to that of the sensors in the MPR-based constructed routing tree. On the other hand Figure 4.1 (b) depicts that in the WMPR-based constructed routing tree, most of the sensors tend to send their packets to the relay rather than the neighboring sensors. As will be shown in Section 4.6, the WMPR algorithm achieves higher lifetime gain than that achieved by the MPR algorithm,

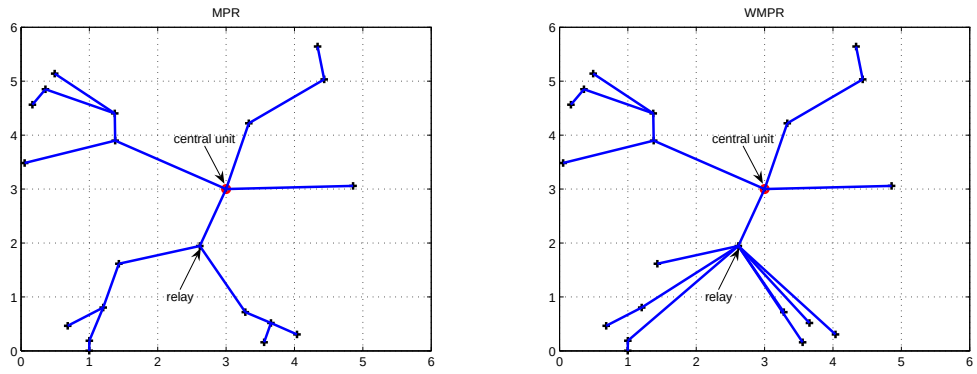

(a) (b)

Figure 4.1: Example of routing trees for $n = 20$ sensors deployed randomly in $6m \times 6m$ square field (a) MPR-based constructed routing tree and (b) WMPR-based constructed routing tree.

when the deployed relays have more initial energy than the sensors. Finally, we point out that many of the lifetime-maximization routing algorithms [57, 58, 75] can be modified in a similar way to that of the WMPR algorithm.

4.4.2 Adaptive Network Maintenance Algorithm

In this subsection, we consider the possibility of relocating the deployed relays. In the fixed network maintenance strategy, as described in Table 4.1, each relay will be deployed in a particular place and will be there until the network dies. Intuitively, the network lifetime can be increased by adaptively relocating the relays based on the status of the network. Such a scheme can be implemented via low-altitude Unmanned Air Vehicles (UAVs) or movable robots depending on the network environment. For instance, we can utilize one UAV or more, which can fly along the obtained relays' locations to improve the connectivity of the ground

network. In each location, UAV acts exactly as a fixed relay connecting a set of sensors through multi-hop relaying.

The proposed adaptive network-maintenance algorithm is implemented as follows. First, the initial locations of the deployed relays are determined using the network-maintenance algorithm described in Table 4.1. Whenever a node dies, the Fiedler value of the remaining network is calculated. If it is greater than certain threshold, then the network is likely to be disconnected soon. Therefore, the deployment algorithm is calculated again and the new relays' locations are obtained. Finally each relay is relocated to the new location, if it is different from its current one. The algorithm is repeated until the network is disconnected.

In the sequel, we present an example to illustrate how effective the adaptive network maintenance algorithm can be. Consider a wireless sensor network of $n = 20$ nodes deployed randomly in a $6m \times 6m$ square area. We assume that only $K = 1$ relay is available. Whenever a node sends a packet, the remaining energy is decreased by the amount of the transmission energy and it dies when it has no remaining energy. In addition, the Fiedler value threshold is chosen to be 0.03.

Figure 4.2 depicts the Fiedler value of the network as a function of the number of dead nodes utilizing the MPR algorithm. The original network is disconnected after the death of 8 nodes. By adding a fixed relay, the network lifetime increases, resulting in a network lifetime gain of 31%. The network lifetime gain due to adding K relays is defined as $G(K) = \frac{T(K)-T(0)}{T(0)}$ where $T(K)$ is the network lifetime after deploying K relays. By considering $K = 1$ relay, the adaptive network-maintenance algorithm achieves lifetime gain of 70%. This example shows that the proposed adaptive network maintenance algorithm can significantly increase the network lifetime. We clarify that these lifetime gains are specific to that

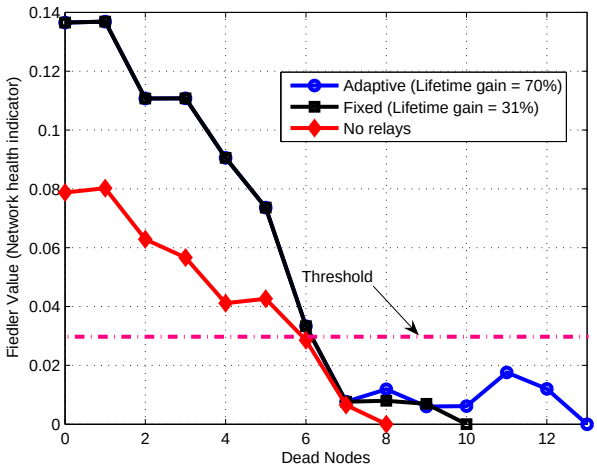

Figure 4.2: Fiedler value (Network health indicator) versus the number of dead nodes, for $n = 20$ sensors deployed randomly in $6m \times 6m$ square field, is plotted. Effects of adaptive and fixed network maintenance algorithms are illustrated.

particular example and do not represent the average results. The average results of the various proposed network maintenance strategies are provided in Section 4.6.

It is worth to note that Figure 4.2 shows that the Fiedler value of the living network can be thought of as a *health indicator* of the network. If the network health is below certain threshold, then the network is in danger of being disconnected. Thus, a network maintenance strategy, either fixed or adaptive, should be implemented. However, if the network becomes disconnected then intuitively we can consider reconnecting the network again via deploying the minimum number of relays. This is the network repair problem and it is discussed in the following section.

4.5 Network Repair

In this section, we consider the network repair problem. In particular, the network is initially disconnected and we need to find the minimum number of relays along with their locations in order to reconnect the network. Let a disconnected base network deployed in a $g \times g$ square area be represented by the graph $G_b = (V_b, E_b)$. Hence, $\lambda_2\Big(\mathbf{L}\big(E_b\big)\Big) = 0$. The network repair problem can be formulated as

$$\begin{aligned} &\min \;\; K \\ &\text{s.t.} \;\; \lambda_2\Big(\mathbf{L}\big(E_b \cup E_c(K)\big)\Big) > \delta \;, \end{aligned} \tag{4.15}$$

where $\delta > 0$ is referred to as *connectivity threshold* and it reflects the degree of desired robustness of the network connectivity and $E_c(K)$ denotes the set of edges resulting from adding a candidate set of K relays. We note that as δ increases the number of relays, required to satisfy the connectivity constraint in (4.15), increases.

In [56], it was shown that the network repair problem is NP-complete and hence we propose a heuristic algorithm to solve it. We utilize our proposed solution for the network maintenance problem in solving the network repair problem. More precisely, we propose an iterative network repair algorithm, which is implemented as follows. First, we assume that $K = 1$ relay is enough to reconnect the network. Second, we solve the network maintenance problem in Table 4.1 to find the location for that relay. If the Fiedler value of the resulting network is strictly greater than δ then the network is reconnected and the algorithm stops. Otherwise, the number of candidate relays is incremented by one and the algorithm is repeated.

Table 4.2 summarizes the proposed network repair algorithm. Similar to the network maintenance algorithm, the network repair algorithm is implemented in polynomial time. In this section, we have presented our proposed network repair problem and in the following section, we show some simulation results for the

network maintenance and network repair proposed strategies.

4.6 Simulation Results

In this section, we present some simulation results to show the performance of our proposed algorithms. We consider $n = 20$ nodes deployed randomly in $6m \times 6m$ square area and the central unit is assumed to be in the center of the network. Data generated at the sensors follows a Poisson process with rate 10 packets per unit time and the path loss exponent is $\alpha = 2$. The desired BER for the transmissions over any link is $\varepsilon^o = 10^{-4}$, the noise variance $N_0 = -20$dBm, the maximum power $P_{max} = 0.15$ watt, the receiver processing power is $P_r = 10^{-4}$ watt, and the initial energy of every sensor is 0.1 joule. The number of candidate relays locations utilized in the network maintenance algorithm, described in Table 4.1, is chosen to be $n_c = 25$ locations. The SDPA-M software package [74] has been utilized to solve the SDP optimization problem in (4.12). The following results are averaged over 1000 independent network realizations.

Figure 4.3 depicts the increase of the Fiedler value as the number of added relays increases. For comparison purposes, we also plot the effect of randomly adding relays. As shown, the random addition performs poorly compared to our proposed algorithm. In Section 4.3, we have chosen the Fiedler value as an intuitive and good measure of the network lifetime, which is our main objective. Figure 4.4 depicts the network lifetime gain as a function of the added number of relays. The network lifetime gain due to adding K relays is defined as

$$G_T(K) = \frac{T(K) - T_{MPR}(0)}{T_{MPR}(0)} \ \% \ , \tag{4.16}$$

where $T(K)$ is the network lifetime after deploying K relays and $T_{MPR}(0)$ de-

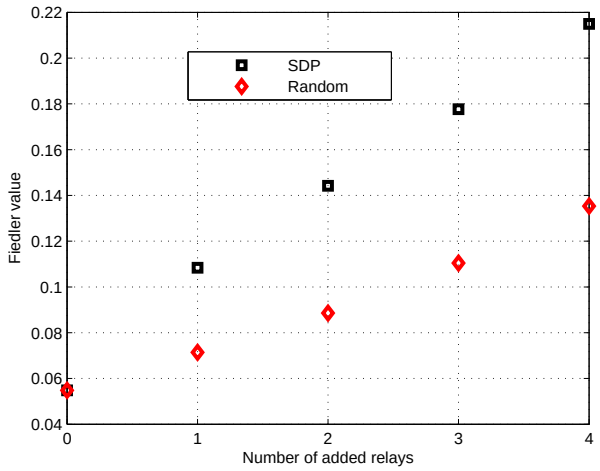

Figure 4.3: The average Fiedler value versus the added number of relays, for $n = 20$ distributed randomly in $6m \times 6m$ square field, is plotted. Effect of deploying relays is illustrated.

notes the network lifetime of the original network utilizing the MPR algorithm. As shown, the proposed SDP-based network maintenance algorithm achieves significant network lifetime gain as the number of added relays increases, which is a direct consequence of increasing the Fiedler value as shown previously in Figure 4.3. At $K = 4$ and by employing the MPR algorithm, the proposed network maintenance algorithm achieves lifetime gain of 105.8%, while the random deployment case achieves lifetime gain of 40.09%.

In Figure 4.4, we also illustrate the impact of the adaptive network maintenance algorithm on the network lifetime gain. At $K = 4$ relays, the lifetime gain jumps to 132.1% for the MPR algorithm. We also compare the performance of our proposed algorithm with the exhaustive search scheme. For practical implementation of the exhaustive search scheme, the optimum locations for a given set of relays are determined consecutively, i.e., one relay at a time. We have implemented the exhaustive search scheme by dividing the network area into many small regions

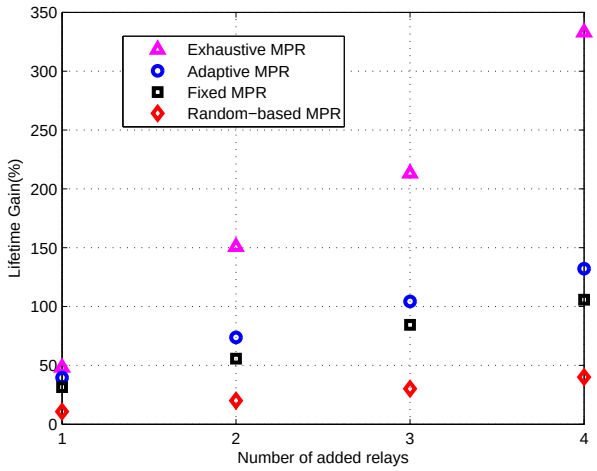

Figure 4.4: The average network lifetime gain versus the added number of relays, for $n = 20$ distributed randomly in $6m \times 6m$ square field, is plotted. Effect of deploying relays is illustrated.

and each region is represented by a relay at its center. The optimum location for the first relay is determined by calculating the lifetime of all the possible locations and choosing the one that results in maximum lifetime. Given the updated network including the first relay, we find the optimum location for the second relay via the same exhaustive search scheme. This algorithm is repeated until all the relays are deployed. In Figure 4.4, we show the network lifetime gain of the exhaustive search case utilizing the MPR algorithm.

As indicated in Section 4.4.1, the proposed WMPR algorithm should intuitively outperform the MPR algorithm when relays have higher initial energy than that of the sensors. We set the weights of the deployed relays to be 0.1, while the weights of the original sensors to be 1. Therefore, sensors tend to send their data to the deployed relays rather than the neighboring sensors. In addition, the relays' energy are set to be 10 times that of the sensors. As a result, the WMPR algorithm achieves higher gain compared to that achieved by the MPR algorithm as shown

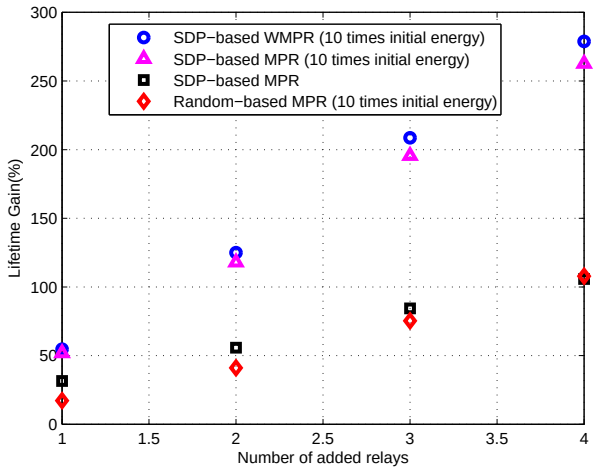

Figure 4.5: The average network lifetime gain versus the added number of relays, for $n = 20$ distributed randomly in $6m \times 6m$ square field, is plotted. Effect of increasing the relays' initial energy 10 times is illustrated.

in Figure 4.5. At $K = 4$, the WMPR and MPR algorithms achieve network lifetime gains of 278.8% and 262.7%, respectively. In Figure 4.5, we notice that the difference between the WMPR and the MPR performance curves increases as the number of relays increases. Intuitively, the WMPR algorithm utilizes the relays more frequently than the MPR algorithm. Hence it achieves higher lifetime gain by increasing the the relays' initial energy.

We also consider a larger sensor network of $n = 50$ nodes deployed randomly in $15m \times 15m$ square area. Figure 4.6 shows the network lifetime gain. At $K = 15$ and by employing the MPR algorithm, the proposed network maintenance algorithm achieves lifetime gain of 113.6%, while the random deployment case achieves lifetime gain of 40.7%. In Figure 4.6, we also illustrate the impact of the adaptive network maintenance algorithm on the network lifetime gain. At $K = 15$ relays, the lifetime gain jumps to 119.7% for the MPR algorithm.

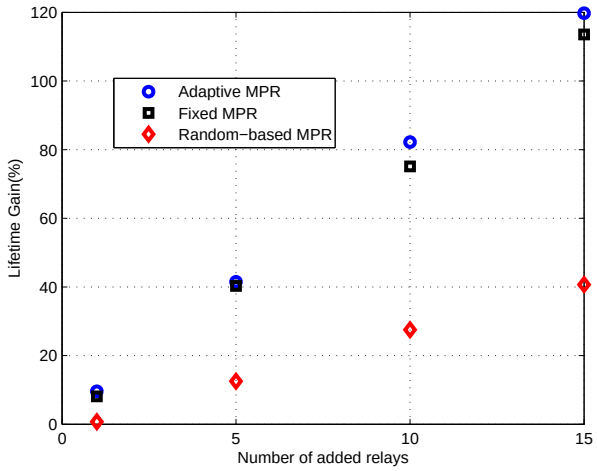

Figure 4.6: The average network lifetime gain versus the added number of relays, for $n = 50$ distributed randomly in $15m \times 15m$ square field, is plotted. Effect of deploying relays is illustrated.

4.6.1 Interference-based Transmission Scenario

In this subsection, we consider a different transmission scenario where some of the sensors are allowed to send their data simultaneously over the same channel. Assuming that node v_i is sending its data to node v_j and the total number of simultaneous transmissions is s. The received symbol can be modeled as

$$y_j = \sqrt{P_i}\, h_{i,j}\, x_i + \sum_{k=1, k\neq i}^{s} \sqrt{P_k}\, h_{k,j}\, x_k + n_j \ . \tag{4.17}$$

Let $m_j = \sum_{k\neq i} \sqrt{P_k}\ h_{k,j}\ x_i + n_j$ denote the random variable representing the summation of the noise and interference terms. For a large enough number of simultaneous transmissions, m_j can be modeled as a complex Gaussian random variable with zero-mean and variance $N_0 + \sum_{k\neq i} P_k\, d_{k,j}^{-\alpha}$ via the central limit theorem [[53], Ch.2], i.e., $m_j \sim CN(0, N_0 + \sum_{k\neq i} P_k\, d_{k,j}^{-\alpha})$. This is a reasonable assumption as the number of sensors, deployed in a sensor network, is often large. Thus, (4.17) can be written as (4.1) with different noise term, which is m_j. Con-

sequently and similar to (4.3), the required power to achieve a desired BER of ε^o can be given by

$$P_i^o = d_{i,j}^{\alpha} \left(N_0 + \sum_{k \neq i} P_k \, d_{k,j}^{-\alpha} \right) \frac{(1 - 2\,\varepsilon^o)^2}{1 - (1 - 2\,\varepsilon^o)^2} \; . \tag{4.18}$$

In (4.18), it is obvious that the transmission power required by each node depends on the transmission powers of the other nodes sending simultaneously over the same channel. We obtain an approximated power expression, by first approximating (4.18) as follows. At low BER, it can be easily shown that

$$P_i \approx \frac{N_0 + \sum_{k \neq i} P_k \, d_{k,j}^{-\alpha}}{4\,\varepsilon^o \, d_{i,j}^{-\alpha}} \; . \tag{4.19}$$

The transmission power can be determined through a power control problem, which can be formulated as the following optimization problem

$$\min \; \sum_i P_i \quad \text{s.t.} \; \frac{N_0 + \sum_{k \neq i} P_k \, d_{k,j}^{-\alpha}}{4\,P_i \, d_{i,j}^{-\alpha}} \leq \varepsilon^o \; , \tag{4.20}$$

Let $\mathbf{p} \in \mathbf{R}^s$ be the power vector, containing the transmission powers P_i, that needs to be calculated. Hence, (4.20) can be formulated in a matrix form as

$$\min \; \sum_i P_i \quad \text{s.t.} \; \left(\mathbf{I} - \frac{1}{4\,\varepsilon^o} \mathbf{F} \right) \mathbf{p} \geq \mathbf{u} \; , \tag{4.21}$$

where $\mathbf{I} \in \mathbf{R}^{s \times s}$ is the identity matrix and the i-th element of the vector $\mathbf{u} \in \mathbf{R}^s$ is $u_i = \frac{N_0}{4\,\varepsilon^o \, d_{i,j}^{-\alpha}}$. With respect to $\mathbf{F} \in \mathbf{R}^{s \times s}$, $F_{i,j} = 0$ if $i = j$ and $F_{i,j} = (\frac{d_{k,j}}{d_{i,j}})^{-\alpha}$ elsewhere. If the spectral radius of $\mathbf{F}$, which is its largest eigenvalue, is less than $(4\,\varepsilon^o)$, then the minimum power set is given by [76]

$$\mathbf{p}^o = \left(\mathbf{I} - \frac{1}{4\,\varepsilon^o} \mathbf{F} \right)^{-1} \mathbf{u} \; . \tag{4.22}$$

At low BER, it can be shown the zero-interference required transmission power given in (4.3) can be approximated as $P_i \approx \frac{N_0}{4\,\varepsilon^o \, d_{i,j}^{-\alpha}}$. By comparing this power with

that required for the interference-based transmission scenario given in (4.19), it is obvious that the interference-based transmission scenario requires more transmission power per node than that required in the zero-interference scenario for the same desired BER. Therefore, nodes will lose their energies with a faster rate in the interference-based transmission scenario. Consequently, the network lifetime is shorter in the interference-based transmission scenario. Therefore if limited batteries is a concern such as in sensor network, it is recommended to have orthogonal transmission between the nodes to maximize the network lifetime.

We consider a network of $n = 10$ nodes deployed randomly in $4m \times 4m$ area. All the nodes operate in half duplex mode, i.e., no node is allowed to transmit and receive at the same node. In addition, nodes sending their data to the same destination are not allowed to send their data at the same time since this requires more complex receiver such as successive interference cancelation (SIC) decoder, which may not be possible for a simple sensor node to have. The route from each sensor to the central unit is determined based on the zero-interference transmission powers, given in (4.3). Then the transmission powers are modified according to (4.22) to represent the interference-based case.

In addition to the network lifetime, the number of the delivered packets from all the sensors to the central unit before the network dies is an important measure of the network performance. Figure 4.7 depicts the number of delivered packets versus the added number of relays for both the zero-interference and interference-based transmission scenarios utilizing the MPR algorithm. First, it is shown for the interference-based scenario that the number of delivered packets slightly increasing as the number of added relays increases. Generally, there are two main factors affecting the net result of the interference-based scenario whenever relays

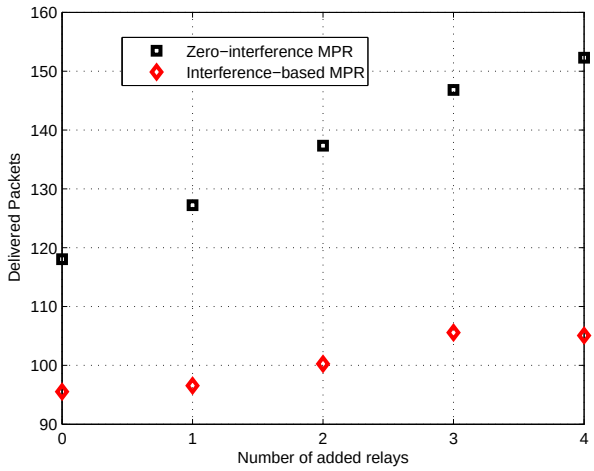

Figure 4.7: The average number of delivered packets versus the added number of relays, for $n = 10$ distributed randomly in $4m \times 4m$ square field, is plotted.

are deployed. Deploying relays increases the number of delivered packets due to performing the relaying task along with the extra energy that the deployed relays have. So, adding more relays increases the number of delivered packets, as shown previously for the zero-interference transmission scenario. On the other hand, deploying relays causes interference to the other existing nodes and forces each existing node to raise its transmission power to overcome the interference effect of the recently added relays. Thus, deploying relays will cause nodes to die faster and consequently will decrease the number of delivered packets. This is the main reason that the network lifetime gains are higher in the zero-interference transmission scenario compared to the interference-based scenarios. We note that the net result of these two factors will determine the performance of the interference-based network maintenance algorithms.

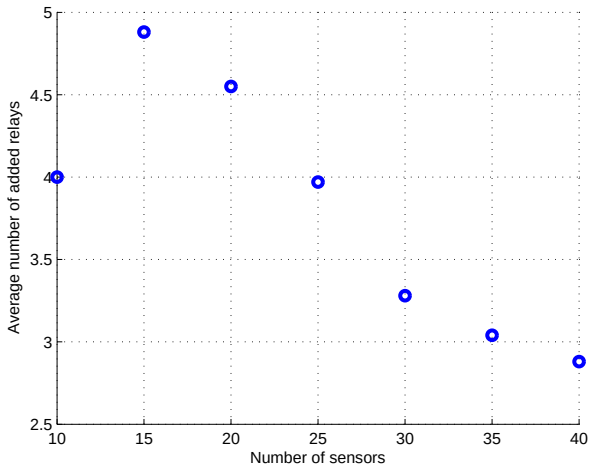

Figure 4.8: The average minimum number of added relays required to reconnect a network versus the number of sensors in the network is plotted.

4.6.2 Network Repair

We consider the network repair problem where the network is originally disconnected. In Figure 4.8, we show the average number of added relays required to reconnect a disconnected network, assuming $\delta = 0$ in (4.15). n sensors are randomly distributed in $6m \times 6m$ square area. The maximum transmission power of any node is $P_{max} = 0.07$ watt. It is shown that for a disconnected network of $n = 25$ nodes deployed randomly in $6m \times 6m$ area, the average number of added relays is 4. For $n < 15$, Figure 4.8 depicts that the average number of added relays increases as n increases. This is because for small n, it is more likely that the added sensors will be deployed in new regions where there are very few or no sensors. Thus, more relays need to be deployed to connect these added sensors. On the other hand, as n increases beyond $n = 15$, the average number of added relays decreases. This is intuitive because as the the number of sensors increases to a moderate state, the network becomes more balanced, i.e., the sensors are uniformly deployed in the whole area. Beyond this moderate state, increasing the

number of sensors keeps filling the gaps in the network. Consequently, the average number of needed relays decreases as n increases.

Let $G_b = (V_b, E_b)$ be the original graph, $\mathbf{L}(K)$ be the Laplacian matrix of the resulting graph after adding the available K relays, and $\lambda_{2,t}\big(\mathbf{L}(K)\big)$ be the Fiedler value at the t-th level (iteration).

1. Initialization: Set $t = 1$ and $\lambda_{2,0}(\mathbf{L}(K)) = \lambda_2(\mathbf{L_b}(0))$, where $\mathbf{L_b}$ is the Laplacian matrix of G_b.

2. Divide the network area into n_c equal square regions. Each region is represented by a relay at its center.

3. Solve the optimization problem in (12) and obtain the best $K < n_c$ relays among the n_c relays defined in 2. Denote the solutions as x_k, $k = 1, 2, \cdots, K$.

4. Calculate $\lambda_{2,t}\big(\mathbf{L}(K)\big)$, which is the Fiedler value of the resulting graph by constructing the Laplacian matrix of the resulting graph.

5. While $\Big(\lambda_{2,t}\big(\mathbf{L}(K)\big) > \lambda_{2,t-1}\big(\mathbf{L}(K)\big)\Big)$

   (a) Increment the level index as: $t = t + 1$.

   (b) For each solution x_k,

      i. Divide the k-th region into n_c equal square regions and obtain the best location for this relay. This can be solved using (12) by setting $K = 1$.

   End For

   (c) Calculate $\lambda_{2,t}\big(\mathbf{L}(K)\big)$ of the resulting graph.

   End While

6. The obtained solutions x_k, $k = 1, 2, \cdots, K$, represent the required locations of the relays.

Table 4.1: Proposed network maintenance algorithm.

Let $G_b = (V_b, E_b)$ be the original graph, $\mathbf{L}(K)$ be the Laplacian matrix of the resulting graph after adding the available K relays, and $\lambda_2(\mathbf{L}(K))$ be its Fiedler value.

1. Initialization: Set $K = 0$.
2. While $(\lambda_2(\mathbf{L}(K) \leq \delta)$
   (a) Increment the number of relays as: $K = K + 1$.
   (b) Implement the network maintenance algorithm, described in Table 4.1, utilizing K candidate relays.
   (c) Calculate $\lambda_2(\mathbf{L}(K))$ of the resulting graph.

   End While
3. The obtained K represents the minimum number of required relays.

Table 4.2: Proposed network repair algorithm.

Chapter 5

Mitigating Channel Estimation Error and Co-channel Interference Effects via Cooperative Communications

In the previous chapters, we have shown the impact of cooperative communications on improving the network performance such as increasing the bandwidth efficiency, reducing the end-to-end transmission power, and maximizing the network lifetime. In these chapters, we have assumed perfect channel estimation and zero-interference scenario. In this chapter, we aim to complete our work by pointing out the possibility of mitigating some of the problems existing in wireless networks such as channel estimation error and co-channel interference (CCI) problems by utilizing cooperative communication scenarios.

Channel estimation error, caused possibly by Doppler shift or noise on the pilot signals, can cause dramatic performance degradation in wireless networks. In [77],

it was examined that channel estimation error results in lower average signal-to-noise ratio (SNR) and higher average error rate in orthogonal frequency division multiplexing (OFDM)-based systems. It was also shown in [78] via simulations results that channel estimation error causes error floor in the amplify-and-forward cooperative scheme. In [79], a superposition coding scheme was proposed to reduce the channel estimation effect when the users have largely different SNR. In addition to the channel estimation error problem, CCI problem also arises in networks such as cellular networks, in which users of different neighboring cells are simultaneously transmitting their data over the same channels (e.g. OFDM subcarriers). CCI results in lower signal to interference plus noise ratio (SINR), which causes dramatic performance degradation. Recently, there have been some works that studied the impact of the multiple-input multiple-output (MIMO) techniques on the CCI problem [76, 80–82], in which it was shown that MIMO techniques can reduce the effect of the CCI problem. In general, we note that in communication systems with channel estimation error or CCI, we cannot get arbitrarily large SNR for high transmission power.

Motivated by the bad impact of channel estimation error and CCI on the direct transmission scenario, we investigate in this chapter the ability of the various cooperative transmission protocols mentioned above to mitigate such impact. We consider two main performance criteria to characterize the impact of cooperative communications on channel estimation error, namely, the traditional outage probability and the proposed SNR gap ratio. The SNR gap ratio quantifies the reduction in the SNR due to channel estimation error. First, we show that the outage probability is reduced due to utilizing cooperative communication scenarios in the presence of channel estimation error. Second, we illustrate that cooperative

transmission protocols, either the conventional or the relay-selection schemes, reduce the SNR gap ratio compared to that of the direct transmission. We find that cooperative communication protocols are less susceptible to channel estimation error by achieving spatial diversity via relays and distributing the total transmission power across multiple transmission phases. Moreover, increasing the number of relays reduces the effect of the channel estimation error more. With respect to CCI, we also show that cooperative communication protocols can mitigate the effect of CCI problem compared to the direct communication.

Unlike the conventional and relay-selection cooperative protocols, distributed space-time cooperative schemes allow simultaneous transmission among the cooperating relays. In these schemes, there is no guarantee that all the cooperating relays start their transmission at the same instant since they are not completely synchronized with each other. Furthermore, the received signals at the destination from the simultaneously transmitting relays experience different propagation delays. Therefore distributed space-time cooperative schemes suffer from timing synchronization error, which results in interference terms that dramatically increase the error rate. Unlike the channel estimation error, increasing the number of relays increases the timing synchronization error effect. In this chapter, we study the tradeoff of the impact of the channel estimation and the timing synchronization errors on the performance of the distributed transmit beamforming cooperative scheme. For a fixed channel estimation error variance, we show that at low data transmission power the effect of the timing synchronization error is more significant, and having more relays results in higher SNR gap ratio. As the transmission power increases, the channel estimation error dominates and having more relays leads to lower SNR gap ratio.

In this work, we focus on the single-carrier analysis, however, the analysis can be easily extended to the multi-carrier OFDM systems. The rest of this chapter is organized as follows. In the next section, we describe the system model of the communication system, taking into consideration the channel estimation error effect, and explain the problem formulation. We Study the impact of various communication scenarios on the channel estimation error and CCI in Section 5.2. In Section 5.3, we consider the timing synchronization error and how it interacts with the channel estimation error.

5.1 System Model and Problem Formulation

Communication scenarios, which are based on training sequences (pilots) for channel estimation, are implemented in two consecutive phases, namely, training phase and data transmission phase. In the training phase, the channel is estimated using a known training sequence with a particular pilot power, denoted by P_{pilot}. A particular pilot transmission power P_{pilot} results in a certain level of channel estimation error variance, referred to as α, which is inversely proportional to the pilot transmission power. In the end of the training phase, the receiver has an estimate of the channel to be utilized in the coherent detection of the transmitted data in the following data transmission phase. In the data transmission phase, the channel estimate is fixed and does not depend on the data transmission power, P. Hence, the channel estimation error does not depend on the data transmission power, P.

The communication system under consideration is shown in Figure 5.1. It consists of the source, s, the destination, d, and a set of N transmitting/receiving nodes, $r_1, r_2, \cdots, r_N$, which will be referred to as relays. We note that each of the nodes $s, r_i, i = 1, 2, \cdots, N$ has a data of its own, and its role interchanges

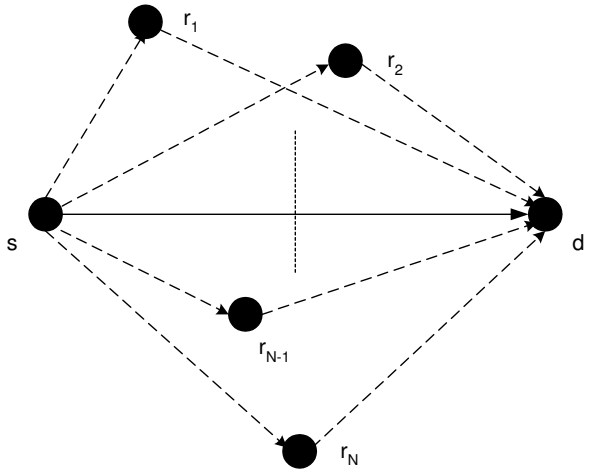

Figure 5.1: Cooperative communication system with a set of N relays. Solid line represents the direct transmission and dashed lines represent the cooperative transmissions via the relays.

between being a source sending its own information or a relay forwarding other nodes information. We assume that all the $N+1$ transmitting nodes utilize the same pilot transmission power, P_{pilot}, to allow the destination to estimate the corresponding channel responses. In the same time, every other receiving node can estimate its corresponding channel response with the sender. Therefore, no extra pilot transmission power is needed in the cooperative transmission protocols compared to that required in the direct transmission case. Finally, we assume that there is a fixed channel estimation error variance, α, resulting from the training phase due to utilizing pilot transmission power of P_{pilot}.

We take into consideration the channel estimation error in the data transmission phase as follows. In the direct transmission scenario, the source sends its data symbol to the destination in one phase, which can be a time or frequency slot. The received symbol at the destination can be modeled as

$$y_{s,d}^{D} = \sqrt{P}\,(h_{s,d} + h_{\alpha})\,x + \sqrt{N_0}\,\eta_{\alpha}, \tag{5.1}$$

where the superscript D denotes the direct transmission scenario, x is the transmitted symbol with unit average energy, i.e., $|x|^2 = 1$, $h_{s,d}$ is the estimated source-destination channel coefficient, h_α denotes the channel estimation error, η_α is a zero-mean additive white Gaussian noise (AWGN) with unit variance, and N_0 is the noise variance. In [79], the additional term resulting from channel estimation error, namely $\sqrt{P}\, x\, h_\alpha$ in (5.1), was called self-noise because it represents an added noise term that scales with the data transmission power.

The channel estimation error is a summation of large number of small quantities representing the inter-carrier interference and noise, and hence it can be modeled as a Gaussian random variable via the central limit theorem [53]. Similar to [77], the channel estimation error h_α is modeled as a zero-mean complex Gaussian random variable with variance α. For a constant modulus transmitted symbol x, the additional self-noise term ($\sqrt{P}\, x\, h_\alpha$) is a zero-mean complex Gaussian random variable with variance $\alpha\, P$. Thus, (5.1) can be rewritten as

$$y_{s,d}^{D} = \sqrt{P}\; h_{s,d}\; x + \sqrt{\alpha\, P + N_0}\; \eta_{s,d}, \tag{5.2}$$

where $\eta_{s,d}$ is a zero-mean Gaussian random variable with unit variance. We note that the system model in (5.2) is similar to the one that was considered to represent the channel estimation error effect in [79].

In the conventional N-relay cooperative transmission scenario, a transmission of one symbol is implemented in $N + 1$ phases. In the first phase, the source broadcasts its symbol to the relays and the destination with a transmission power of P_0. Taking into consideration the channel estimation error as in (5.2), the received symbols at the destination and the i-th relay can be modeled as

$$\begin{aligned} y_{s,d}^{C} &= \sqrt{P_0}\; h_{s,d}\; x + \sqrt{\alpha\, P_0 + N_0}\; \eta_{s,d}, \\ y_{s,r_i}^{C} &= \sqrt{P_0}\; h_{s,r_i}\; x + \sqrt{\alpha\, P_0 + N_0}\; \eta_{s,r_i}\,, \quad i = 1, 2, \cdots, N. \end{aligned} \tag{5.3}$$

respectively, where the superscript C denotes the cooperative transmission scenario, h_{s,r_i} is the estimated channel coefficient between the source and the i-th relay, and η_{s,r_i} is a zero-mean AWGN with unit variance.

In this chapter, we consider the decode-and-forward cooperative protocol [7,17]. However, the system model and the following performance analysis can be easily extended to other cooperative protocols such as amplify-and-forward [7,15]. In the decode-and-forward protocol, each relay decides whether to forward the received information or not according to the quality of the received signal. We assume that every relay can tell whether the received information is correctly decoded or not [7,17]. If the i-th relay correctly decodes the received symbol, then it forwards the decoded symbol to the destination in the $(i+1)$-th phase, otherwise it remains idle. The received symbol at the destination in the $(i+1)$-th phase is given by

$$y^C_{r_i,d} = \sqrt{\widetilde{P}_i}\, h_{r_i,d}\, x + \sqrt{\alpha\, \widetilde{P}_i + N_0}\, \eta_{r_i,d}, \tag{5.4}$$

where $\widetilde{P}_i = P_i$ if the relay decodes the symbol correctly, otherwise $\widetilde{P}_i = 0$, $h_{r_i,d}$ is the estimated channel coefficient between the i-th relay and destination, and $\eta_{r_i,d}$ is a zero-mean AWGN with unit variance. The transmission powers, $P_i, i = 0, 1, \cdots, N$, are allocated subject to a total power constraint of $P_0 + \sum_{i=1}^{N} P_i = P$ [17]. This power constraint is imposed to guarantee a fair comparison with the direct transmission scenario.

Flat Rayleigh fading channels are considered. Let $h_{u,v}$ be a generic channel coefficient representing the channel between any two nodes, where $h_{u,v}$ is modeled as zero-mean complex Gaussian random variable with variance $\delta^2_{u,v}$. The channel gain squared $|h_{u,v}|^2$ follows an exponential random variable with mean $\delta^2_{u,v}$ [53]. We assume that the channel coefficients between each two nodes are independent of each other [7, 17], which can be practically achieved by deploying the nodes far

enough from each other.

Below, we illustrate the performance degradation due to channel estimation error in the direct transmission case. For the direct transmission scenario defined in (5.2), the destination applies the conventional matched filter [53] as $h_{s,d}^{*}\, y_{s,d}$. The output SNR, denoted as γ, can be computed as

$$\gamma^{D} = \frac{P}{N_0 + \alpha\, P} \left|h_{s,d}\right|^2 . \tag{5.5}$$

In the perfect channel estimation scenario, i.e., $\alpha = 0$, the SNR at the destination increases with the data transmission power P. However with channel estimation error, increasing the data transmission power cannot lead to arbitrarily large SNR. This limits the performance of the direct transmission scenario and causes dramatic performance degradation. We also note that the effect of the channel estimation error, which is $\alpha\, P$ in (5.5), increases with high data transmission power. Motivated by the bad impact of channel estimation error on the direct transmission scenario, we investigate in the next section the ability of the various cooperative transmission protocols to mitigate such impact.

5.2 Effects of Cooperative Communications

5.2.1 On Channel Estimation Error

In this subsection, we analyze the performance of the direct and cooperative transmission scenarios introduced in Section 5.1. For each scenario, we calculate the outage probability and the SNR gap ratio, which is defined as

$$R = \frac{\gamma|_{(\alpha=0)} - \gamma|_{(\alpha\neq 0)}}{E\{\gamma|_{(\alpha=0)}\}} , \tag{5.6}$$

where $E\{.\}$ denotes the statistical expectation of a particular random variable. Intuitively, the SNR gap ratio measures the reduction in the SNR, $(\gamma|_{(\alpha=0)} - \gamma|_{(\alpha\neq 0)})$, compared to the average SNR without channel estimation error, i.e., it measures the relative SNR gap ratio.

For the direct transmission scenario defined in (5.2), the output SNR in (5.5) is an exponential random variable with mean $(P\,\delta_{s,d}^2)/(N_0 + \alpha\,P)$, i.e., $\gamma^D \sim \exp\big((N_0 + \alpha\,P)/(P\,\delta_{s,d}^2)\big)$. The outage probability, which is defined as the probability that the output SNR is less than a particular threshold γ_{th}, is computed as

$$F_{\gamma^D}(\gamma_{th}) \triangleq \Pr(\gamma^D \leq \gamma_{th}) = 1 - \exp\Big(-\frac{N_0 + \alpha\,P}{P\,\delta_{s,d}^2}\,\gamma_{th}\Big)\,. \tag{5.7}$$

By substituting (5.5) into (5.6), the direct transmission SNR gap ratio can be written as

$$R^D = \frac{\alpha\,P}{\delta_{s,d}^2\,(N_0 + \alpha\,P)}\,|h_{s,d}|^2\,. \tag{5.8}$$

The source-destination channel gain squared $|h_{s,d}|^2$ is an exponential random variable with mean $\delta_{s,d}^2$. Hence, the direct transmission SNR gap ratio in (5.8) is an exponential random variable, i.e., $R^D \sim \exp\big((N_0 + \alpha\,P)/(\alpha\,P)\big)$. Finally, the average SNR gap ratio can be calculated as

$$E\{R^D\} = \frac{\alpha\,P}{N_0 + \alpha\,P}\,. \tag{5.9}$$

In the conventional cooperative transmission scenario, the destination applies maximal-ratio combining (MRC) [8] to coherently combine the signals received from the source and the N relays. The output of the MRC detector at the destination is given by

$$y^C = \frac{\sqrt{P_0}}{N_0 + \alpha\,P_0}\,h_{s,d}^*\,y_{s,d}^C + \sum_{i=1}^{N}\frac{\sqrt{\widetilde{P}_i}}{N_0 + \alpha\,\widetilde{P}_i}\,h_{r_i,d}^*\,y_{r_i,d}^C\,. \tag{5.10}$$

Let $\widetilde{\mathbf{P}} \triangleq [P_0, \widetilde{P}_1, \cdots, \widetilde{P}_N]^T$ denote the power distribution vector, where T denotes vector transpose. For a fixed power vector $\widetilde{\mathbf{P}}$, the conditional SNR can be computed as

$$\gamma^C(\widetilde{\mathbf{P}}) = \frac{P_0}{N_0 + \alpha\, P_0}\, |h_{s,d}|^2 + \sum_{i=1}^{N} \frac{\widetilde{P}_i}{N_0 + \alpha\, \widetilde{P}_i}\, |h_{r_i,d}|^2 \,. \tag{5.11}$$

In the sequel, we obtain the distribution of the power vector $\widetilde{\mathbf{P}}$, which is based on the transmission between the user and the i-th relay, modeled in (5.3). We assume M-PSK modulation type. The conditional SER at the i-th relay, which is conditioned on the the channel coefficient h_{s,r_i}, can be written as [41]

$$\varepsilon^{h_{s,r_i}} = \Psi(\gamma_i) \triangleq \frac{1}{\pi} \int_0^{(M-1)\pi/M} \exp\Big(- \frac{b\gamma_i}{\sin^2\theta} \Big)\, d\theta \,, \tag{5.12}$$

where $\gamma_i = P_0\, |h_{s,r_i}|^2 / (N_0 + \alpha\, P_0)$ is the instantaneous SNR at the i-th relay and $b = \sin^2(\pi/M)$. By averaging (5.12) with respect to the exponential random variable $|h_{s,r_i}|^2$, the SER can be given by

$$\varepsilon = F_1\Big(1 + \frac{b\, P_0\, \delta^2_{s,r_i}}{(N_0 + \alpha\, P_0)\, \sin^2\theta}\Big) \,, \tag{5.13}$$

where $F_1\big(x(\theta)\big) = 1/\pi \int_0^{(M-1)\pi/M} 1/x(\theta)\, d\theta$.

As described in Section 5.1, the i-th relay retransmits the source's symbol only if it has correctly decoded that symbol. Hence the power of the i-th relay, $\widetilde{P}_i, i = 1, 2 \cdots, N$, is distributed as a Bernoulli random variable with success probability equal to $(1 - \varepsilon)$, i.e.,

$$\widetilde{P}_i = \begin{cases} P_i & \text{w.p.} \quad 1 - F_1\Big(1 + \frac{b\, P_0\, \delta^2_{s,r_i}}{(N_0 + \alpha\, P_0)\, \sin^2\theta}\Big) \\ 0 & \text{w.p.} \quad F_1\Big(1 + \frac{b\, P_0\, \delta^2_{s,r_i}}{(N_0 + \alpha\, P_0)\, \sin^2\theta}\Big) \end{cases} , \tag{5.14}$$

where w.p. stands for "with probability". We note that the relays' powers $\widetilde{P}_i, i = 1, 2 \cdots, N$ are independent random variables since each one depends on its own

source-relay channel gain $|h_{s,r_i}|$, which are independent of each other as assumed in Section 5.1.

By averaging the conditional SNR in (5.11) with respect to $\widetilde{\mathbf{P}}$, the cooperative transmission SNR can be obtained as

$$\gamma^C = \frac{P_0}{N_0 + \alpha\, P_0}\,|h_{s,d}|^2 + \sum_{i=1}^{N} \frac{P_i}{N_0 + \alpha\, P_i}\left(1 - F_1\Big(1 + \frac{b\, P_0\, \delta_{s,r_i}^2}{(N_0 + \alpha\, P_0)\, \sin^2\theta}\Big)\right)|h_{r_i,d}|^2\,. \tag{5.15}$$

Let $h_0 = h_{s,d}/\delta_{s,d}$ and $h_i = h_{r_i,d}/\delta_{r_i,d}, i = 1, 2, \cdots, N$, where $h_i, i = 0, 1, \cdots, N$, is distributed as a zero-mean complex Gaussian random variable with unit variance. Consequently, the SNR in (5.15) can be rewritten as

$$\gamma^C = \sum_{i=0}^{N} a_i\,|h_i|^2\,, \tag{5.16}$$

where $a_0 = \frac{P_0\,\delta_{s,d}^2}{N_0 + \alpha\, P_0}$ and $a_i = \frac{P_i\,\delta_{r_i,d}^2}{N_0 + \alpha\, P_i}\left(1 - F_1\Big(1 + \frac{b\, P_0\, \delta_{s,r_i}^2}{(N_0 + \alpha\, P_0)\, \sin^2\theta}\Big)\right),\ i = 1, 2, \cdots, N$. Furthermore, the outage probability is calculated as

$$F_{\gamma^C}(\gamma_{th}) = \sum_{i=0}^{N} b_i\Big(1 - \exp(-\frac{\gamma_{th}}{a_i})\Big)\,, \tag{5.17}$$

where $b_i = \prod_{k=0, k\neq i}^{N} \frac{a_i}{a_i - a_k}, i = 0, 1, \cdots, N$.

By substituting (5.16) into (5.6), the cooperative transmission SNR gap ratio can be given by

$$R^C = \frac{\gamma^C|_{(\alpha=0)} - \gamma^C}{E\{\gamma^C|_{(\alpha=0)}\}} = \sum_{i=0}^{N} c_i\,|h_i|^2\,, \tag{5.18}$$

where

$$\begin{aligned} c_0 &= \frac{\delta_{s,d}^2}{S}\,\frac{\alpha\, P_0^2}{N_0\,(N_0 + \alpha\, P_0)}\,, \\ c_i &= \frac{\delta_{r_i,d}^2}{S}\left(\frac{\alpha\, P_i^2}{N_0\,(N_0 + \alpha\, P_i)} - \frac{P_i}{N_0}\,F_1\Big(1 + \frac{b\, P_0\, \delta_{s,r_i}^2}{N_0\, \sin^2\theta}\Big)\right. \\ &\quad \left. + \frac{P_i}{N_0 + \alpha\, P_i}\,F_1\Big(1 + \frac{b\, P_0\, \delta_{s,r_i}^2}{(N_0 + \alpha\, P_0)\, \sin^2\theta}\Big)\right), \end{aligned} \tag{5.19}$$

Parameter	Value
Cell radius	1 km
Site-to-site distance	2 km
Thermal noise	-100dBm
Max transmission power	25 dBm
Carrier frequency	1.9 GHz
Propagation model	31.5 + 35$\log_{10}$(d in m)dB

Table 5.1: Simulation parameters of a typical cellular system.

in which $S = E\{\gamma^C|_{(\alpha=0)}\} = \sum_{i=0}^{N} a_i|_{(\alpha=0)}$. The cooperative transmission SNR gap ratio defined in (5.18) represents a weighted sum of a set of independent chi-square random variables [53] and its probability density function (PDF) can be written as

$$f_{R^C}(r) = \sum_{i=0}^{N} \frac{d_i}{c_i} \exp(-\frac{r}{c_i})\, U(r)\,, \tag{5.20}$$

where $d_i = \prod_{k=0,k\neq i}^{N} \frac{c_i}{c_i - c_k}, i = 0, 1, \cdots, N$. Finally, the average of the cooperative transmission SNR gap ratio is computed as

$$E\{R^C\} = \sum_{i=0}^{N} c_i\,. \tag{5.21}$$

Numerical Comparisons

Now, we present some numerical results to illustrate the impact of the cooperative transmission scheme on the channel estimation error. The outage probability and SNR gap ratio are utilized to characterize such impact. For fair comparison, we assume that a total power P is available for the direct and cooperative transmission scenarios. We assume maximum of $N = 6$ relays are available and we consider power allocation policy, in which $P_0 = P/2$ and $P_i = P/(2\,N), i = 1, 2, \cdots, N$ [17].

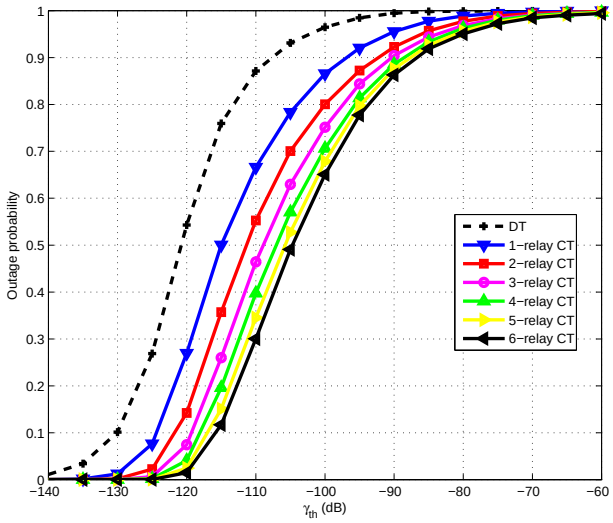

Figure 5.2: Channel estimator error: outage probability of the direct and cooperative transmission scenarios for $\alpha = 0.05$ and $P/N_0 = 20$dB. Cooperative transmission reduces the outage probability as the number of relays increases.

QPSK modulation type is assumed throughout this chapter. Table 5.1 summarizes a typical set of simulation parameters for cellular networks. Finally, the shown results are averaged over 1000 independent network realizations, where the locations of the users and the relays are randomly distributed in each realization.

We assume that the channel estimation error variance is $\alpha = 0.05$. As indicated in Section 5.1, the channel estimation error variance, α, is fixed and does not depend on the data transmission power, P. Figure 5.2 depicts the outage probability, given by (5.7) and (5.17) for the direct and cooperative transmission scenarios, respectively, at $P/N_0 = 20$ dB. As shown, the direct transmission has the highest outage probability for any SNR threshold, γ_{th}. It is also shown that as the number of relays increases, the cooperative transmission outage probability reduces. This is due to the fact that cooperative transmission with N relays pro-

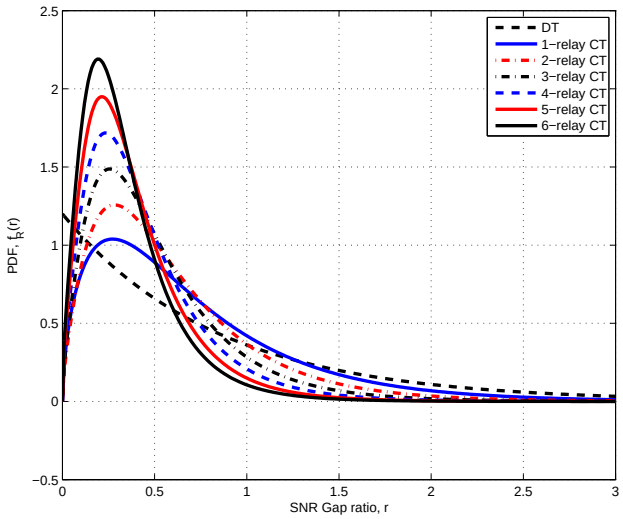

Figure 5.3: Channel estimator error: probability density function of the direct and cooperative transmission scenarios for $\alpha = 0.05$ and $P/N_0 = 20$dB. Direct transmission has an exponential distribution while cooperative transmission has weighted-sum chi-square distribution.

vides $N+1$ independently-faded paths from the source to the destination. Hence, diversity order $N+1$ is achieved. Furthermore, the effect of adding relays decreases as the number of relays increases. Intuitively the available relays provide enough reliability and increasing the number of relays will slightly improve the performance.

In addition to the outage probability, the average SNR gap ratio is of great interest. Figure 5.3 depicts the PDF of the SNR gap ratio at $P/N_0 = 20$ dB for the direct and cooperative transmissions. As shown, the direct transmission SNR gap ratio has an exponential distribution. On the other hand, the cooperative transmission SNR gap ratio has a weighted-sum chi-square distribution (5.20) that depends on the number of relays. It is also shown that as the number of

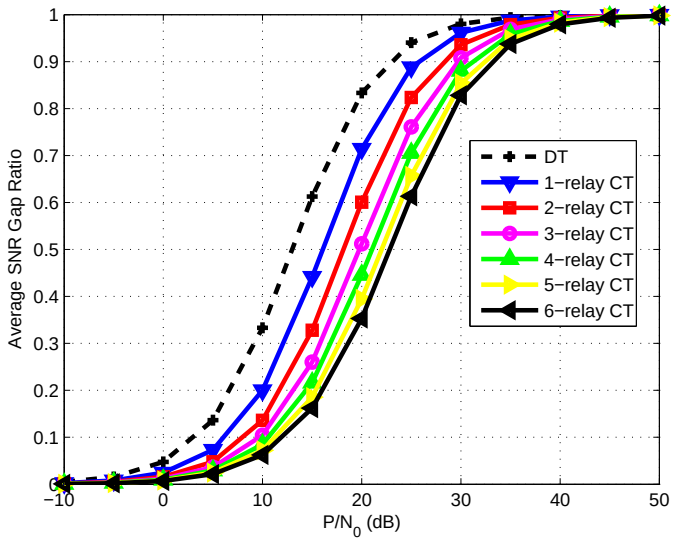

Figure 5.4: Channel estimator error: average SNR gap ratio of the direct and cooperative transmission scenarios for $\alpha = 0.05$. Cooperative transmission reduces the average SNR gap ratio as the number of relays increases.

relays increases, the PDF of the cooperative transmission SNR gap ratio gets more concentrated in the low-ratio region.

Figure 5.4 depicts the average SNR gap ratio for the different transmission scenarios as a function of P/N_0. For fixed N_0, Figure 5.4 shows that the average SNR gap ratio increases with the data transmission power, P. This is due to the fact that the channel estimation error effect, which is αP in (5.2), is more significant at high transmission power compared to the noise variance. At high transmission power, the average SNR gap ratio is 1 as can be shown using (5.9). It is also depicted in Figure 5.4 that the direct transmission scenario has the largest SNR gap ratio compared to the conventional cooperative transmission scenario. Furthermore, increasing the number of utilized relays reduces the average SNR gap ratio. At $P/N_0 = 10$ dB, the direct transmission scenario suffers SNR gap ratio of

0.33, while the cooperative transmission scenario with $N = 6$ relays suffers SNR gap ratio of 0.06. From Figure 5.4, we conclude that the cooperative communication protocol reduces the effect of the channel estimation error, which is one of the main results of this chapter. In this subsection, we have investigated the impact of the conventional cooperative transmission scenario on the channel estimation error. In the next subsection, we investigate such impact on the CCI problem.

5.2.2 On Co-channel Interference

In this subsection, we investigate the impact of the cooperative communications on the CCI problem in cellular networks (e.g. OFDM-based cellular networks). Reuse factor 1 is assumed, and hence the available frequency band is utilized by all the cells. For a particular mobile unit sending its data to the base station over a specific sub-carrier, it experiences a large number of interfering signals coming from users in its main cell as well as other cells who are occupying the same frequency sub-carrier. In each cell, there is usually a number of users transmitting their data over the same sub-carrier utilizing, for instance, space-division multiple access technique (SDMA) [1]. Moreover, a number of users can be applying MIMO schemes such as Vertical Bell Labs Space-Time Architecture (V-BLAST) [83], by which an independent symbol is transmitted from each transmit antenna over the same sub-carrier. Having reuse factor 1 in addition to these intra-cell interfering signals result in a large number of interfering signals, denoted by K, each contributing by a small effect. The summation of these large number of small interference quantities can be modeled, via the central limit theorem [53], as a complex Gaussian random variable. In [1], a similar argument was presented to justify approximating the inter-cell and intra-cell interference in practical systems, such as code division

multiple access (CDMA) networks, as complex Gaussian random variable.

We assume that all the cells are utilizing the same transmission scenario, whether direct or cooperative transmission scenario. Below, we calculate the SNR gap ratio and the outage probability, as defined previously, for each transmission scenario. In the direct transmission scenario, the received symbol at the base station over a particular sub-carrier can be modeled as

$$y^{D}_{s,d,CCI} = \sqrt{P}\, h_{s,d}\, x + \sum_{k=1}^{K} \sqrt{P_k}\, h_{s_k,d}\, x_k + \sqrt{N_0}\, \eta_{s,d}\,, \tag{5.22}$$

where P_k and x_k denote the transmission power and the unit-energy transmitted symbol of user k, respectively. In (5.22), $h_{s_k,d}$ represents the channel coefficient from user k to the main base station and it is modeled as a zero-mean complex Gaussian random variable with variance $\delta^2_{s_k,d}$. For sufficiently large number of interferers K, which is a reasonable assumption as discussed above, the interference term $\Big(\sum_{k=1}^{K} \sqrt{P_k}\ h_{s_k,d}\ x_k\Big)$ can be modeled as a zero-mean complex Gaussian random variable with variance $\Big(\sum_{k=1}^{K} P_k\ \delta^2_{s_k,d}\Big)$. Thus, (5.22) can be rewritten as

$$y^{D}_{s,d,CCI} = \sqrt{P}\, h_{s,d}\, x + \sqrt{\sum_{k=1}^{K} P_k\ \delta^2_{s_k,d} + N_0}\ \eta_{s,d}\,. \tag{5.23}$$

By applying matched filter at the receiver, the SINR at the main base station is given by

$$\gamma^{D}_{CCI} = \frac{P}{N_0 + \sum_{k=1}^{K} P_k\ \delta^2_{s_k,d}}\, |h_{s,d}|^2\,. \tag{5.24}$$

As shown in (5.24), we cannot get arbitrarily large SINR for high transmission power P, and this shows the dramatic effect of the CCI on the direct transmission scenario. The outage probability, defined in (5.7), can be computed as

$$F_{\gamma^D,CCI}(\gamma_{th}) = 1 - \exp\Big(-\frac{N_0 + \sum_{k=1}^{K} P_k\ \delta^2_{s_k,d}}{P\,\delta^2_{s,d}}\,\gamma_{th}\Big)\,. \tag{5.25}$$

Similar to (5.6), the SINR gap ratio due to CCI can be defined as

$$R_{CCI} = \frac{\gamma|_{(K=0)} - \gamma|_{(K\neq 0)}}{E\{\gamma|_{(K=0)}\}} \,. \tag{5.26}$$

Substituting (5.24) into (5.26), the direct transmission SINR gap ratio is

$$R^{D}_{CCI} = \frac{\sum_{k=1}^{K} P_k \, \delta^2_{s_k,d}}{(N_0 + \sum_{k=1}^{K} P_k \, \delta^2_{s_k,d}) \, \delta^2_{s,d}} \, |h_{s,d}|^2 \,, \tag{5.27}$$

where $R^{D}_{CCI} \sim \exp\big((N_0 + \sum_{k=1}^{K} P_k \, \delta^2_{s_k,d})/(\sum_{k=1}^{K} P_k \, \delta^2_{s_k,d})\big)$. Finally, the average SINR gap ratio can be calculated as

$$E\{R^{D}_{CCI}\} = \frac{\sum_{k=1}^{K} P_k \, \delta^2_{s_k,d}}{N_0 + \sum_{k=1}^{K} P_k \, \delta^2_{s_k,d}} \,. \tag{5.28}$$

As for the cooperative transmission mode, we assume that there exists the same number of relays in every cell. Moreover, we assume that all the relays helping the interfering users always decode their received data correctly and hence they are always retransmitting their sources' data. We note that this scenario represents the worst-case performance. In the cooperative transmission mode, the transmission scenario can be written in a similar way to that in (5.3) and (5.4) taking into consideration the CCI effect as in (5.23). Similar to (5.15), it can be shown that the received SINR is given by

$$\begin{aligned}\gamma^{C}_{CCI} = {} & \frac{P_0}{N_0 + \sum_{k=1}^{K} P_{k,0} \, \delta^2_{s_k,d}} \, |h_{s,d}|^2 \\ & + \sum_{i=1}^{N} \frac{P_i}{N_0 + \sum_{k=1}^{K} P_{k,i} \, \delta^2_{r_{k,i},d}} \left(1 - F_1\Big(1 + \frac{b \, P_0 \, \delta^2_{s,r_i}}{(N_0 + \sum_{k=1}^{K} P_{k,0} \, \delta^2_{s_k,r_i}) \, \sin^2\theta}\Big)\right) |h_{r_i,d}|^2 \,,\end{aligned} \tag{5.29}$$

where $r_{k,i}$ denotes the i-th relay in the k-th cell and $P_{k,i}$ denotes its transmission

power. The SINR in (5.29) can be written as in (5.16), in which

$$a_{0,CCI} = \frac{P_0\,\delta^2_{s,d}}{N_0 + \sum_{k=1}^{K} P_{k,0}\,\delta^2_{s_k,d}}$$
$$a_{i,CCI} = \frac{P_i\,\delta^2_{r_i,d}}{N_0 + \sum_{k=1}^{K} P_{k,i}\,\delta^2_{r_{k,i},d}}\left(1 - F_1\Big(1 + \frac{b\,P_0\,\delta^2_{s,r_i}}{(N_0 + \sum_{k=1}^{K} P_{k,0}\,\delta^2_{s_k,r_i})\,\sin^2\theta}\Big)\right). \tag{5.30}$$

Similarly, the outage probability can be computed using (5.17), and the cooperative transmission SINR gap ratio can be given by (5.18), in which

$$c_{0,CCI} = \frac{\delta^2_{s,d}}{S_{CCI}}\,\frac{P_0\,(\sum_{k=1}^{K} P_{k,0}\,\delta^2_{s_k,d})}{N_0\,(N_0 + \sum_{k=1}^{K} P_{k,0}\,\delta^2_{s_k,d})},$$
$$c_{i,CCI} = \frac{\delta^2_{r_i,d}}{S_{CCI}}\left(\frac{P_i\,(\sum_{k=1}^{K} P_{k,i}\,\delta^2_{r_{k,i},d})}{N_0\,(N_0 + \sum_{k=1}^{K} P_{k,i}\,\delta^2_{r_{k,i},d})} - \frac{P_i}{N_0}\,F_1\Big(1 + \frac{b\,P_0\,\delta^2_{s,r_i}}{N_0\,\sin^2\theta}\Big)\right.$$
$$\left. + \frac{P_i}{N_0 + \sum_{k=1}^{K} P_{k,i}\,\delta^2_{r_{k,i},d}} \times F_1\Big(1 + \frac{b\,P_0\,\delta^2_{s,r_i}}{(N_0 + \sum_{k=1}^{K} P_{k,0}\,\delta^2_{s_k,r_i})\,\sin^2\theta}\Big)\right), \tag{5.31}$$

in which $S_{CCI} = E\{\gamma^C_{CCI}|_{(K=0)}\} = \sum_{i=0}^{N} a_{i,CCI}|_{(K=0)}$. Finally, the PDF and average of the cooperative transmission SINR gap ratio can be calculated as in (5.20) and (5.21), respectively.

We present the CCI numerical results as follows. We assume $K = 7$ interfering users, which exist in K neighboring cells that have noticeable effect on the main user. In addition, we assume that all the users in the various cells are having the same power allocation policy, i.e., $P_0 = P_{k,0} = P/2$ and $P_i = P_{k,i} = P/(2\,N), i = 1, 2, \cdots, N$. The rest of the simulation parameters are given in Table 5.1. In Figure 5.5, we show the outage probability of the SNR for the direct and cooperative transmission scenarios. Similar to the channel estimation error case, it is shown that the cooperative transmission reduces the outage probability as the number of relays increases. Figure 5.6 depicts the average SNR

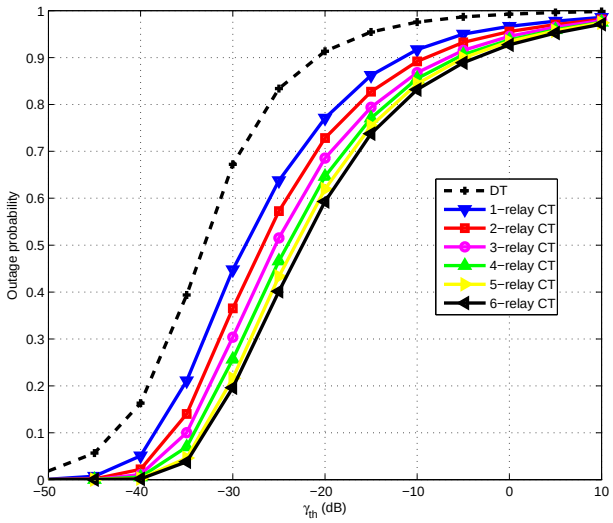

Figure 5.5: CCI: outage probability of the direct and cooperative transmission scenarios for equal power and $P/N_0 = 100$dB. Cooperative transmission reduces the outage probability as the number of relays increases.

gap ratio and it is shown that the CCI effect is reduced by utilizing relays. Moreover, increasing the number of cooperating relays results in lower SNR gap ratio. It is shown that at $P/N_0 = 130$ dB, the direct transmission scenario suffers SNR gap ratio of 0.18, while the cooperative transmission scenario with $N = 6$ relays suffers SNR gap ratio of 0.07. From Figure 5.6, we conclude that the conventional cooperative communication protocol is less susceptible to CCI compared to the direct transmission, which is one of the main results of this chapter.

In this subsection, we have presented the CCI problem in a similar fashion to that of the channel estimation error. In the rest of this chapter, we will focus on the channel estimation error, however, the obtained results can be easily extended to the CCI case. In the following subsections, we study the impact of additional transmission protocols, namely, relay selection and multi-phase direct transmission,

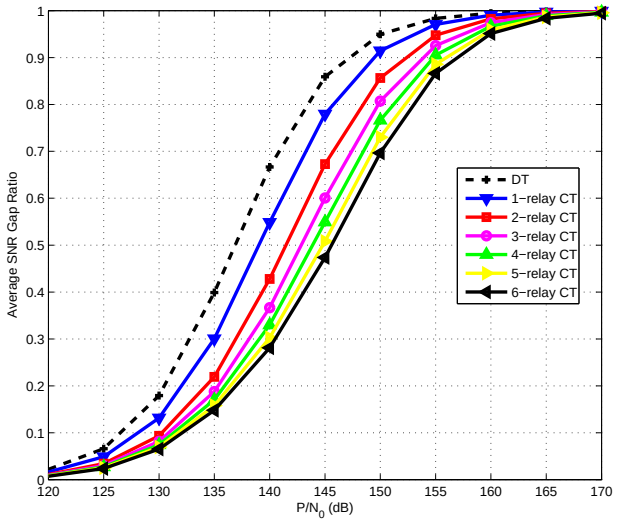

Figure 5.6: CCI: average SNR gap ratio of the direct and cooperative transmission scenarios for equal power. Cooperative transmission reduces the SNR gap ratio as the number of relays increases.

on the channel estimation error effect.

5.2.3 Relay Selection

In this subsection, we consider a different cooperative transmission scenario, namely, cooperative communications with relay selection [24]. In the relay-selection cooperative scheme, one optimal relay among a set of N available relays is chosen based on the instantaneous channel gains. This protocol guarantees full diversity order of $N+1$ as was proven in [24]. Unlike the conventional cooperative scheme with bandwidth efficiency of $1/(N+1)$ SPCU, the relay selection scheme achieves bandwidth efficiency of $1/2$ SPCU. In [24], it was shown that the effective channel from the source to the destination via the i-th relay can be quantified using the following

relay metric

$$\beta_i = \mu_H(\frac{A^2}{q^2}\,|h_{r_i,d}|^2, \frac{B}{q\,(1-q)}\,|h_{s,r_i}|^2) \triangleq \frac{2\,\frac{A^2}{q^2}\;\frac{B}{q\,(1-q)}\,|h_{s,r_i}|^2\,|h_{r_i,d}|^2}{\frac{A^2}{q^2}\,|h_{r_i,d}|^2 + \frac{B}{q\,(1-q)}\,|h_{s,r_i}|^2}\,, \tag{5.32}$$

where $\mu_H(.,.)$ denotes the standard harmonic mean function, $q \triangleq \frac{P_o}{P}$ represents the portion of the total transmission power assigned to the user, and for M-PSK modulation $A = \frac{M-1}{2M} + \frac{\sin(\frac{2\pi}{M})}{4\pi}$ and $B = \frac{3(M-1)}{8M} + \frac{\sin(\frac{2\pi}{M})}{4\pi} - \frac{\sin(\frac{4\pi}{M})}{32\pi}$ [24].

The i-th relay metric β_i in (5.32) gives an instantaneous indication about the relay's ability to cooperate with the user. Consequently, the optimal relay is the one that has the maximum instantaneous relay metric among the set of available relays. The user utilizes the optimal relay only to forward its data to the destination. The relay-selection cooperative scheme can be modeled by (5.3) and (5.4) utilizing one relay only, i.e., $K = 1$. Let $\widetilde{P}_m$ denote the transmission power of the optimal relay, r_m. Similar to (5.11), for a given $\widetilde{P}_m$ the conditional SNR is calculated as

$$\gamma^S(\widetilde{P_m}) = \frac{P_0}{N_0 + \alpha\,P_0}\,|h_{s,d}|^2 + \frac{\widetilde{P}_m}{N_0 + \alpha\,\widetilde{P_m}}\,|h_{r_m,d}|^2\,, \tag{5.33}$$

where the superscript S denotes relay selection scheme. The transmission power of the optimal relay P_m is a Bernoulli random variable, with PDF given by (5.14). By averaging (5.33) with respect to P_m, the SNR can be computed as

$$\gamma^S = \frac{P_0}{N_0 + \alpha\,P_0}\,|h_{s,d}|^2 + \frac{P_m}{N_0 + \alpha\,P_m}\Big(1 - F_1\Big(\exp(\frac{b\,P_0\,|h_{s,r_m}|^2}{(N_0 + \alpha\,P_0)\,\sin^2\theta})\Big)\Big)\,|h_{r_m,d}|^2\,. \tag{5.34}$$

We note that the channel gains of the optimal relay, namely, $|h_{s,r_m}|^2$ and $|h_{r_m,d}|^2$ are no longer exponentially distributed random variables as was shown in [24]. It is very complicated to analytically obtain the probability distribution of the optimal relay channels. Therefore, we show by simulations the performance of the relay-selection cooperative scheme.

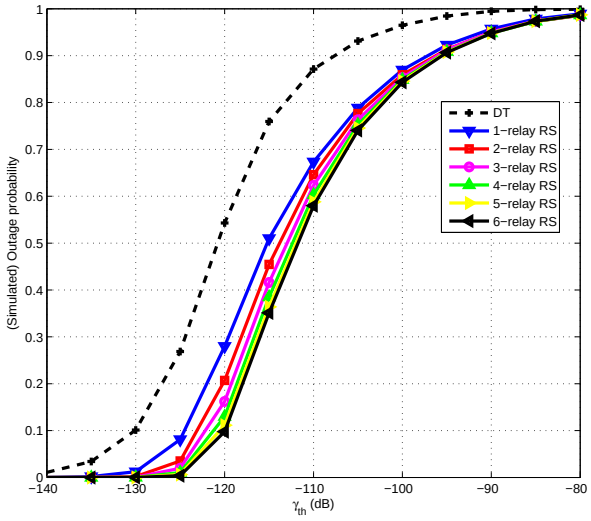

Figure 5.7: Channel estimator error: outage probability of the direct and relay-selection cooperative transmission scenarios for $P/N_0 = 20$ dB and $\alpha = 0.05$. Cooperative transmission reduces the outage probability as the number of relays increases.

The simulated outage probability of the relay-selection cooperative transmission scheme at $P/N_0 = 20$ dB and $\alpha = 0.05$ is depicted in Figure 5.7. As shown, the outage probability of the cooperative protocol is lower than that of the the direct transmission and it decreases as the number of relays increases due to achieving diversity order equal to $N+1$. Figure 5.8 depicts the average SNR gap ratio of the relay-selection cooperative transmission scenario. As shown, all the relay-selection curves with different number of available relays have the same average SNR gap ratio, which is lower than that of the direct transmission scenario. Moreover, the average SNR gap ratio of the relay-selection scheme is the same as that of the conventional cooperative scheme with one relay only, which was shown in Figure 5.4. From Figure 5.8, we conclude that relay-selection cooperative scheme does not reduce the effect of the channel estimation error by adding more relays. This case is

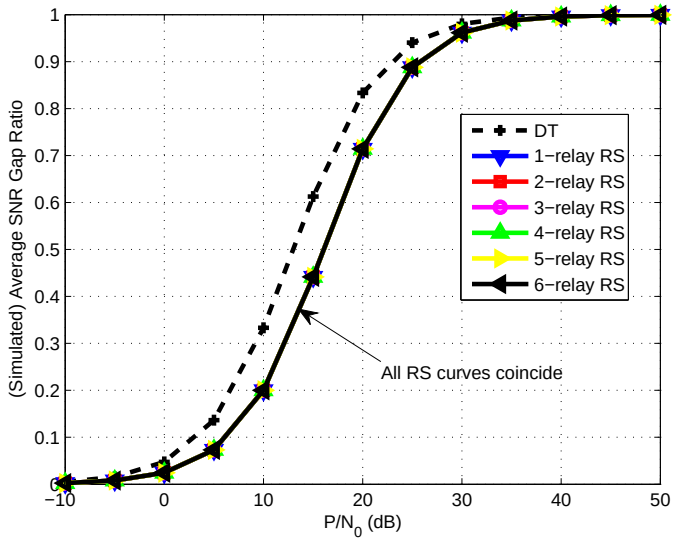

Figure 5.8: Channel estimator error: average SNR gap ratio of the direct and relay-selection cooperative transmission scenarios for $\alpha = 0.05$. The average SNR gap ratio is almost constant as the number of relays increases.

different from the conventional cooperative scheme, in which increasing the number of relays reduces the effect of the channel estimation error. From Figure 5.4 and Figure 5.8, we conclude that achieving higher diversity order is not the only factor for mitigating the effect of channel estimation error. In order to find out the other factors, we consider in the following subsection the multi-phase direct transmission scheme.

5.2.4 Multi-phase Direct transmission

In this subsection, we consider the multi-phase direct transmission scenario, in which a user sends its data to its destination in N consecutive channel uses, each with a transmission power of P/N. The N consecutive transmissions experience the same channel. There is no relays utilized in this scheme. Similar to (5.8), it

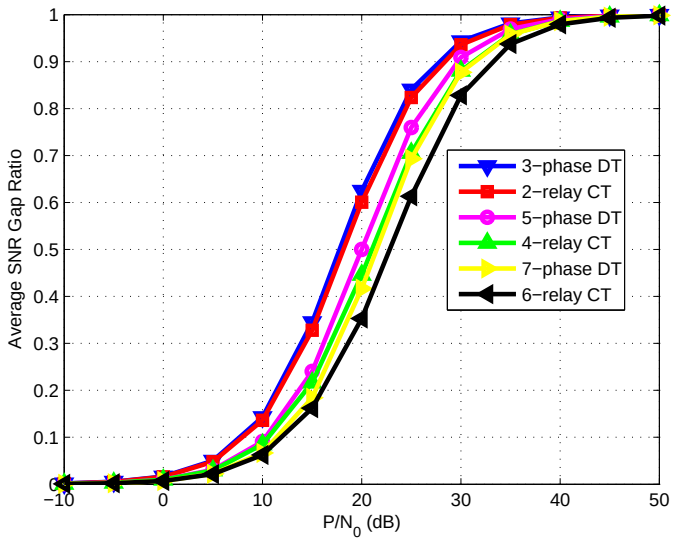

Figure 5.9: Channel estimator error: average SNR gap ratio of the multi-phase direct and cooperative transmission scenarios for $\alpha = 0.05$. Cooperative transmission scenarios reduces the SNR gap ratio more than the multi-phase direct transmission for the same number of phases.

can be shown that the SNR gap ratio is given by

$$R^D(N) = \frac{\alpha\, P}{N\, \delta_{s,d}^2\, (N_0 + \alpha\, P/N)}\, |h_{s,d}|^2\,, \tag{5.35}$$

i.e., $R^D(N) \sim \exp\big(N\,(N_0 + \alpha\, P/N)/(\alpha\, P)\big)$. The average SNR gap ratio can be calculated as

$$E\{R^D(N)\} = \frac{\alpha\, P}{N(N_0 + \alpha\, P/N)}\,. \tag{5.36}$$

We note that the multi-phase direct transmission scenario achieves diversity order equal to 1, and has outage probability similar to that of the conventional direct transmission.

Figure 5.9 depicts the average SNR gap ratio for the multi-phase and conventional cooperative transmission scenarios. As shown, the multi-phase direct transmission protocol reduces the SNR gap ratio as the number of relays increases.

Therefore by distributing the total transmission power across multiple transmission phases, the effect of the channel estimation error can be mitigated. In Figure 5.9, it is also shown that the cooperative transmission scenario reduces the SNR gap ratio more compared to the multi-phase direct transmission, for the same total number of transmission phases.

From Figure 5.4, Figure 5.8, and Figure 5.9, we conclude that the reduction in the SNR gap ratio is due to two main factors. The first factor is the distribution of the transmission power across multiple transmission phases. This reduces the transmission power in each phase, and accordingly the channel estimation error portion, αP, in each transmission is reduced. This first reduction factor exists in both the multi-phase direct transmission and conventional cooperative transmission scenarios, and hence both of them mitigate the effect of channel estimation error by increasing the number of transmission phases as was shown in Figure 5.9. On the contrary, the relay-selection cooperative scheme does not distribute the transmission power more by having more available relays.

The second factor of reducing the effect of channel estimation error is the achieved diversity order. The conventional cooperative transmission scenario utilizes relays, other than retransmission over the same channel. The cooperation gain resulting from utilizing relays reduces the channel estimation error effect more. This is clear in the SNR gap ratio PDF, as was shown previously in Figure 5.3, where the direct transmission SNR gap ratio is exponentially distributed while the conventional cooperative transmission SNR gap ratio is distributed as a weighted sum chi-square random variable. Since the conventional cooperative scheme achieves full diversity order along with distributing the transmission power, it reduces the SNR gap ratio compared to that of the multi-phase direct transmis-

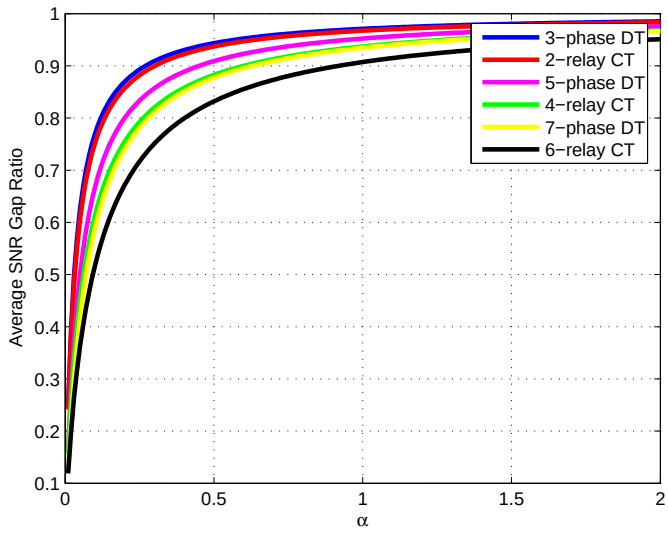

Figure 5.10: Channel estimator error: average SNR gap ratio of the multi-phase direct and cooperative transmission scenarios for $P/N_0 = 20$dB. Cooperative transmission scenarios reduces the SNR gap ratio more than the multi-phase direct transmission for the same number of phases.

sion, as was shown in Figure 5.9.

Finally, Figure 5.10 depicts the effect of the channel estimation error variance α on the average SNR gap ratio at P/N_0 =20dB. As expected, the average SNR gap ratio increases as α increases. Moreover, it is shown that cooperative transmission reduces the SNR gap ratio compared to the multi-phase direct transmission for the same number of transmission phases, which agrees with the result previously shown in Figure 5.9.

5.3 Timing Synchronization Error

In addition to the conventional and relay-selection cooperative schemes, we consider distributed space-time cooperative schemes [19, 20, 84], in which all the coop-

erating relays are simultaneously transmitting their designated codes. Assuming perfect timing synchronization among the relays, distributed space-time cooperative schemes achieve bandwidth efficiency equal to 1/2 SPCU while guaranteeing full diversity order [20]. Distributed space-time cooperative schemes suffer from timing synchronization error, which is a result of having the start of the transmission time of the cooperating relays not completely synchronized with each other. Moreover, due to the different geographic locations of the relays, signals transmitted from different relays experience different propagation delays and consequently arrive at the destination at different time instants. The destination picks a particular sampling instant, which definitely does not match the signals from all the relays. At the chosen sampling instant, the destination reads the mixture of a number of interfering signals that come from various multipaths, which dramatically increases the error rate. Finally, we note that the timing synchronization error increases as the number of relays increases.

In distributed space-time cooperative communication, there are two main contradicting factors that affect the system performance, which are the channel estimation error and the timing synchronization error. The channel estimation error effect decreases as the number of relays increases, as was previously shown in Figure 5.4. On the contrary, timing synchronization error increases as the number of relays increases. In this section, we investigate the tradeoff between these two contradicting types of error and their net impact on the system performance. In particular, we analyze one of the distributed space-time cooperative schemes, namely, distributed transmit beamforming scheme [84]. In distributed transmit beamforming transmission, the set of cooperating relays applies transmit beamforming via the available instantaneous relay-destination channel gain at each relay.

The distributed transmit beamforming scheme can be implemented in two consecutive transmission phases as follows. In the first phase, the source broadcasts its symbol, which is received by the set of N relays and the destination. The received symbols at the destination and the i-th relay can be modeled as in (5.3), with $P_0 = P/2$. Each relay decodes the received symbol and transmits it to the destination if correctly decoded, otherwise, it remains idle. The k-th transmitted sample from the i-th relay at time $k\,T$, where T is the symbol time, is given by

$$x_i(k) = I_{r_i}(k)\,\frac{h_{r_i,d}(k)^*}{||\mathbf{h}_{r,d}(k)||}\,x(k)\,, \tag{5.37}$$

where $\mathbf{h}_{r,d}(k) = [h_{r_1,d}(k), h_{r_2,d}(k), \cdots, h_{r_N,d}(k)]^T$ and $||.||$ denotes the vector norm. In (5.37), $I(.)$ is the indicator function of the i-th relay and it is given by

$$I_{r_i}(k) = \begin{cases} 1, & \text{if } r_i \text{ correctly decoded the } k\text{-th symbol} \\ 0. & \text{Otherwise} \end{cases}, \tag{5.38}$$

Each relay multiples its transmitted sample by a pulse shape function, denoted by $p(.)$, before transmission. We consider raised cosine pulse shape, $p(.)$, with roll-off factor of 0.5. In this chapter, we take into consideration the contribution from the first-order sidelobes of $p(.)$ and neglect that of the higher-order sidelobes due to its smaller effect [85]. We assume that the sampling instant at the destination is $(k\,T + \Delta_o)$, where Δ_o is a timing shift chosen by the destination to compensate for the average propagation delay. The received signal at the destination can be written as

$$y^B(k) = \sqrt{P/2}\sum_{i=1}^{N}\sum_{l=-1}^{1} x_i(k-l)\left(h_{r_i,d}(k-l) + h_{r_i,\alpha}(k-l)\right)p(\Delta_o - T_i + l\,T) + \eta(k)\,, \tag{5.39}$$

where the superscript B denotes the distributed beamforming scheme. In (5.39), T_i is the propagation delay of the i-th relay and $h_{r_i,\alpha}$ represents the channel estimation

error at the destination for the channel from the i-th relay to the destination. Finally, $\eta(k)$ is a zero-mean AWGN with variance N_o.

The received signal in (5.39) can be rewritten as

$$y^B(k) = y_{des}(k) + y_{int}(k) + \eta_\alpha(k)\,, \tag{5.40}$$

where $y_{des}(.)$, $y_{int}(.)$, and $\eta_\alpha(.)$ denote the desired signal, the interference signal, and the noise term including the channel estimation error, respectively. The desired signal is given by

$$y_{des}(k) = \sqrt{P/2}\,\frac{x(k)}{||\mathbf{h}(k)||}\,\sum_{i=1}^{N}\big(\,|h_{r_i,d}(k)|^2\,I_{r_i}(k)\,p(\Delta_o - T_i)\big)\,. \tag{5.41}$$

In addition, the interference signal can be modeled as

$$\begin{aligned} y_{int}(k) = {} & \sqrt{P/2}\,\frac{x(k+1)}{||\mathbf{h}(k+1)||}\,\sum_{i=1}^{N}\big(\,|h_{r_i,d}(k+1)|^2\,I_{r_i}(k+1)\,p(\Delta_o - T_i - T)\big) \\ & + \sqrt{P/2}\,\frac{x(k-1)}{||\mathbf{h}(k-1)||}\,\sum_{i=1}^{N}\big(\,|h_{r_i,d}(k-1)|^2\,I_{r_i}(k-1)\,p(\Delta_o - T_i + T)\big)\,. \end{aligned} \tag{5.42}$$

The composite noise term is

$$\begin{aligned} \eta_\alpha(k) = \sqrt{P/2}\,\sum_{i=1}^{N}\sum_{l=-1}^{1}\frac{x(k-l)}{||\mathbf{h}(k-l)||}\,\big(\,h_{r_i,d}(k-l)^*\,h_{r_i,\alpha}(k-l)\,I_{r_i}(k-l) \\ \times\,p(\Delta_o - T_i + l\,T)\big)\,+\eta(k)\,. \end{aligned} \tag{5.43}$$

The channel estimation error terms, $h_{r_i,\alpha}$, for different relays r_i and time instants $l\,T$ are independent and identically distributed with variance α. For a fixed x and $\mathbf{h}$, the noise variance can be calculated as

$$E\{\eta_\alpha(k)^2\} = \frac{\alpha\,P}{2}\,\sum_{i=1}^{N}\sum_{l=-1}^{1}\Big(\,\frac{|h_{r_i,d}(k-l)|^2}{||\mathbf{h}(k-l)||^2}\,I_{r_i}(k-l)\,p^2(\Delta_o - T_i + l\,T)\Big) + N_o\,. \tag{5.44}$$

Finally, the conditional received SNR can be computed as

$$\gamma^B(k) = \frac{P}{2\,(N_0 + \alpha\,P/2)}\,|h_{s,d}(k)|^2 + \frac{y_{des}(k)^2}{y_{int}(k)^2 + E\{\eta_\alpha(k)^2\}}\,, \tag{5.45}$$

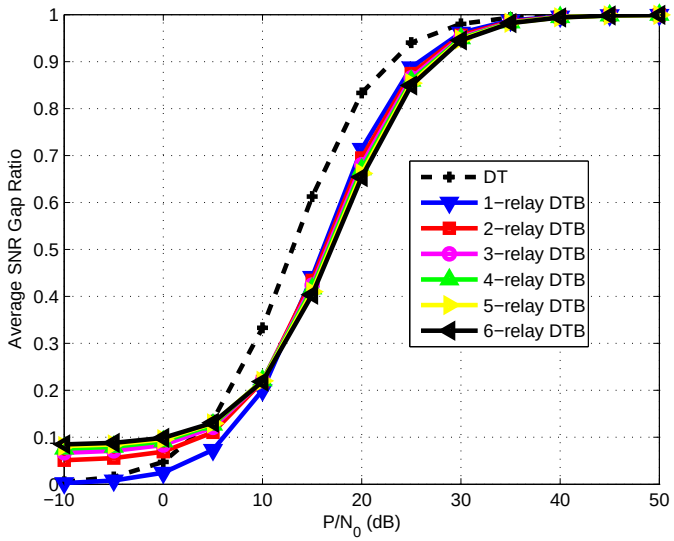

Figure 5.11: Channel estimator error: average SNR gap ratio of the direct and distributed transmit beamforming cooperative transmission scenarios for $\alpha = 0.05$ and $\Delta T = 0.15\,T$. The average SNR gap ratio increases at low transmission power, and decreases at high transmission power with increasing the number of relays.

where the first term represents the SNR due to the first phase, which is similar to the first term in (5.11).

We assume that the timing synchronization error is distributed uniformly as $(\Delta_o - T_i) \sim U[-\Delta T/2, \Delta T/2]$. Figure 5.11 depicts the average SNR gap ratio for a particular deployment scenario, in which the relays are close to the middle between the source and destination and $\Delta T = 0.15T$. The average SNR gap ratio is obtained via simulations by averaging over independent channel and independent timing synchronization error realizations. For each realization, the SNR and SNR gap ratio are calculated as in (5.45) and (5.6), respectively. In (5.6), $\gamma|_{(\alpha=0)}$ refers to having perfect channel estimation and perfect timing synchronization case. Finally, the outage probability is calculated based on the SNR expression given in (5.45).

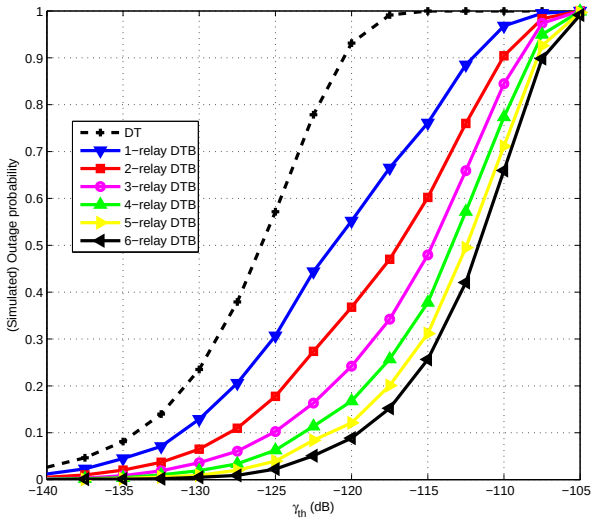

Figure 5.12: Channel estimator error: outage probability of the direct and distributed transmit beamforming transmission scenarios for $\alpha = 0.05$, $\Delta T = 0.15\,T$, and $P/N_0 =$ 20dB. Distributed transmit beamforming transmission reduces the outage probability as the number of relays increases.

Figure 5.11 depicts the average SNR gap ratio of the distributed transmit beamforming scheme. As shown, the net impact of the two contradicting error effects depends on the data transmission power, P. We note that the timing synchronization error effect does not depend on the transmission power. On the contrary, the effect of the channel estimation error, αP, increases with increasing the data transmission power. At low transmission power, the effect of the synchronization error is more significant compared to that of the channel estimation error. Hence at low transmission power, having more relays increases the average SNR gap ratio as shown in Figure 5.11. As the transmission power increases, the effect of channel estimation error gets more significant compared to that of the timing synchronization error. Therefore at high transmission power, adding more relays leads to net effect of lower average SNR gap ratio. Finally, Figure 5.12 depicts the outage probability of the distributed transmit beamforming transmission at $P/N_0 = 20$. As shown, the outage probability decreases as the number of relays increases due to achieving higher spatial diversity order, which is equal to $N + 1$.

Chapter 6

Conclusions and Future Work

6.1 Conclusions

In this thesis, we have developed and analyzed a cross-layer framework for utilizing the cooperative communication paradigm in wireless networks. In particular, we have developed new relay deployment and selection protocols across the network layers that can increase the bandwidth efficiency, reduce the required transmission power needed to achieve a desired network throughput, maximize the lifetime of a given network, maintain a given network to be connected as long as possible, rebuild a given network in case it is disconnected, and mitigate the effect of channel estimation error and co-channel interference (CCI). More specifically, we have addressed the following problems.

In Chapter 2, we have proposed a cross-layer design for relay-selection decode-and-forward cooperative scenario, which utilizes the partial channel state information (CSI) available at the source and the relays. The main objective of this work is to achieve higher bandwidth efficiency and to guarantee full diversity order. We have defined the optimal relay as the one which has the maximum instantaneous

scaled harmonic mean function of its source-relay and relay-destination channel gains among the N helping relays. We have introduced an approximate expression of the achievable bandwidth efficiency, which decreases with increasing the number of employed relays. Furthermore, we have derived the SER upper bound, which proves that full diversity order is guaranteed as long as there is cooperation. We have shown that the bandwidth efficiency is boosted up from 0.2 to 0.82 symbol per channel use (SPCU) for $N = 4$ relays and unity channel variances case. The optimum power allocation between the source and the relay is determined by minimizing the symbol error rate expression. Moreover, we have shown the bandwidth efficiency-SER tradeoff curve, which determines the optimum cooperation threshold. Finally, we have presented some simulation results to verify the obtained analytical results.

In Chapter 3, we have generalized the relay-selection problem considered in Chapter 2 to a general routing problem. In particular, we have investigated the impact of the cooperative communications on the minimum-power routing problem in wireless networks. For a given source-destination pair, the optimum route requires the minimum end-to-end transmission power while guaranteeing certain throughput. We have proposed a cross-layer design of routing scheme, namely, Minimum Power Cooperative Routing (MPCR) algorithm, which applies the cooperative communication while constructing the route. The MPCR algorithm constructs the minimum-power route using any number of the proposed cooperation-based building blocks, which require the least possible transmission power.

We have also presented the Cooperation Along the Shortest Non-Cooperative Path (CASNCP) algorithm, which is similar to most of the existing cooperative routing algorithms. The CASNCP algorithm first constructs the conventional

shortest-path route then applies a cooperative-communication protocol upon the established route. We have shown that for random networks of $N = 100$ nodes, the power savings of the MPCR algorithm with respect to the conventional shortest-path and CASNCP routing algorithms are 57.36% and 37.64%, respectively. In addition, we have considered regular linear and grid networks, and we have derived the analytical results for the power savings due to cooperation in these cases. We have shown that in a regular linear network with $N = 100$ nodes, the power savings of the MPCR algorithm with respect to shortest-path and CASNCP routing algorithms are 73.91% and 65.61%, respectively. Similarly, the power savings of the MPCR algorithm with respect to shortest-path and CASNCP routing algorithms in a grid network of 100 nodes are 65.63% and 29.8%, respectively.

Utilizing relays can not only reduce the transmission power, as it was investigated in Chapter 3, but also increase the network lifetime of a given network. In Chapter 4, we have addressed the problems of network maintenance and network repair in wireless sensor networks via relay deployment. We have considered the Fiedler value, which is the algebraic connectivity of a graph, as a network health indicator. First, we have proposed a network maintenance algorithm, which finds the locations for an available set of relays that result in the maximum possible Fiedler value. This algorithm finds the location through a small number of levels. In each level, the network maintenance problem is formulated as a semi-definite programming (SDP) optimization problem, which can be solved using the available standard SDP solvers. In a sensor network of $n = 50$ sensors deployed in a 15×15 area, the network lifetime has increased by 113.6% due to the addition of 15 relays.

Second, we have proposed an adaptive network maintenance algorithm, where

the relays' locations can be changed depending on the network health indicator. We have shown that a lifetime gain of 119.7% is achieved due to the proposed adaptive network maintenance algorithm. Third, we have proposed the Weighted Minimum Power Routing (WMPR) algorithm, which balances the load of the network among the sensors and the relays. We have also illustrated that in sensor networks, where sensors have limited supplies, nodes should transmit their data over orthogonal channels with no interference from the other nodes. Finally, we have proposed an iterative network repair algorithm, which finds the minimum number of relays needed to connect a disconnected network.

In Chapter 5, we have investigated the impact of the cooperative communications on mitigating channel estimation error and CCI effects. The SNR gap ratio, which measures the reduction in the SNR, and the conventional outage probability were utilized to characterize the system performance. We have shown that the cooperative transmission schemes are less susceptible to the channel estimation error compared to the direct transmission. Furthermore, increasing the number of relays results in lower SNR gap ratio. At $P/N_0 = 10$ dB and channel estimation error variance $\alpha = 0.05$, the direct transmission scenario suffers SNR gap ratio of 0.33, while the cooperative transmission scenario with $N = 6$ relays suffers SNR gap ratio of 0.06 only. We have illustrated that cooperative transmission reduces the channel estimation error effect due to two main factors: 1) achieving spatial diversity via relays and 2) distributing the transmission power across multiple transmission phases.

We have also considered distributed transmit beamforming cooperative scheme, and we have studied the tradeoff between the timing synchronization error and channel estimation error. At low data transmission power, the timing synchro-

nization error is more significant. As the data transmission power increases, we find that the effect of channel estimation error overcomes that of the timing synchronization error. Finally, we have shown that cooperative schemes are less susceptible to the CCI problem, compared to that of the direct transmission. At $P/N_0 = 130$ dB, the direct transmission scenario suffers SNR gap ratio of 0.18, while the cooperative transmission scenario with $N = 6$ relays suffers SNR gap ratio of 0.07.

6.2 Future Work: Relay Deployment in 4G Cellular Networks

Currently, there is a huge interest in integrating relays and employing cooperative communication protocols into the fourth generation (4G) cellular systems, namely, the Worldwide Interoperability for Microwave Access (WiMAX) and the Long Term Evolution (LTE). Integrating relays into cellular networks can combat the shadowing effect, extend the coverage area, increase the total throughput, and reduce the infrastructure deployment costs compared to that of the base stations [86]. For relay-based cellular networks, there are many interesting issues that need to be addressed. In this section, we shed the light on an important aspect which is related to relay deployment. In particular, what is the optimum number of relays to be deployed in each cell, along with their optimum locations?

We start solving this question by defining an optimization metric. In cellular networks, cell-edge users usually experience the worst performance. Therefore, we consider the performance of the cell-edge users as the optimization criterion. In the sequel we discuss two relay deployment strategies, which aim to significantly

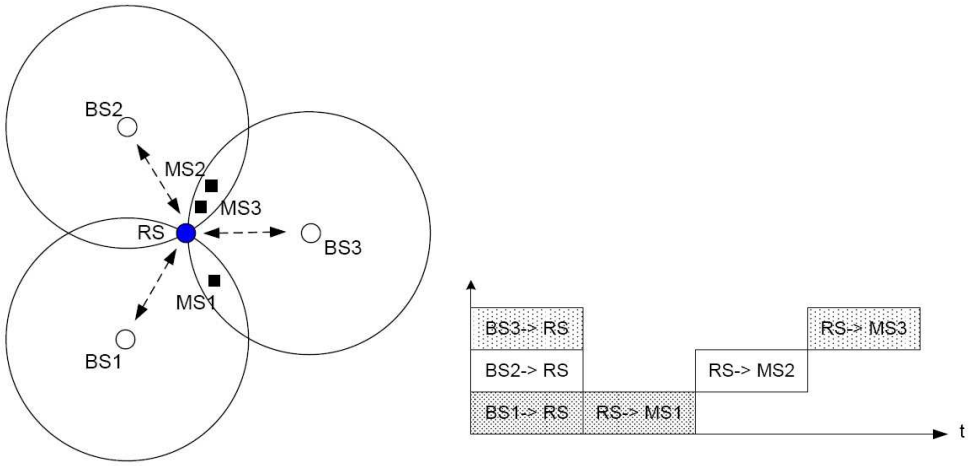

(a) (b)

Figure 6.1: Single-relay deployment: (a) network diagram, (b) timing diagram.

improve the performance of the cell-edge users. Particularly, we consider single-relay and multiple-relay deployment strategies in Section 6.2.1 and Section 6.2.2, respectively.

6.2.1 Single-Relay Deployment

Figure 6.1 (a) depicts multiple-antenna single-relay deployment scenario, in which one Relay Station (RS) serves the cell-edge Mobile Stations (MSs) associated with 3 neighboring Base Stations (BSs). For best utilization, the RS is deployed at the intersection of the 3 neighboring cells. In practice, the RS is deployed at a relatively high position. Hence the channels between the BSs and the RS provide line-of-sight communication, and these channels are very reliable with high probability. Thus with high probability, the BS and RS have identical copies of the same information.

We note that having the BSs geographically separated provides spatial multiplexing gain to the network by utilizing Space Division Multiple Access (SDMA)

technique. In other words, the 3 BSs can simultaneously transmit their information to the multiple-antenna RS, with low interference effect due to the spatial decorrelation of the corresponding channels. It should be noted though that the spatial multiplexing gain is limited by the minimum of the number of the RS antennas and the sum of the number of the BSs antennas.

In the downlink transmission, we assume that the i-th BS has one symbol to be sent to the i-th MS, for $i = 1, 2, 3$. In Figure 6.1 (b), we show the timing diagram of the reliable downlink transmission, which consists of 4 time slots. In the first time slot, the 3 BSs send their information simultaneously to the RS. Then, the RS sends each symbol separately to its designated MS. Various space-time schemes can be implemented at the RS to achieve full transmit diversity and reliably transmits the information to each MS. Since 4 time slots are required for the transmission of 3 symbols, hence, the bandwidth efficiency can be calculated as

$$R_s = 3/4 \text{ SPCU}\,, \tag{6.1}$$

where SPCU denotes Symbols Per Channel Use.

A similar procedure can be implemented in the uplink transmission, in which MSs transmit their information to the designated BSs. In this sub-section we have introduced the single-relay deployment scenario, which significantly improves the performance of the cell-edge users with relatively high bandwidth efficiency. In the next sub-section, we investigate multiple-relay deployment strategy that significantly increases the bandwidth efficiency via deploying multiple relays in each cell.

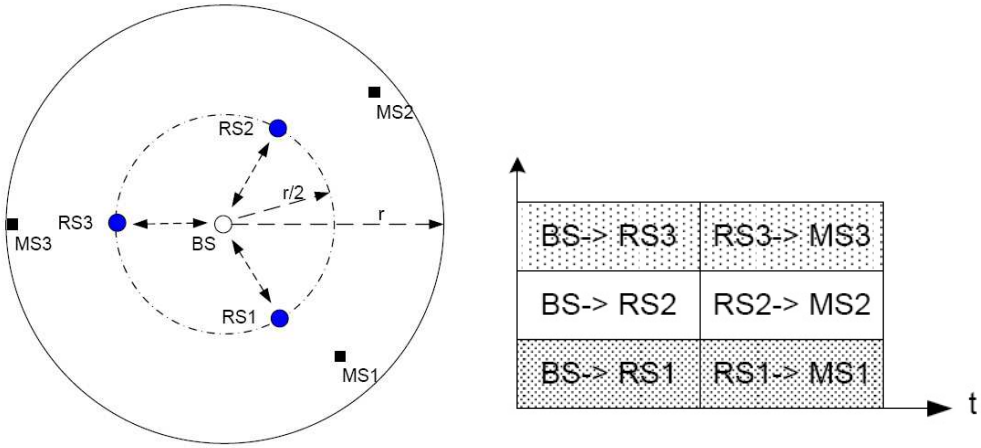

(a) (b)

Figure 6.2: Multiple-relay deployment: (a) network diagram, (b) timing diagram.

6.2.2 Multiple-Relay Deployment

The proposed relay deployment strategy is based on the result that the optimum relay location helping a particular MS will be in the mid-point between the MS and the BS, in the case of amplify-and-forward [18] or incremental relaying decode-and-forward with no maximal ratio combining (MRC) at the MS [9]. The proposed scheme, which aims to significantly enhance the performance of the cell-edge users, deploys the available relays uniformly across a circle with radius $r/2$, where r is the cell radius. Figure 6.2 (a) depicts the multiple-relay deployment strategy, in which 3 RSs are deployed in each cell.

The multiple-relay deployment strategy also provides spatial multiplexing gain. Because the RSs are geographically separated and hence the BS can simultaneously transmit independent data to the RSs, taking advantage of the low spatial decorrelation of the BS-RS channels. The spatial multiplexing gain in this case is limited by the minimum number of antennas at the BS and the sum of the number of

antennas at the RSs. Moreover, the relays are relatively far apart from each other. Thus, the RSs can send their information simultaneously to their designated MSs with low interference effect.

In Figure 6.2 (b) we show the timing diagram of the downlink transmission, in which the BS sends 3 different symbols to their designated MSs in 2 consecutive time slots. In the first time slot, the BS transmits the 3 symbols to the 3 RSs simultaneously employing superposition coding and transmit beamforming. In the second time slot, each RS sends 1 symbol to its designated MS using any transmit diversity scheme. The bandwidth efficiency of the multiple-relay scenario can be computed as

$$R_m = 3/2 \text{ SPCU}\,, \tag{6.2}$$

which is higher than that achieved by the single-relay deployment strategy in (6.1). A similar transmission procedure can be implemented in the uplink transmission.

In this section, we have discussed two possible relay deployment scenarios that improve the performance of the cell-edge users in the 4G cellular networks. We have shown that the multiple-relay deployment strategy achieves higher bandwidth efficiency compared to that achieved by the single-relay deployment strategy. In the future, we aim to provide more analytical analysis and simulation results for these relay deployment strategies.

BIBLIOGRAPHY

[1] D. Tse and P. Viswanath, *Fundamentals of wireless communication*, Cambridge University Press, 2005.

[2] V. Tarokh, N. Seshadri, and A. R. Calderbank, "Space-time codes for high data rate wireless communication: Performance criterion and code construction," *IEEE Trans. Information Theory*, vol. 44, no. 2, pp. 744–765, Mar. 1998.

[3] S. M. Alamouti, "A simple transmit diversity technique for wireless communiucations," *IEEE Journal on Selected Areas in Communications*, vol. 16, no. 8, pp. 1451–1458, Oct. 1998.

[4] G. J. Foschini and M. Gans, "On the limits of wireless communication in a fading environment when using multiple antennas," *Wireless Personal Communications*, vol. 6, pp. 311–335, Mar. 1998.

[5] E. Telatar, "Capacity of multi-antenna gaussian channels," *Eur. Trans. Telecom.*, vol. 10, pp. 585–595, Nov. 1999.

[6] K. J. R. Liu, A. K. Sadek, W. Su, and A. Kwasinski, *Cooperative communications and networking*, Cambridge University Press, 2008.

[7] W. Su, A. K. Sadek, and K. J. R. Liu, "Cooperative communication protocols in wireless networks: performance analysis and optimum power allocation," *Wireless Personal Communications*, vol. 44, pp. 181–217, Jan. 2008.

[8] D. G. Brennan, "Linear diversity combining techniques," *Proc. IEEE*, vol. 91, no. 2, pp. 331–356, Feb. 2003.

[9] A. K. Sadek, Z. Han, and K. J. R. Liu, "A distributed relay-assignment algorithm for cooperative communications in wireless networks," *Proc. IEEE International Conference on Communications (ICC'06)*, vol. 4, pp. 1592–1597, Jun. 2006.

[10] E. C. van der Meulen, "Three-terminal communication channels," *Adv. Appl. Probab.*, 1971.

[11] T. M. Cover and A. A. El Gamal, "Capacity theorems for the relay channel," *IEEE Trans. Information Theory*, vol. 25, no. 9, pp. 572–584, Sep. 1979.

[12] G. Kramer, M. Gatspar, and P. Gupta, "Cooperative strategies and capacity theorems for relay networks," *IEEE Trans. Information Theory*, vol. 51, no. 9, pp. 3037–3063, Sep. 2005.

[13] A. Sendonaris, E. Erkip, and B. Aazhang, "User cooperation diversity, part I: System description," *IEEE Trans. Communications*, vol. 51, no. 11, pp. 1927–1938, Nov. 2003.

[14] A. Sendonaris, E. Erkip, and B. Aazhang, "User cooperation diversity, part II: Implementation aspects and performance analysis," *IEEE Trans. Communications*, vol. 51, no. 11, pp. 1939–1948, Nov. 2003.

[15] J. N. Laneman, D. N. C. Tse, and G. W. Wornell, "Cooperative diversity in wireless networks: efficient protocols and outage behavior," *IEEE Trans. Information Theory*, vol. 50, no. 12, pp. 3062–3080, Dec. 2004.

[16] J. Boyer, D. D. Falconer, and H. Yanikomeroglu, "Multihop diversity in wireless relaying channels," *IEEE Trans. Communications*, vol. 52, no. 16, pp. 1020–1030, Oct. 2004.

[17] A. K. Sadek, W. Su, and K. J. R. Liu, "Multi-node cooperative communications in wireless networks," *IEEE Trans. Signal Processing*, vol. 55, pp. 341–355, Jan. 2007.

[18] A. Ribeiro, X. Cai, and G. B. Giannakis, "Symbol error probabilities for general cooperative links," *IEEE Trans. Wireless Communications*, vol. 4, pp. 1264–1273, May 2005.

[19] J. N. Laneman and G. W. Wornell, "Distributed space-time coded protocols for exploiting cooperative diversity in wireless networks," *IEEE Trans. Information Theory*, vol. 49, no. 10, pp. 2415–2425, Oct. 2003.

[20] K. G. Seddik, A. K. Sadek, A. S. Ibrahim, and K. J. R. Liu, "Design criteria and performance analysis for distributed space-time coding," *IEEE Trans. on Vehicular Technology*, vol. 57, pp. 2280 – 2292, Jul. 2008.

[21] T. E. Hunter and A. Nosratinia, "Diversity through coded cooperation," *IEEE Trans. Communications*, vol. 5, pp. 283–289, Feb. 2006.

[22] A. Wittneben and B. Rankov, "Impact of cooperative relays on the capacity of rank-deficient MIMO channels," *Proc. of the 12th IST Summit on Mobile and Wireless Communications*, pp. 421–425, Jun. 2003.

[23] X. Tang and Y. Hua, "Optimal design of non-regenerative MIMO wireless relays," *IEEE Trans. Wireless Communications*, vol. 6, pp. 1398–1407, Apr. 2007.

[24] A. S. Ibrahim, A. K. Sadek, W. Su, and K. J. R. Liu, "Cooperative communications with relay-selection: when to cooperate and whom to cooperate with?," *IEEE Trans. on Wireless Comm.*, vol. 7, pp. 2814 – 2827, Jul. 2008.

[25] A. S. Ibrahim, A. K. Sadek, W. Su, and K. J. R. Liu, "Cooperative communications with partial channel state information: when to cooperate?," *Proc. IEEE Global Telecommunications Conference (Globecom'05)*, vol. 5, pp. 3068 – 3072, Nov. 2005.

[26] A. S. Ibrahim, A. K. Sadek, W. Su, and K. J. R. Liu, "Relay selection in multi-node cooperative communications: When to cooperate and whom to cooperate with?," *Proc. IEEE Global Telecommunications Conference (Globecom'06)*, pp. 1 – 5, Nov. 2006.

[27] A. S. Ibrahim, Z. Han, and K. J. R. Liu, "Distributed energy-efficient cooperative routing in wireless networks," *IEEE Trans. on Wireless Comm.*, vol. 7, pp. 3930–3941, Oct. 2008.

[28] A. S. Ibrahim, Z. Han, and K. J. R. Liu, "Distributed energy-efficient cooperative routing in wireless networks," *Proc. IEEE Global Telecommunications Conference (Globecom'07)*, pp. 4413 – 4418, Nov. 2007.

[29] I. Akyildiz, W. Su, Y. Sankarasubramanian, and E. Cayirci, "A survey on sensor networks," *IEEE Comm. Magazine*, vol. 40, pp. 102 – 114, Aug. 2002.

[30] A. S. Ibrahim, K.G. Seddik, and K. J. R. Liu, "Connectivity-aware network maintenance and repair via relays deployment," *IEEE Trans. on Wireless Comm.*, vol. 8, pp. 356–366, Jan. 2009.

[31] A.S. Ibrahim, K.G. Seddik, and K.J.R. Liu, "Improving connectivity via relays deployment in wireless sensor networks," *Proc. IEEE Global Telecommunications Conference (Globecom'07)*, pp. 1159–1163, Nov. 2007.

[32] A.S. Ibrahim, K. G. Seddik, and K.J.R. Liu, "Connectivity-aware network maintenance via relays deployment," *Proc. IEEE Wireless Comm. and Networking Conference 2008 (WCNC'08)*, pp. 2573–2578, Apr. 2008.

[33] A.S. Ibrahim and K.J.R. Liu, "Mitigating channel estimation error via cooperative communications," *to appear in IEEE International Conference on Communications (ICC'09)*, Jun. 2009.

[34] A.S. Ibrahim and K.J.R. Liu, "Mitigating channel estimation error and co-channel interference effects via cooperative communications," *submitted to IEEE Trans. on Signal Processing*, Dec. 2008.

[35] B. Zhao and M. C. Valenti, "Practical relay networks: A generalization of hybrid-ARQ," *IEEE J. Sel. Areas Commun.*, vol. 23, pp. 7–18, Jan. 2005.

[36] M. Zorzi and R. R. Rao, "Geographic random forwarding (GeRaF) for ad hoc and sensor networks: Multihop performance," *IEEE Trans. Mobile Comput.*, vol. 2, pp. 337 – 348, Oct.-Dec. 2003.

[37] M. Zorzi and R. R. Rao, "Geographic random forwarding (GeRaF) for ad hoc and sensor networks: Energy and latency performance," *IEEE Trans. Mobile Comput.*, vol. 2, pp. 349 – 365, Oct.-Dec. 2003.

[38] J. Luo, R. S. Blum, L. J. Greenstein, L. J. Cimini, and A. M. Haimovich, "New approaches for cooperative use of multiple antennas in ad hoc wireless networks," *Proc. IEEE 60th Vehicular Technology Conference*, vol. 4, pp. 2769 – 2773, Sep. 2004.

[39] M. O. Hasna and M. S. Alouini, "Performance analysis of two-hop relayed transmssions over rayleigh fading channels," *Proc. IEEE Vehicular Technology Conference*, vol. 4, pp. 1992–1996, Sep. 2002.

[40] M. Abramowitz and I. A. Stegun, *Handbook of mathematical functions with formulas, graphs, and mathematical tables*, New York, NY: Dover publications, 9th ed., 1970.

[41] M.K. Simon and M.-S. Alouini, "A unified approach to the performance analysis of digital communication over generalized fading channels," *Proc. IEEE*, vol. 86, pp. 1860–1877, Sep. 1998.

[42] I. S. Gradshteyn and I. M. Ryzhik, *Tables of integrals, series, and products*, San Diego, CA: Academic press, 5th ed., 1994.

[43] J. H. Chang and L. Tassiulas, "Energy conserving routing in wireless ad-hoc networks," *Proc. IEEE Conference on Computer Communications (INFOCOM'00)*, pp. 22–31, Mar. 2000.

[44] M. Younis, M. Youssef, and K. Arisha, "Energy-aware management for cluster-based sensor networks," *Journal of Computer Networks*, vol. 43, pp. 539 – 694, Dec. 2003.

[45] L. M. Feeney and M. Nilsson, "Investigating the energy consumption of a wireless network interface in an ad hoc networking environment," *Proc. IEEE Conference on Computer Communications (INFOCOM'01)*, vol. 3, pp. 1548 – 1557, Apr. 2001.

[46] B. Zhang and H. T. Mouftah, "QoS routing for wireless ad hoc networks: problems, algorithms, and protocols," *IEEE Communications Magazine*, vol. 43, pp. 110–117, Oct. 2005.

[47] A. E. Khandani, E. Modiano, L. Zheng, and J. Abounadi, "Cooperative routing in wireless networks," *Chapter in Advannces in Pervasive Computing and Networking, Kluwer Academic Publishers, Eds. B. K. Szymanski and B. Yener*, 2004.

[48] Z. Yang and A. Host-Madsen, "Routing and power allocation in asynchronous gaussian multiple-relay channels," *EURASIP Journal on Wireless Communications and Networking*, 2006.

[49] F. Li, K. Wu, and A. Lippman, "Energy-efficient cooperative routing in multi-hop wireless ad hoc networks," *Proc. IEEE International Performance, Computing, and Communications Conference*, pp. 215 – 222, Apr. 2006.

[50] M. Sikora, J. N. Laneman, M. Haenggi, D. J. Costello, and T. E. Fuja, "Bandwidth- and power-efficient routing in linear wireless networks," *IEEE Trans. Inform. Theory*, vol. 52, pp. 2624 – 2633, Jun. 2006.

[51] C. Pandana, W. P. Siriwongpairat, T. Himsoon, and K. J. R. Liu, "Distributed cooperative routing algorithms for maximizing network lifetime," *Proc. IEEE Wireless Communications and Networking Conference (WCNC'06)*, vol. 1, pp. 451–456, 2006.

[52] *SDPA-M package*, Available online at: http://grid.r.dendai.ac.jp/sdpa/.

[53] J. G. Proakis, *Digital Communications*, McGraw-Hill Inc., 4th ed., 2000.

[54] I.F. Akyildiz, W. Su, Y. Sankarasubramaniam, and E. Cayirci, "A survey on sensor networks," *IEEE Communications Magazine*, vol. 40, pp. 102–114, Aug. 2002.

[55] Y. T. Hou, Y. Shi, H. D. Sherali, and S. F. Midkiff, "Prolonging sensor network lifetime with energy provisioning and relay node placement," *Proc. IEEE Sensor and Ad Hoc Communications and Networks (SECON'05)*, pp. 295–304, Sep. 2005.

[56] N. Li and J. C. Hou, "Improving connectivity of wireless ad hoc networks," *Proc. The Second Annual International Conference on Mobile and Ubiquitous Systems: Networking and Services (MobiQuitous'05)*, pp. 314–324, Jul. 2005.

[57] C. Pandana and K. J. R. Liu, "Maximum connectivity and maximum lifetime energy-aware routing for wireless sensor networks," *Proc. IEEE Global Telecommunications Conference (Globecom'05)*, vol. 2, pp. 1034–1038, Nov. 2005.

[58] C. Pandana and K. J. R. Liu, "Robust connectivity-aware energy-efficient routing for wireless sensor networks," *IEEE Trans. on Wireless Communications*, vol. 7, pp. 3904–3916, Oct. 2008.

[59] T. Himsoon, W.P. Siriwongpairat, Z. Han, and K.J.R. Liu, "Lifetime maximization via cooperative nodes and relay deployment in wireless networks," *IEEE Journal of Selected Areas in Communications, Special Issue on Cooperative Communications and Networking*, vol. 25, pp. 306–317, Feb. 2007.

[60] Y. Xin, T. Guven, and M. Shayman, "Relay deployment and power control for lifetime elongation in sensor networks," *Proc. IEEE International Conference on Communications (ICC'06)*, vol. 8, pp. 3461–3466, Jun. 2006.

[61] S. Maruyama, K. Nakano, K. Meguro, M. Sengoku, and S. Shinoda, "On location of relay facilities to improve connectivity of multi-hop wireless networks," *Proc. 10th Asia-Pacific Conference on Communications and 5th International Symposiym on Multi-Dimensional Mobile Communications*, pp. 749–753, 2004.

[62] K. Xu, H. Hassanein, and G. Takahara, "Relay node deployment strategies in heterogeneous wireless sensor networks: multiple-hop communication case," *Proc. IEEE Sensor and Ad Hoc Communications and Networks (SECON'05)*, pp. 575–585, Sep. 2005.

[63] Zhu Han, A. L. Swindlehurst, and K. J. R. Liu, "Smart deployment/movement of unmanned air vehicle to improve connectivity in manet," *Proc. IEEE Wireless Communications and Networking Conference (WCNC'06)*, vol. 1, pp. 252–257, Apr. 2006.

[64] G. Lin and G. Xue, "Steiner tree problem with minimum number of steiner points and bounded edge-length," *Information Processing Letters*, vol. 69, pp. 53–57, 1999.

[65] D. Chen, D.Z. Du, X.-D. Hu, G.H. Lin, L. Wang, and G. Xue, "Approximations for steiner trees with minimum number of steiner points," *J. Global Optimization*, vol. 18, pp. 17–33, 2000.

[66] X. Cheng, D.Z. Du, L. Wang, and B. Xu, "Relay sensor placement in wireless sensor networks," *ACM/Springer J. Wireless Networks*, 2004.

[67] E. Lloyd and G. Xue, "Relay node placement in wireless sensor networks," *IEEE Transactions on Computers*, vol. 56, pp. 134–138, Jan. 2007.

[68] A. Kashyap, S. Khuller, and M. Shayman, "Relay placement for higher order connectivity in wireless sensor networks," *Proc. 25th IEEE International*

Conference on Computer Communications (INFOCOM'06), pp. 1–12, Apr. 2006.

[69] M. Fiedler, "Algebraic connectivity of graphs," *Czechoslovak Lathematics Journal*, pp. 298–305, 1973.

[70] A. Ghosh and S. Boyd, "Growing well-connected graphs," *Proc. IEEE Conference on Decision and Control (CDC'06)*, pp. 6605–6611, Dec. 2006.

[71] B. Mohar, "Some applications of laplace eigenvalues of graphs," *In G. Hahn and G. Sabidussi, editors, Graph Symmetry: Algebraic Methods and Applications, NATO ASI Series C*, vol. 497, pp. 227–275, Jul. 1997.

[72] S. Boyd, "Convex optimization of graph laplacian eigenvalues," *Proc. International Congress of Mathematicians, 3:1311-1319*, 2006.

[73] S. Boyd and L. Vandenberghe, *Convex Optimization*, Cambridge University Press, 2003.

[74] D. Bertsekas and R. Gallager, *Data Networks*, Prentice Hall.

[75] J. H. Chang and L. Tassiulas, "Energy conserving routing in wireless ad-hoc networks," *Proc. IEEE Conference on Computer Communications (INFOCOM'00)*, pp. 22 – 31, Mar. 2000.

[76] F. Rashid-Farrokhi, L. Tassiulas, and K. J. R. Liu, "Joint optimal power control and beamforming in wireless networks using antenna arrays," *IEEE Trans. on Communications*, vol. 46, pp. 1313 – 1324, Oct. 1998.

[77] H. Cheon and D. Hong, "Effect of channel estimation error in OFDM-based WLAN," *IEEE Communications Letters*, vol. 6, pp. 190 – 192, May 2002.

[78] L. Li, X. Zhao, H. Hu, and H. Yu, "Effect of imperfect channel estimation on multi-branch cooperative links in fading channels," *Proc. IEEE International Conference on Wireless Communications, Networking and Mobile Computing(WiCom'07)*, pp. 1087 – 1090, Sep. 2007.

[79] H. Jin, R. Laroia, and T. Richardson, "Superposition by position," *Proc. IEEE Information Theory Workshop*, pp. 222 – 226, Mar. 2006.

[80] F. Rashid-Farrokhi, K. J. R. Liu, and L. Tassiulas, "Transmit beamforming and power control for cellular wireless systems," *IEEE Journal of Selected Areas in Communications, Special Issue on Signal Processing for Wireless Communications*, vol. 16, pp. 1437 – 1450, Oct. 1998.

[81] W. Choi, N. Himayat, S. Talwar, and M. Ho, "The effects of co-channel interference on spatial diversity techniques," *Proc. IEEE Wireless Communications and Networking Conference (WCNC'07)*, pp. 1938 – 1943, Mar. 2007.

[82] Y. Akyildiz and B.D. Rao, "Statistical performance analysis of optimum combining with co-channel interferers and flat rayleigh fading," *Proc. IEEE Global Telecommunications Conference (GLOBECOM'01)*, vol. 6, pp. 3663 – 3667, Nov. 2001.

[83] G. J. Foschini, "Layered space-time architecture for wireless communication in a fading environment when using multiple antennas," *Bell Lab. Tech. J.*, vol. 1, pp. 41–59, 1996.

[84] S. Jagannathan, H. Aghajan, and A. Goldsmith, "The effect of time synchronization errors on the performance of cooperative MISO systems," *Proc. IEEE Global Telecommunications Conference (GLOBECOM'04)*, pp. 102 – 107, Nov. 2004.

[85] Y. Mei, Y. Hua, A. Swami, and B. Daneshrad, "Combating synchronization errors in cooperative relays," *Proc. IEEE International Conference on Acoustics, Speech, and Signal Processing(ICASSP'05)*, pp. iii/369 – iii/372, Mar. 2005.

[86] R. Pabst, B. H. Walke, D. C. Schultz, P. Herhold, H. Yanikomeroglu, S. Mukherjee, H. Viswanathan, M. Lott, W. Zirwas, M. Dohler, H. Aghvami, D. D. Falconer, and G. P. Fettweis, "Relay-based deployment concepts for wireless and mobile broadband radio," *IEEE Communications Magazine*, vol. 42, pp. 80–89, Sep. 2004.